

**SENSORY NEURON SUBPOPULATION-SPECIFIC REGULATION OF
INTRACELLULAR CALCIUM IN A RAT MODEL OF CHEMOTHERAPY- INDUCED
PERIPHERAL NEUROPATHY**

by

Eser Yilmaz

B.S. in Biology and Biochemistry, University of Massachusetts at Amherst, 2004

M.S. in Neuroscience, University of Pittsburgh, 2010

Submitted to the Graduate Faculty of
University of Pittsburgh School of Medicine in partial fulfillment
of the requirements for the degree of
Ph.D. in Neuroscience

University of Pittsburgh

2016

UNIVERSITY OF PITTSBURGH

SCHOOL OF MEDICINE

This dissertation was presented

by

Eser Yilmaz

It was defended on

June 8, 2016

and approved by

Gerald Gebhart, PhD, Professor

Theresa Hastings, PhD, Associate Professor

Elias Aizenman, PhD, Professor

Stephen Meriney, PhD, Professor

James Ibinson, MD PhD, Assistant Professor

Patrick Dougherty, PhD, Professor

Dissertation Advisor: Michael Gold, PhD, Professor

Copyright © by Eser Yilmaz

2016

**SENSORY NEURON SUBPOPULATION-SPECIFIC REGULATION OF
INTRACELLULAR CALCIUM IN A RAT MODEL OF CHEMOTHERAPY-
INDUCED PERIPHERAL NEUROPATHY**

Eser Yilmaz, Ph.D.

University of Pittsburgh, 2016

Chemotherapeutic-induced peripheral neuropathy (CIPN) is associated with a unique stocking-glove distribution of signs and symptoms. CIPN starts with numbness and tingling and proceeds to ongoing pain. The potential impact of target of innervation on CIPN has been largely ignored despite the tremendous heterogeneity among sensory neurons regarding their resting and injury-induced properties. Moreover, there is compelling evidence from other neuropathy models indicating that dysregulation of intracellular Ca^{2+} in sensory neurons contributes to the signs and symptoms of the neuropathy. Therefore, the central hypothesis I pursued in this thesis was that both the positive and negative signs of CIPN are due to subpopulation-specific changes in Ca^{2+} regulation, which I tested in a paclitaxel-induced peripheral neuropathy model. Paclitaxel was associated with a persistent decrease in mechanical nociceptive threshold in response to stimuli applied to the glabrous hindpaw skin, but not the other areas that were tested. While paclitaxel had no detectable influence on either resting or depolarization-evoked Ca^{2+} transients in putative non-nociceptive neurons, there was a significant paclitaxel-induced decrease in the evoked Ca^{2+} transient duration in putative nociceptive glabrous neurons, which correlated with the paclitaxel-induced nociceptive behavior. This paclitaxel-induced change in Ca^{2+} regulation was not due to increased activity of Na^+ - Ca^{2+} -exchanger (NCX), which contributes to the regulation of evoked Ca^{2+} transient durations in this subpopulation of neurons. However, the paclitaxel-induced decrease in the duration of the evoked Ca^{2+} transient did appear to be due to both direct and

indirect influences of mitochondria. The direct influence reflected an increase in mitochondria volume, enabling an increase in total Ca^{2+} uptake, while the indirect influence reflected an increase in the activity of ATP-dependent Ca^{2+} regulatory mechanisms, such as the sarco-endoplasmic-reticulum-ATPase (SERCA). The results generated in this dissertation expand the current view of CIPN mechanisms and constitute an important step towards understanding the roles of intracellular Ca^{2+} as well as mitochondrial changes to the pain associated with CIPN, paving the road for novel therapeutic strategies to limit the side effects of chemotherapy.

TABLE OF CONTENTS

PREFACE.....	XIV
1.0 INTRODUCTION.....	1
1.1 CHEMOTHERAPY-INDUCED PERIPHERAL NEUROPATHY	1
1.1.1 Clinical Presentation	2
1.1.2 Temporal Profile.....	4
1.2 MECHANISMS IMPLICATED IN CIPN	4
1.2.1 Primary Antineoplastic Mechanisms.....	4
1.2.1.1 DNA Targeting	5
1.2.1.2 Inhibition of the Mitotic Spindle.....	6
1.2.1.3 Metabolic Inhibitors	7
1.2.2 Inflammatory Pathways.....	8
1.2.3 Axonal Length and Loss of Intraepidermal Nerve Fibers.....	11
1.2.4 Mitotoxicity	12
1.3 HETEROGENEITY OF PRIMARY AFFERENTS	16
1.3.1 Classification of Primary Afferent Subpopulations	17
1.3.2 Multi-criterion Approach for Subpopulation Classification.....	19
1.4 REGULATION OF INTRACELLULAR CALCIUM SIGNALING	21
1.4.1 Regulation of Ca²⁺ in primary afferents.....	23

1.4.2	Regulation of Ca ²⁺ and pain models	24
1.5	A NEW HYPOTHESIS FOR CIPN.....	25
2.0	SENSORY NEURON SUBPOPULATION-SPECIFIC DYSREGULATION OF INTRACELLULAR CALCIUM IN A RAT MODEL OF CHEMOTHERAPY- INDUCED PERIPHERAL NEUROPATHY	27
2.1	INTRODUCTION	27
2.2	METHODS.....	30
2.2.1	Animals.....	30
2.2.2	Tissue Labeling	30
2.2.3	Paclitaxel Treatment	31
2.2.4	Behavioral Assessment of Mechanical Hypersensitivity.....	31
2.2.5	Sensory Neuron Isolation.....	32
2.2.6	Ca ²⁺ Imaging	32
2.2.7	Chemicals	33
2.2.8	Data Analysis.....	34
2.3	RESULTS	35
2.3.1	Paclitaxel-Induced Mechanical Hypersensitivity	35
2.3.2	The impact of target of innervation on resting and evoked intracellular calcium concentration [Ca ²⁺] _i in putative nociceptive cutaneous neurons	36
2.3.3	Paclitaxel attenuates the duration of the evoked Ca ²⁺ transient in putative nociceptors.....	38
2.3.4	Paclitaxel does not affect the resting or evoked Ca ²⁺ transient properties in putative non-nociceptive sensory neurons.	41

2.4	DISCUSSION.....	43
3.0	PACLITAXEL-INDUCED INCREASE IN NCX ACTIVITY IN SUBPOPULATIONS OF NOCICEPTIVE AFFERENTS: A PROTECTIVE MECHANISM AGAINST CHEMOTHERAPY-INDUCED PERIPHERAL NEUROPATHY?	48
3.1	INTRODUCTION	48
3.2	METHODS.....	50
3.2.1	Animals.....	50
3.2.2	Tissue labeling.....	50
3.2.3	Paclitaxel treatment.....	51
3.2.4	Sensory Neuron Isolation.....	51
3.2.5	Ca ²⁺ Imaging	51
3.2.6	Chemicals	52
3.2.7	Data Analysis.....	53
3.3	RESULTS	55
3.3.1	NCX does not mediate the paclitaxel-induced attenuation of the depolarization-evokedCa ²⁺ transient duration in putative glabrous nociceptors.....	55
3.3.2	NCX is sensitized by the vehicle of paclitaxel.	56
3.3.3	The impact of paclitaxel on NCX activity is dependent on target of innervation.	59
3.3.4	Paclitaxel-induced increase in NCX activity in thigh neurons is not due to NCX3 activity.....	62

3.4	DISCUSSION.....	66
4.0	ROLE OF PACLITAXEL-INDUCED INCREASE IN MITOCHONDRIAL VOLUME ON CALCIUM DYSREGULATION IN SUBPOPULATIONS OF NOCICEPTIVE AFFERENTS: DIRECT AND INDIRECT MECHANISMS	71
4.1	INTRODUCTION	71
4.2	METHODS.....	75
4.2.1	Animals.....	75
4.2.2	Retrograde labeling.....	75
4.2.3	Paclitaxel treatment.....	76
4.2.4	Behavioral Assessment.....	76
4.2.5	Sensory Neuron Isolation.....	77
4.2.6	Fura-2 and Rhod-2 Ca ²⁺ Imaging	77
4.2.7	Live cell confocal microscopy	79
4.2.8	Fluorescent Immunocytochemistry.....	80
4.2.9	Chemicals	81
4.2.10	Statistical Analysis.....	82
4.3	RESULTS.....	84
4.3.1	The recovery of the paclitaxel-induced decrease in the duration of the depolarization evoked Ca ²⁺ transient correlates with the resolution of paclitaxel-induced hypersensitivity.....	84
4.3.2	Mitochondrial [Ca ²⁺] _i buffering is increased in putative nociceptive glabrous skin neurons from paclitaxel-treated rats.	86

4.3.3	While there are differences between putative nociceptive and non-nociceptive DRG neurons with respect to resting mitochondrial Ca ²⁺ levels, paclitaxel was not associated with an increase in mitochondrial Ca ²⁺ uptake in putative nociceptive glabrous skin neurons.	89
4.3.4	Paclitaxel is associated with an increase in mitochondria in putative nociceptive glabrous skin neurons.	92
4.3.5	Paclitaxel does not reduce the health and functionality of mitochondria in putative nociceptive glabrous skin neurons.	97
4.3.6	Paclitaxel increases ATP-dependent Ca ²⁺ uptake into endoplasmic reticulum.....	100
4.4	DISCUSSION.....	103
5.0	DISCUSSION	111
5.1	SUMMARY OF THE DISSERTATION.....	111
5.1.1	The Goal of the Study.....	111
5.1.2	Summary of the Findings.....	112
5.2	COMPLEXITY OF CA ²⁺ REGULATION	114
5.3	HETEROGENEITY OF NEURONS BASED ON PHENOTYPE AND TARGET OF INNERVATION	116
5.4	EXPERIMENTAL LIMITATIONS	118
5.4.1	Isolated Cell Body.....	118
5.4.2	Generalizability of Paclitaxel Model to CIPN.....	119
5.4.3	Species Differences	122
5.4.4	Sex Differences.....	123

5.5	FUTURE DIRECTIONS.....	123
5.5.1	Paclitaxel-Induced Changes in Ca²⁺ Regulation and Pain-Related Behavior.....	123
5.5.2	Compensatory Mechanisms.....	124
5.5.3	Clinical Implications.....	125
	BIBLIOGRAPHY	130

LIST OF FIGURES

Figure 1. Paclitaxel-Induced Mechanical Hypersensitivity	36
Figure 2. The impact of target of innervation on resting and evoked intracellular calcium concentration $[Ca^{2+}]_i$ in putative nociceptive cutaneous neurons.	38
Figure 3. Paclitaxel attenuates the duration of the evoked Ca^{2+} transient in putative nociceptors.	40
Figure 4. Paclitaxel does not affect the resting or evoked Ca^{2+} transient properties in putative non-nociceptive sensory neurons.	42
Figure 5. NCX does not mediate the paclitaxel-induced attenuation of the depolarization evoked Ca^{2+} transient duration in putative glabrous nociceptors.	56
Figure 6. NCX is sensitized by the vehicle of paclitaxel.	59
Figure 7. The impact of paclitaxel on NCX activity is dependent on target of innervation.	61
Figure 8. Paclitaxel-induced increase in NCX activity in thigh neurons is not due to NCX3 activity.	64
Figure 9. The recovery of the paclitaxel-induced decrease in the duration of the depolarization evoked Ca^{2+} transient correlates with the resolution of paclitaxel-induced hypersensitivity.	85
Figure 10. Mitochondrial $[Ca^{2+}]_i$ buffering is increased in putative nociceptive glabrous skin neurons from paclitaxel-treated rats.	88

Figure 11. Paclitaxel was not associated with an increase in mitochondrial Ca^{2+} uptake in putative nociceptive glabrous skin neurons.	91
Figure 12. Paclitaxel is associated with an increase in the mitochondria in putative nociceptive glabrous skin neurons.	94
Figure 13. Paclitaxel is associated with an increase in the mitochondrial volume in putative nociceptive glabrous skin neurons.	96
Figure 14. Paclitaxel does not reduce the functionality of mitochondria in putative nociceptive glabrous skin neurons.	98
Figure 15. Paclitaxel does not reduce the health of mitochondria in putative nociceptive glabrous skin neurons.	100
Figure 16. Paclitaxel increases ATP-dependent Ca^{2+} uptake into endoplasmic reticulum.	102

PREFACE

I consider myself to be lucky for having such a great committee and I appreciate all the advice I received throughout my dissertation. I could not ask for a better committee chair than Dr. Gebhart, who has been very supportive. Dr. Hastings was always there to answer my questions and discuss experiments or techniques. I would also like to thank Drs. Meriney, Aizenman, and Ibinson for their guidance and Dr. Dougherty for traveling all the way to Pittsburgh as my outside examiner and his valuable feedback.

In addition to my committee, I am also grateful for all the help and training I received from Dr. Zachary Wills and Dr. Simon Watkins. Without their support, I would not be able to do the experiments involving confocal microscopy. I also owe it to the members of the Gold laboratory, all of whom gave me feedback during lab meetings and practice talks. An amazing undergraduate assistant, Greta Volpedo, who is about to become a graduate student herself, deserves special thanks for her help with the behavioral experiments.

You would not be reading this page, if it weren't for Dr. Gold. I met him as a technician who was considering other career options to be able to take care of a growing human being. But Dr. Gold encouraged me to finish "what I've started" first. So, I joined graduate school again. I cannot thank him enough for many reasons. First, he adopted me as his graduate student and made it possible for me to finish my degree. More importantly, however, I learned how science is done. Maybe it is wishful thinking, but I am also hoping that I became a better writer over time

after coauthoring a few documents together. One last thing I learned from him is that to be successful one has to be very passionate about what they are doing. I have never seen another person so dedicated, so knowledgeable, so passionate about their work than Dr. Gold. He is the human form of pain biology. This observation encouraged me to do some soul searching and figure out what I was really passionate about.

I also owe so much to my amazing family. My parents were supportive in all dimensions imaginable, from traveling halfway across the globe to help with childcare to financially assisting me at the times of need. My husband Jim is probably the coolest person I have ever met; he is very knowledgeable in many science fields from physics to ecology, even if he would deny it, he is a living philosopher, and his creative writing skills make me “literally” envious. I owe him so much for all his love and support, for co-parenting with me, for listening to my daily research experiences, for all his feedback, and for being a very supportive boyfriend/fiancé/spouse during my studies. And his family has been wonderful; his mother Lisa became a very good friend and my biggest support system for childcare. She was always there when I needed her help. My “mellow little fellow” Dennis was also phenomenal. He was well-behaved, lovely, and very healthy the entire time. And no matter how tired, upset, angry, etc. I was in a given day, going home and seeing the faces of Jim and Dennis just made it all go away and be replaced with happiness. I am very proud of them both and I hope that I can make them proud as well.

Last, working in a windowless facility with dim artificial lights for 9 to 14 hours a day can be lonely and depressing. I owe completion of this work without losing my sanity to numerous headphones and Pandora radio, NPR, iTunes University, TED talks, and free Audiobooks.

1.0 INTRODUCTION

1.1 CHEMOTHERAPY-INDUCED PERIPHERAL NEUROPATHY

Cancer is the second leading cause of death in the United States following heart disease, claiming approximately 1620 lives per day (American Cancer Society, 2015). Thus early intervention and the use of aggressive treatments are often essential to save lives. Chemotherapeutics, drugs from a variety of different classes that share the essential ability to arrest cell division, are widely used for the treatment of a most cancers. In addition to the impact of chemotherapeutics on dividing cells, these drugs have effects on post-mitotic cells, including sensory neurons of the peripheral nervous system (Windebank and Grisold, 2008, Gornstein and Schwarz, 2014). This side effect of chemotherapy is associated with the development of chemotherapy-induced peripheral neuropathy (CIPN) in a significant fraction of cancer patients (Jaggi and Singh, 2012). Sensory disturbances associated with CIPN can range from mild tingling to severe ongoing pain in distal appendages. The severity of symptoms often increases with continued therapy, resulting in dose limitation or even therapy cessation (Dougherty et al., 2004, Windebank and Grisold, 2008, Pachman et al., 2011, Jaggi and Singh, 2012, Schneider et al., 2015). Understanding the mechanisms underlying CIPN may enable the development adjuvant treatments that prevent or reverse CIPN so that it is possible to increase dosing and consequently, the efficacy for existing chemotherapeutics.

1.1.1 Clinical Presentation

There is general agreement between studies that 30 - 40 % of chemotherapy patients develop CIPN (Xiao et al., 2008, Pachman et al., 2011, Jaggi and Singh, 2012, Gornstein and Schwarz, 2014). This prevalence as well as the severity of CIPN is thought to be directly related to initial and cumulative doses of chemotherapeutics and duration of the therapy. Co-administration of other drugs, and the presence of other conditions, such as diabetes, may also increase the likelihood of developing painful symptoms (Chaudhry et al., 2003, Cata et al., 2008). CIPN is reported to be a predominantly sensory neuropathy that is manifest in a “stocking-glove” distribution, i.e. with signs and symptoms of the neuropathy that occur most frequently in distal appendages (Dougherty et al., 2004, Windebank and Grisold, 2008, Wolf et al., 2008, Jaggi and Singh, 2012).

As with other forms for neuropathy, the sensory changes associated with CIPN are referred to as both gain of function and loss of function (Schneider et al., 2015). The most common gain-of-function symptoms are paresthesias, tingling, and pain, whereas the most common loss-of-function symptoms are numbness, reduced proprioception, and/or vibratory sense (Schneider et al., 2015). The gain-of-function symptoms appear to be due to increased spontaneous activity of sensory neurons as well as a decrease in the threshold for activation, whereas the loss-of-function symptoms are thought to reflect a dieback of large diameter sensory axons or loss of intraepidermal nerve fibers (IENFs).

Since loss of the loss of IENFs has been associated with various neuropathic conditions such as complex regional pain syndrome and diabetic neuropathy (Shun et al., 2004, Albrecht et al.,

2006) a series of studies were conducted to determine whether CIPN was likewise associated with loss of IENFs. Indeed, skin biopsies taken from chemotherapy patients receiving bortezomib, paclitaxel, and vincristine showed significant decreases Meissner's corpuscles and IENFs compared to healthy control subjects (Boyette-Davis et al., 2011b, Boyette-Davis et al., 2013). Animal models of oxaliplatin- and paclitaxel-induced peripheral neuropathy are also associated with loss of IENFs at the time of peak (maximal) mechanical hypersensitivity, which was reversed with minocycline treatment in both cases (Liu et al., 2010, Boyette-Davis and Dougherty, 2011, Boyette-Davis et al., 2011a). This suggested that loss of IENFs is downstream of an inflammatory response. Nevertheless, the observation of a decrease in the density of IENF in both painful areas as well as pain-free areas in patient studies (Boyette-Davis et al., 2013) suggests that loss of IENF and pain are not causally linked.

Whereas, sensory disturbances of CIPN are a major concern, effects of chemotherapeutics on motor and autonomic systems are less likely to lead to dose limitation or therapy cessation. Signs and symptoms relating to motor system abnormalities are fairly uncommon and have been generally reported for cases treated with significantly high doses of chemotherapeutics (Windebank and Grisold, 2008, Jaggi and Singh, 2012, Gornstein and Schwarz, 2014). Thus, it is not clear whether occurrence of chemotherapy-induced motor neuropathy is simply a severe variant of the same processes leading to sensory neuropathy or whether it reflects completely different mechanisms (Schneider et al., 2015). Similarly, while chemotherapy is associated with nausea, vomiting and other digestive tract symptoms (Windebank and Grisold, 2008) as well as orthostatic hypotension and arrhythmia (Windebank and Grisold, 2008), autonomic system problems are also not a primary reason for dose limitation or cessation.

1.1.2 Temporal Profile

Treatment with certain chemotherapy agents, such as paclitaxel and oxaliplatin, leads to acute painful symptoms (Loprinzi et al., 2007, Hill et al., 2010). Even though chemotherapy-induced acute pain syndrome can resolve within days (Loprinzi et al., 2007), a significant fraction of patients develops a persistent form of CIPN (Jaggi and Singh, 2012). This persistent form of CIPN develops days to weeks after the initiation of chemotherapy, and most patients experience it for months even after the cessation of treatment (Boyette-Davis et al., 2013). Moreover, the time-courses of loss- and gain-of-function symptoms are also temporally dissociated and loss-of-function symptoms, such as numbness, are reported generally earlier than painful symptoms (Schneider et al., 2015).

1.2 MECHANISMS IMPLICATED IN CIPN

Various mechanisms have been proposed to underlie CIPN. These include: primary antineoplastic mechanisms of chemotherapeutic drugs, inflammatory mechanisms, dying back of long axons and as well as mitotoxicity.

1.2.1 Primary Antineoplastic Mechanisms

Multiple classes of chemotherapeutic drugs with distinct primary mechanisms of action were designed to kill rapidly dividing cancer cells. These actions can be roughly grouped according to whether the target is transcription of nuclear DNA or the assembly of the mitotic spindle during

cell division. Commonly used classes of chemotherapeutics that target the nuclear DNA are platinum compounds, DNA alkylating agents, and antineoplastic antibiotics, such as actinomycin derivatives. Taxane compounds and vinca alkaloids are examples of mitotic spindle inhibitors. Since cancer cells have very high metabolic rates and inhibition of their metabolism leads them to commit apoptosis, metabolic inhibitors represent a third group of chemotherapeutics examples of which include the proteasome inhibitor bortezomib and the antimetabolites such as methotrexate, gemcitabine, and 5-fluorouracil.

1.2.1.1 DNA Targeting

Many heavy metals are of environmental concern due their high affinity to cellular structures, especially to cellular DNA. For more than three decades cancer biology has been taking advantage of one heavy metal, platinum, which has strong covalent binding properties to N7 on purines (Bonetti et al., 2009). Commonly used platinum compounds are cisplatin, oxaliplatin, and carboplatin, all of which lead to irreparable DNA damage, which in turn initiates apoptosis (Windebank and Grisold, 2008, Bonetti et al., 2009). Use of each of these platinum compounds has been linked to a sensory neuropathy; 60-80% of patients on an oxaliplatin regimen develop stereotypical acute sensory symptoms (Windebank and Grisold, 2008, Jaggi and Singh, 2012) and patients receiving either of the three drugs develop a persistent neuropathy, which starts with paresthesias in distal limbs and progresses even after the last dose of chemotherapy (Grunberg et al., 1989). In advanced stages, sensory ataxia and severe neuropathic pain are reported (Jaggi and Singh, 2012).

Antineoplastic antibiotics, such as actinomycin derivatives and doxorubicin, block transcription by intercalating into the DNA. Since these compounds are generally used in

combination with other chemotherapeutic agents, there is not enough data to conclude that their use leads to CIPN. Experimental evidence suggests doxorubicin can damage dorsal root ganglia (DRG) neurons in animal models however it does not seem to be associated with neurotoxicity in humans (Windebank and Grisold, 2008).

As for DNA alkylating agents, neuropathy is not a prominent effect. For example, little to no peripheral neuropathy symptoms are reported in association with cyclophosphamide (Windebank and Grisold, 2008) and signs of neuropathy are reported in less than 10 percent of the patients treated with high-dose ifosfamide (Patel et al., 1997). Therefore among DNA-targeting chemotherapeutic agents, the platinum compounds are the only ones clearly linked to CIPN, suggesting that targeting DNA in general is unlikely to be the underlying mechanism of CIPN.

1.2.1.2 Inhibition of the Mitotic Spindle

The mitotic spindle is the machinery that binds and segregates chromosomes during cell division (Walczak and Heald, 2008) and is composed of microtubule polymers with a bipolar organization. The intrinsic polarity and dynamic properties of microtubules are essential for mitotic spindle function (Walczak and Heald, 2008). Microtubules are therefore targeted by drugs that either stabilize or inhibit the assembly of microtubules or such as taxanes or vinca alkaloids (Windebank and Grisold, 2008, Boyette-Davis et al., 2013). Disruption of the mitotic spindle arrests mitosis and ultimately activates apoptotic mechanisms (Windebank and Grisold, 2008, Gornstein and Schwarz, 2014). Vinca alkaloids, such as vincristine, vinblastine, and vinorelbine inhibit assembly and promote disassembly of microtubules (Windebank and Grisold, 2008, Boyette-Davis et al., 2013). On the other hand, taxanes, such as paclitaxel and docetaxel, stabilize microtubules (Windebank and Grisold, 2008, Boyette-Davis et al., 2013). More

specifically, taxanes bind along the microtubule lumen to β -tubulin that has been incorporated into the microtubules (Nogales et al., 1995), strengthening lateral contacts between subunits, hence suppressing microtubule depolarization (Prota et al., 2013). At higher concentrations, paclitaxel even enhances the polymerization of microtubules (Gornstein and Schwarz, 2014).

The clinical features with each of these microtubule-targeting agents are similar; a dose dependent, predominantly-sensory neuropathy in a stocking-glove distribution (Dougherty et al., 2004, Windebank and Grisold, 2008, Wolf et al., 2008, Jaggi and Singh, 2012, Boyette-Davis et al., 2013, Gornstein and Schwarz, 2014, Schneider et al., 2015). It has been suggested that microtubule-targeting drugs cause CIPN via disrupting axonal transport, which in turn may disrupt axonal structure and function resulting in axon degeneration (Windebank and Grisold, 2008, Jaggi and Singh, 2012, Gornstein and Schwarz, 2014). However, other microtubule-disrupting drugs such as colchicine and TZT-1027 do not induce neuropathic pain (Raffa et al., 2012), suggesting that even if microtubule-disruption contributes to CIPN, there is another mechanism underlying CIPN at large.

1.2.1.3 Metabolic Inhibitors

Rapidly dividing cancer cells have high metabolic activity, and interfering with their metabolism leads to apoptosis. Bortezomib, a boronic acid derivative, interferes with cellular metabolism by inhibiting the mammalian 26S proteasome complex of the ubiquitin degradation pathway (Windebank and Grisold, 2008). Bortezomib-induced neuropathy, similar to CIPN observed with taxanes, vinca alkaloids, and platinum compounds, is predominantly sensory and distal (Wolf et al., 2008, Jaggi and Singh, 2012, Zheng et al., 2012). The sensory neuropathy caused by bortezomib often involves significant neuropathic pain and is thought to involve a small fiber

neuropathy (Windebank and Grisold, 2008). On the other hand, there is another class of metabolic inhibitors known as antimetabolites, which are biologically inactive folic acid, pyrimidine or purine analogues. Antimetabolites induce apoptosis after getting incorporated into nucleic acids or inhibit crucial metabolic enzymes. However these drugs rarely cause neuropathy and if any, are associated with central rather than peripheral neuropathy (Windebank and Grisold, 2008). These differences between bortezomib and antimetabolites argue against metabolic interference as a primary mechanism of CIPN.

In conclusion, sensory disruption leading to painful paresthesias is associated with members of all major classes of chemotherapeutic agents. Although some of these primary mechanisms can contribute to the signs and symptoms of CIPN, none of these primary mechanisms alone appear sufficient to cause CIPN both because of the common phenotype of the neuropathy independent of the primary mechanism and because not all members of each class are associated with neuropathy. This led many groups to search for a common mechanism of CIPN that might be employed by different classes of chemotherapeutic agents.

1.2.2 Inflammatory Pathways

Inflammation is generally associated with tissue injury or infection. One of the five cardinal signs of inflammation is pain and/or hypersensitivity. While changes in tissue have been implicated in inflammatory pain, the bulk of evidence indicates that the pain presented at the site of injury is due to the actions of inflammatory mediators on nociceptive afferents. Many mediators, such as protons, $\text{TNF}\alpha$, or TRPV1 ligands, are able to directly activate nociceptive afferents, others, such as bradykinin, PGI₂, and ATP are able to activate and sensitize nociceptive afferents, while others still, as such as PGE₂, NGF, and IL-1 β are only able to

sensitize nociceptive afferents (Kidd and Urban, 2001, Koltzenburg et al., 2013). Resident and recruited immune cells are an important source of inflammatory mediators, but nonimmune cells also have been shown to release inflammatory mediators in response to injury. These cells include keratinocytes in the skin, endothelial cells, as well as glial cells and Schwann cells in the nervous system (Koltzenburg et al., 2013).

While the focus on neuropathic pain, as least in the context of underlying mechanisms, has historically been on the changes in the injured nerves, it is now clear that inflammatory processes also contribute to pain associated with nerve injury. In the context of traumatic nerve injury, mediators are released from Schwann cells and resident immune cells, such as mast cells and macrophages (Scholz and Woolf, 2007, Ellis and Bennett, 2013) which are initially activated as part of the process of wallerian degeneration of damaged fibers (Scholz and Woolf, 2007). Macrophages, as well as lymphocytes and satellite cells also drive an immune response within the DRG (Scholz and Woolf, 2007, Koltzenburg et al., 2013). Moreover, peripheral nerve injury leads to activation of spinal microglia and subsequently activation and proliferation of astrocytes, which are responsible for the release of inflammatory mediators within the spinal cord (Scholz and Woolf, 2007). In addition, proinflammatory cytokines and chemokines have been shown to be crucial for the development and maintenance of painful peripheral neuropathy (Watkins and Maier, 2002) and induction of proinflammatory mediators was proposed as an underlying mechanism for CIPN as well (Wang et al., 2012).

Both neuronal and non-neuronal cells are involved in the immunomodulation due to chemotherapy and the release of cytokines and chemokines is one of the primary mechanisms facilitating these changes. There is evidence that paclitaxel treatment in rats is associated with infiltration of activated macrophages into the DRG, sciatic nerve, and the spinal cord (Peters et

al., 2007, Nishida et al., 2008, Zhang et al., 2016). This macrophage infiltration as a response to chemotherapy initiates production and secretion of various cytokines, chemokines, growth factors, inflammatory mediators, prostaglandins, and serotonin (Wang et al., 2012). Moreover, Schwann cells start undergoing phenotype modulation and releasing TNF- α , IL-1 β , IL-6, PGE2, ATP, leukemia inhibitory factor (LIF) and monocyte chemoattractant protein-1 (MCP-1) (Wang et al., 2012). In addition, primary afferents themselves have also been implicated in the immunomodulation; paclitaxel was shown to induce MCP-1 in small diameter neurons whereas its receptor CCR2 was shown to be expressed in large myelinated neurons (Zhang et al., 2013), suggesting a potential paracrine MCP-1/CCR2 signaling in DRG.

Inflammatory mediators have been implicated in the pain associated with CIPN, although there appears to be differences between traumatic nerve injury and CIPN, with respect to the mechanisms responsible for the “inflammatory” component of these neuropathic pains. Chemotherapeutic agents with distinct primary antineoplastic mechanisms have been shown to induce upregulation of genes associated with inflammatory and immune responses in DRG (Wang et al., 2012). Remarkably, in a rat model of paclitaxel-induced peripheral neuropathy, nearly half of upregulated genes from the DRG were associated with inflammatory and immune responses (Nishida et al., 2008). Expression of the proinflammatory cytokine IL-6 was found to be increased in a bortezomib-induced peripheral neuropathy model (Mangiacavalli et al., 2010). Similarly, TNF α and IL-1 β mRNA levels were shown to be elevated in the DRG in a rat model of paclitaxel-induced neuropathy (Ledebøer et al., 2007). Importantly, intrathecal administration of IL1 receptor antagonist reversed paclitaxel-induced allodynia (Ledebøer et al., 2007). Immunomodulatory agents such as thalidomide and minocycline that have been shown to attenuate mechanical allodynia in a sciatic nerve inflammation model (Ledebøer et al., 2005),

effectively reduced paclitaxel-induced mechanical allodynia and hyperalgesia (Cata et al., 2008, Liu et al., 2010). Similarly, another such inhibitor, propentophylline, attenuated vincristine-induced pain symptoms (Sweitzer et al., 2006). Recently paclitaxel-induced neuropathy was also shown to involve activation of cellular immune responses via the toll-like receptor 4 (TLR4) pathway (Li et al., 2015a, Li et al., 2015b). Thus, in contrast to traumatic nerve injury, where immune activation appears to be a consequence of the tissue injury, at least some of the immune activation associated with CIPN appears to be due to direct actions of the chemotherapeutics.

While the evidence for the role of inflammatory mediators in CIPN is compelling, there are several lines of evidence against a primary role for inflammatory mediators, alone, in either the positive or the negative signs of CIPN. First, anti-inflammatory medications fail to relieve pain associated with CIPN (Wang et al., 2012). Moreover, a general activation of inflammatory pathways is not sufficient to explain the stocking-glove manifestation of the CIPN symptoms.

1.2.3 Axonal Length and Loss of Intraepidermal Nerve Fibers

An intuitive explanation for the stocking-glove distribution of CIPN, is that longer axons will be more susceptible to disruption of axonal transport, and therefore more likely to be deleteriously impacted by the accumulation of drug effects over longer distances. The result would be a die-back of the nerve endings (Windebank and Grisold, 2008). Early evidence indicating that mechanisms involved in axonal degeneration may underlie symptoms caused by paclitaxel treatment came from slow wallerian degeneration (Wld^s) mice that possess a unique resistance to axonal degeneration. These mice have also been shown to be resistant to paclitaxel-induced peripheral neuropathy (Wang et al., 2002). Thus, the long nerve hypothesis can account for the loss of IENF in CIPN, where there is no loss of fibers for short axons and toxicity is peripherally

manifest. Loss of IENF density, which is proposed to account for the negative signs, could also contribute to pain, if there is a decrease in the low-threshold input based on the gate theory.

However, the link between CIPN and damage to long axons falls short of providing a generalizable mechanism for CIPN. First, even in paclitaxel-induced pain models, there is no evidence of microtubule anomalies along the sensory and motor axons (Polomano et al., 2001, Flatters and Bennett, 2006, Xiao et al., 2011). Second, motor axons with comparable lengths appear to be spared from the effects of chemotherapy. Last, acute pain symptoms and rapid prognosis with some chemotherapeutics cannot be explained with a slow-scale die-back hypothesis of long axons. Therefore, even though damage to long axons might be responsible for some symptoms of CIPN, another mechanism is necessary to account for the full spectrum of signs and symptoms.

1.2.4 Mitotoxicity

Mitochondria are versatile organelles responsible for vital and interdependent functions including adenosine triphosphate (ATP) production, intracellular Ca^{2+} regulation, the generation of reactive oxygen species, and the regulation of apoptotic signaling pathways. Therefore a change in mitochondrial homeostasis may have a tremendous impact on the health and function of a cell.

Mitochondria were the focus of some of the earliest mechanistic studies of CIPN. Mitochondrial damage is associated with the release of the electron transfer chain protein, cytochrome c, into the cytosol (Kulikov et al., 2012). Indeed, incubating mitochondria isolated from human neuroblastoma cells with taxanes resulted in release of cytochrome c (Andre et al., 2000), as well as activation of the apoptotic protease caspase-8 (Goncalves et al., 2000). It has

been proposed that association of β -tubulin with the mitochondrial permeability transition pore (mPTP) provides paclitaxel a mitochondrial binding site (Flatters and Bennett, 2006). Consistent with the suggestion that chemotherapeutics were directly responsible for mitotoxicity, *in vitro* data linked paclitaxel to mitochondrial calcium release in cancer cells and pancreatic acinar cells via the mPTP (Evtodienko et al., 1996, Kidd et al., 2002).

That mitotoxicity may also be a mechanism of CIPN *in vivo*, was suggested by data from animal models of paclitaxel- oxaliplatin-, and bortezomib-induced CIPN, in which there was evidence of mitotoxicity along sensory axons. Toxicity was manifest in the form of mitochondrial swelling, increase in the percentage of vacuolated mitochondria, reduced rate of ATP production and respiration, as well as an increase in the production of reactive oxygen species (ROS) (Flatters and Bennett, 2006, Xiao et al., 2011, Zheng et al., 2011, 2012). This chemotherapeutic-induced mitotoxicity was observed in both small diameter slow-conducting fibers and large diameter myelinated sensory fibers, but was absent in motor fibers (Xiao et al., 2011). The authors suggested that the sensory fiber specific changes in mitochondria in CIPN models stems from high levels of paclitaxel accumulation in DRG, where the sensory neuron cell bodies are located (Xiao et al., 2011). In addition, an increase in the number of atypical mitochondria was detectable within days after the initiation of chemotherapy and returned back to normal levels when the pain behavior had resolved (Flatters and Bennett, 2006), providing correlational evidence of a link between toxicity and the hypersensitivity associated with CIPN.

According to the mitotoxicity model, it is the increase in ROS combined with the chronic energy deficit that are responsible for both spontaneous discharges (thus, tingling and pain) and degeneration in primary afferents (Bennett et al., 2014). Superoxide is the major ROS made in mitochondria, produced during oxidative phosphorylation. In support of this model are data from

studies in which it was demonstrated that manipulations that increase mitochondrial health or reduce ROS levels were effective at preventing painful symptoms of CIPN in animal models. For example, inhibition of superoxide production by systemic injection of complex I inhibitor rotenone or complex III inhibitor Antimycin A (Griffiths and Flatters, 2015) attenuated the established paclitaxel-induced mechanical hypersensitivity. Antimycin A also attenuated the development of paclitaxel-induced hypersensitivity (Griffiths and Flatters, 2015). However, in a study using a general ROS scavenger and a superoxide-selective scavenger, the general ROS scavenger, phenyl N-tert-butyl nitron (PBN), has been shown to attenuate the development of paclitaxel-induced mechanical hypersensitivity, however the superoxide selective scavenger, 4-hydroxy-2,2,6,6-tetramethylpiperidine-1-oxyl (TEMPOL) inhibited mechanical hypersensitivity only when administered at high doses but to a lesser degree than PBN, and daily systemic administration of TEMPOL failed to prevent the development of paclitaxel-induced mechanical hypersensitivity (Fidanboyly et al., 2011), suggesting a role for ROS but not necessarily for superoxide.

Acetyl-L-carnitine received a fair amount of attention in the context of CIPN and ROS production. This compound is naturally produced inside the mitochondria from L-carnitine and acetyl-CoA during periods of high energy demand and transported to the cytoplasm, where it converts back to its original constituents. Subsequently, L-carnitine enters mitochondria transporting fatty acids and facilitating fat metabolism, while acetyl-CoA stays in the cytoplasm. Enhancing this L-carnitine cycle is believed to improve mitochondrial function (Jin et al., 2008). Indeed, treatment with acetyl-L-carnitine was shown to block pain behavior and neurotoxicity in animal models of paclitaxel-, cisplatin-, oxaliplatin-, bortezomib-, and vincristine-induced

peripheral neuropathy (Ghirardi et al., 2005a, Ghirardi et al., 2005b, Jin et al., 2008, Xiao et al., 2012, Zheng et al., 2012), suggesting reduced mitochondrial health in CIPN.

While there is compelling evidence both for the presence of mitotoxicity in response to chemotherapeutic administration, as well as the contribution of mitotoxicity to both the positive and negative signs of CIPN, there are several important limitations of this model. First, it is unclear how a global change in mitochondria in sensory axons would result in stocking-glove manifestation of the CIPN that affects predominantly the glabrous skin. It has been suggested that the effects of mitotoxicity will be more detrimental in regions of high metabolic demand (Xiao and Bennett, 2008). These authors argued that the nerve endings of relatively longer primary afferent fibers have high levels of metabolic activity due to greater energy demands for maintenance and signal transmission over longer distance (Xiao and Bennett, 2008), however, there is no reason to suggest that the demands of the terminals in the glabrous skin, are any different than the demands to terminals throughout the body. Furthermore, there are afferents, such as muscle spindles, that have even higher metabolic demands than cutaneous afferents, yet there are no reports of paclitaxel-induced ill effects on muscle function. The mitotoxicity model does not account for relative restriction of CIPN symptoms to the glabrous but not to the dorsal surfaces of extremities (Dougherty et al., 2004) even though both surfaces are innervated by axons of comparable length. Furthermore, if there was a length-dependent influence of mitotoxicity, one would predict that there should be an increase in atypical mitochondria further along the axons. However, the percentage of atypical mitochondria were actually higher in dorsal roots than along the peripheral nerves from both control and paclitaxel treated rats (Xiao et al., 2011). Moreover, while rotenone and Antimycin A were used to block complex I and complex III of electron transport chain in order to reduce superoxide production (Griffiths and Flatters,

2015), these substances are actually thought to increase superoxide levels (Li et al., 2003, Drose and Brandt, 2008). Furthermore, even though CIPN models are associated with mitotoxicity in both small diameter and myelinated larger diameter axons, ameliorating effect of acetyl-L-carnitine was limited to only mitochondria along small diameter fibers (Jin et al., 2008). And despite the success of acetyl-L-carnitine to alleviate CIPN symptoms in preclinical models, and promising findings from pilot studies (Maestri et al., 2005), there was no detectable benefit to acetyl-L-carnitine treatment in a randomized double-blind trial (Hershman et al., 2013). In fact, acetyl-L-carnitine significantly worsened the symptoms of CIPN in participating patients (Hershman et al., 2013). As a result, the American Society of Clinical Oncology advises against the use of acetyl-L-carnitine for the management of CIPN (Hershman et al., 2014). In conclusion, even though there is accumulating evidence that certain symptoms of preclinical chemotherapy models are associated with mitotoxicity along sensory axons, crucial pieces of the puzzle are still missing.

1.3 HETEROGENEITY OF PRIMARY AFFERENTS

The main function of the peripheral nervous system (PNS) is to serve as a communication relay between the central nervous system (CNS) and the rest of the body. The PNS includes both a sensory component, the somatosensory nervous system (SNS) that carries information from the periphery to the CNS, and a motor component that carries information from the CNS to the effector areas. (Patestas and Gartner, 2016). Anatomically, cell bodies of sensory neurons, called primary afferents, are located in eight of the 12 cranial ganglia and all of the 31 pairs of dorsal

root ganglia (DRG) that lie in the intervertebral foramina on both sides of the spinal cord (Patestas and Gartner, 2016). There are no synapses within the ganglia and neurons leave their respective ganglion with a single bifurcating axon (Woolf and Ma, 2007, Mai and Paxinos, 2011, Patestas and Gartner, 2016). The peripheral branch of the axon terminates in the target somatic tissue whereas the central branch projects to the superficial dorsal horn of the spinal cord (Mai and Paxinos, 2011). Despite the uniformity of their general anatomical organization, primary afferents relay a variety of information, such as information relevant to the maintenance of homeostasis and the internal state of the organism including the temperature of the body, cardiovascular state, proprioception; information about the external environment including the modality, intensity, location of stimuli, as well as the features of the stimuli that appear to have affective valence such as pleasant, painful, itchy or tickling (Greger and Windhorst, 2013).

1.3.1 Classification of Primary Afferent Subpopulations

Currently multiple criteria are used to classify primary afferents into specific subpopulations based on their anatomical, physiological, and biochemical characteristics (Koerber et al., 1988, Lawson, 2002). Primary afferent cell soma can be classified roughly in three subpopulations based on cell body size. The ranges generally used to define small, medium and large diameter rat sensory neurons are less than 30 μm , 30 - 40 μm , and greater than 40 μm , respectively (Caffrey et al., 1992). Evidence suggests that the cell body diameter and axon conduction velocity of a primary afferent are at least roughly correlated (Harper and Lawson, 1985). Neurons with a small cell body diameter tend to give rise to non-myelinated, slow-conducting (C-fibers) axons, while those with a large cell body diameter tend to give rise to large diameter, myelinated fast-conducting ($A\beta$ fibers) axons (Harper and Lawson, 1985, Lawson, 2002).

Furthermore, given that nociceptors tend to have slowly conducting axons and neurons with rapidly conducting axons generally convey non-nociceptive information, neurons with small cell body diameter are likely to relay nociceptive information whereas those with a large cell body diameter are likely to be non-nociceptive (Lawson, 2002). Medium diameter neurons are thought to relay both nociceptive and non-nociceptive information (Lawson, 2002).

A way to further classify primary afferents takes advantage of their biochemical profiles. Primary afferents can be roughly divided into as peptidergic and non-peptidergic. These two classes of afferents express different repertoires of receptors and ion channels as well as project to distinct target areas in the dorsal horn (Woolf and Ma, 2007). During early development, all afferent neurons express the receptor for the nerve growth factor (NGF) *trkA*, however at later stages approximately half of these neurons switch off *TrkA* and instead begin to express the transmembrane signaling component of the receptor for glial cell-derived growth factor (GDNF) in addition to other associated factors (Molliver et al., 1997, Woolf and Ma, 2007). The cells that continue to express *TrkA* also express the neuropeptides calcitonin related gene peptide (CGRP) and substance P, hence become the peptidergic primary afferents, whereas the cell expressing GDNF that do not express CGRP or substance P become non-peptidergic primary afferents (Woolf and Ma, 2007).

Primary afferents can also be categorized by the modality of stimuli they are responsive to (i.e., mechanical, thermal or chemical). They are often referred to by their response profile as chemoreceptors, mechanoreceptors, baroreceptors, thermoreceptors, among others. These response properties are usually not mutually exclusive nor anatomically homogenous (Caterina and Julius, 1999). Some afferents are activated by multiple types of stimuli and thus are referred to as polymodal, while others are activated only by a single stimulus modality. Even within a

single modality, neurons are likely to be responsive to a narrow range of stimuli. For example, thermoreceptors that are activated by noxious heat are not necessarily activated by cold or even ambient temperatures.

Although sensory neurons can be classified into different subpopulations using various criteria, one should not rely on a single criterion for classification. For example, as discussed earlier, small diameter neurons are likely to be nociceptive and large diameter neurons non-nociceptive. However, neurons with similar sizes often have different biochemical profiles and distinct modalities, thus not all small diameter neurons are nociceptive and large diameter fibers are non-nociceptive, thus classification of neurons into nociceptive/non-nociceptive subpopulations should not be done by using the cell body diameter alone. In summary, heterogeneity of primary afferents makes it hard to classify subpopulations based on a single criterion.

1.3.2 Multi-criterion Approach for Subpopulation Classification

Studying differences between neurons using isolated neurons provides precise control over extracellular environment and facilitates identification of intrinsic changes in neurons that are not dependent on the influence of other cell types. However, isolated neuron preparations lack axons and terminals hence neither conduction velocity nor functional analysis of response properties of peripheral terminals can be utilized to further identify subpopulations. As discussed earlier, categorization of primary afferent neurons using single criteria has limitations, therefore in this dissertation I used a multi-criterion approach to categorize subpopulations of primary afferents using target of innervation, cell body diameter (Caffrey et al., 1992, Lawson, 2002), Isolectin B4 (IB4) binding (Fang et al., 2006), and sensitivity to capsaicin (Holzer, 1991).

An important factor that contributes to differences in subpopulations of primary afferents is the targets of innervation. Our laboratory as well as others have identified electrophysiological and biochemical differences between afferents identified based on target of innervation (Yoshimura et al., 2003, Beyak et al., 2004, Gold and Traub, 2004, Harriott et al., 2006, Harriott and Gold, 2009, Vaughn and Gold, 2010, Malin et al., 2011). For example, cutaneous and colonic afferents differ in their passive and active electrophysiological characteristics in both the absence and the presence of prostaglandin stimulation (Gold and Traub, 2004). Of note, these differences that are based on target of innervation appear to be most pronounced under pathological conditions, such as the presence of inflammatory mediators (Gold and Traub, 2004, Vaughn and Gold, 2010) or persistent inflammation (Harriott et al., 2006, Zhang et al., 2012b). I hypothesized that differences between neurons based on target of innervation contribute to the unique pattern in which CIPN is manifest, target of innervation was therefore used as a primary criteria with which to define subpopulations of neurons.

IB4 preferentially binds to the outer plasma membrane of the non-peptidergic afferents (Fang et al., 2006). IB4-binding, referred to as IB4+, and those that do not bind IB4, referred to as IB4- populations have been associated with distinct but somewhat overlapping innervation patterns, even though both populations are thought to be activated by all noxious stimulus modalities in the rat (Silverman and Kruger, 1990). Moreover, it has been shown that IB4+ afferents had longer duration action potentials (APs) and a higher density of voltage-gated tetrodotoxin (TTX)-resistant sodium channels while IB4- afferents had larger heat-evoked currents (Stucky and Lewin, 1999). Due to these differences between IB4+ and IB4- populations, IB4 binding was included in the multi-criterion approach in this dissertation.

Application of capsaicin to the skin causes a burning pain sensation (Martin et al., 1987). The receptor for capsaicin, transient receptor potential vanilloid 1 (TRPV1) is implicated in inflammatory thermal sensitivity and capsaicin application is widely used to identify nociceptors. The advantage of using capsaicin is that it is easily applied to dissociated neurons and produce a Ca^{2+} influx, thus using capsaicin is a valuable criterion since dissociated neurons lack axons that would enable functional characterization.

1.4 REGULATION OF INTRACELLULAR CALCIUM SIGNALING

Calcium is the Swiss army knife of a cell, versatile and useful as a secondary messenger capable of helping a cell do, just about everything a cell needs to do (Berridge et al., 2000, Berridge et al., 2003). Ca^{2+} can influence transcriptional and translational regulation, differentiation, apoptosis, contraction, excitability, and neurotransmitter release (Berridge et al., 2000). The versatility of Ca^{2+} dictates that its levels be tightly regulated. To achieve this level of regulation, cells possess a variety of Ca^{2+} regulatory mechanisms, generically referred to as the Ca^{2+} signaling toolkit. The specific features of the tool-kit depend in part on the function of the cell, enabling Ca^{2+} signaling with different spatial and temporal properties (Berridge et al., 2003).

Ca^{2+} signals are initiated via influx across the cell membrane or release from internal stores. There are a variety of influx pathways, which are most often ion channels activated by membrane depolarization, mechanical, thermal and chemical stimuli, as well as depletion of intracellular stores (Berridge et al., 2003). One of the most common stores from which Ca^{2+} is released is the endoplasmic reticulum (ER), where release is triggered via activation of inositol-

1,4,5-trisphosphate receptor (IP₃R) or ryanodine receptor (RyR) (Berridge et al., 2003, Verkhratsky and Toescu, 2003).

Once cytosolic Ca²⁺ levels start increasing, regulatory mechanisms are engaged that attenuate or amplify the increase. These regulatory mechanisms often include, cytosolic buffers, uptake into the mitochondria (via the mitochondrial calcium uniporter (MCU)) or the ER via the sarcoplasmic reticulum ATPase (SERCA), or extrusion via the Na⁺-Ca²⁺ exchanger (NCX) or the plasma membrane calcium ATPase (PMCA).

All of these mechanisms act over different ranges of Ca²⁺ levels, reflecting their density, distribution, and biophysical and pharmacological properties. For example PMCA and SERCA pumps have lower transport rates but high affinities allowing them to respond to modest elevations in Ca²⁺ concentration and set resting Ca²⁺ levels inside the cell. On the other hand, NCX and the MCU have higher rates of Ca²⁺ transport, enabling them to limit the duration and the magnitude of Ca²⁺ increases (Berridge et al., 2003). Similarly, the differential distribution of these regulatory mechanisms contributes to the spatial and temporal regulation of Ca²⁺ resulting in yet another layer of versatility to this important second messenger (Berridge et al., 2000, Berridge et al., 2003). Often Ca²⁺ regulatory proteins are organized into microdomains, which can function as autonomous units to create diverse signaling networks within the same cell (Berridge et al., 2000). For example, individual spines on neurons have been shown to operate as autonomous Ca²⁺-signaling units with diverse responses (Berridge et al., 2003).

1.4.1 Regulation of Ca²⁺ in primary afferents

Given the heterogeneity among the primary afferents with respect to every other property assessed, it should not be surprising that there is also heterogeneity in the regulation of intracellular Ca²⁺. Consistent with this expectation it was demonstrated in an early study, that caffeine-induced Ca²⁺ release from the ER was only observed in 2/3 of the DRG neurons (Shmigol et al., 1995). Another study has shown that NCX contributed to the regulation of resting Ca²⁺ in some neurons, but the duration of the evoked Ca²⁺ transient in others (Verdru et al., 1997). Others have reported that components of mitochondrial Ca²⁺ buffering differed depending on the size of the DRG neuron (Kostyuk et al., 1999). Although these studies provided evidence about differential regulation of Ca²⁺ in sensory neuron subpopulations, a comprehensive characterization of Ca²⁺ regulatory components in healthy primary afferents was not completed until later (Lu et al., 2006). Clear differences among DRG neuron subpopulations with respect to both the magnitude and the duration of the depolarization-evoked Ca²⁺ transients were documented (Lu et al., 2006). More specifically, small diameter, IB4-binding, and capsaicin responsive “putative nociceptor” neurons had longer lasting Ca²⁺ transients with large amplitudes, whereas the large diameter IB4-negative and capsaicin unresponsive neurons had fast decaying transients with small amplitudes (Lu et al., 2006). These differences were not attributable to differences in voltage gated Ca²⁺ currents, instead revealed a differential contribution of Ca²⁺ regulatory mechanisms among subpopulations of afferents (Lu et al., 2006). For example, RyR-mediated Ca²⁺ release, removal of Ca²⁺ via SERCA and PMCA, and mitochondrial Ca²⁺ buffering were found to play prominent roles in large diameter IB4-negative and capsaicin unresponsive afferents, however store operated Ca²⁺ entry and NCX were shown to play a major role in putative nociceptor subpopulation of DRG neurons (Lu et al., 2006).

1.4.2 Regulation of Ca²⁺ and pain models

In addition to the heterogeneity in Ca²⁺ regulation in subpopulations of afferents, there is growing evidence of changes in the regulation of Ca²⁺ in disease states. For example, inflammation increases the magnitude and the duration of the evoked Ca²⁺ transients in putative nociceptors (Lu and Gold, 2008). The increase in the duration of evoked Ca²⁺ transients in this inflammatory model was due to loss of NCX3 in the soma of putative nociceptors that innervated the site of inflammation due to an increase in unidirectional NCX3 trafficking to the periphery (Scheff and Gold, 2015). A distinct pattern of changes in Ca²⁺ have been described in response to nerve injury as well. For example, in models of traumatic nerve injury, the duration of evoked Ca²⁺ transients were shorter in injured but longer in adjacent putative nociceptive neurons (Fuchs et al., 2007). There was also a decrease in resting Ca²⁺ concentration in injured non-nociceptors, while adjacent putative nociceptive neurons did not manifest such changes (Fuchs et al., 2005). However, a diabetic neuropathy model was associated with an increase in both resting Ca²⁺ levels and the duration of the evoked Ca²⁺ transient in nociceptive afferents (Kostyuk et al., 2001). Taken together, these studies emphasize the impact of the nature of the injury on the specific changes in Ca²⁺ regulation.

Dysregulation of Ca²⁺ has been implicated to be critical in peripheral neuropathy models. In a diabetic neuropathy model, Fernyhough and Calcutt characterized dysregulation of both depolarization and caffeine-evoked Ca²⁺ transients in the axons (Fernyhough and Calcutt, 2010). These authors found evidence of axonal damage without any signs of oxidative stress or degeneration in the cell bodies of the same neurons (Fernyhough and Calcutt, 2010). Therefore,

it is likely that loss of function symptoms associated with the diabetic neuropathy model may be mediated by changes in Ca^{2+} regulation. In another study, drugs reducing intra- and extracellular Ca^{2+} inhibited mechanical hypersensitivity and allodynia in rat models of paclitaxel- and vincristine-induced neuropathy (Siau and Bennett, 2006), providing evidence that regulation of Ca^{2+} is critical for pain-related behaviors of at least some peripheral neuropathy models. Taken together, dysregulation of Ca^{2+} can underlie both the loss of function and gain of function symptoms associated with peripheral neuropathy.

1.5 A NEW HYPOTHESIS FOR CIPN

In this chapter, I have laid out the major lines of evidence that served as the basis for the central hypothesis pursued in this thesis. These included 1) the unique features of CIPN, which includes both positive and negative signs that are largely restricted to the glabrous skin and appear to reflect changes in both nociceptive and non-nociceptive afferent; 2) evidence of the tremendous heterogeneity among sensory neurons that includes resting properties, as well as the response to injury. In this regard, it was important to highlight the impact of target of innervation as well as the regulation of intracellular Ca^{2+} . 3) I also summarized evidence indicating that Ca^{2+} is not only dysregulated in the presence of injury, but that dysregulation contributes to the manifestation of both positive and negative signs of neuropathic pain. Based on these lines of evidence in combination with the limitation associated with the current models of CIPN, I hypothesize that both the positive and negative signs of CIPN are due to subpopulation and

target-of-innervation specific changes in Ca^{2+} regulation. The experiments described in the following chapters constitute the work completed so far towards the test of this hypothesis.

2.0 SENSORY NEURON SUBPOPULATION-SPECIFIC DYSREGULATION OF INTRACELLULAR CALCIUM IN A RAT MODEL OF CHEMOTHERAPY-INDUCED PERIPHERAL NEUROPATHY

2.1 INTRODUCTION

The impact of peripheral nerve injury on the regulation of the intracellular Ca^{2+} concentration ($[\text{Ca}^{2+}]_i$) in sensory neurons has received considerable attention because of the importance of neural $[\text{Ca}^{2+}]_i$ to transmitter release (Parnas and Parnas, 2010), gene expression (Fields et al., 2005), excitability (Hogan, 2007), and neurotoxicity (Berridge et al., 2000). These are all neural processes that are not only changed by nerve injury (Lekan et al., 1997, Costigan et al., 2002, Yaksh, 2006, Wilson et al., 2012, Ratte et al., 2014) but appear to contribute to the signs and symptoms of peripheral neuropathy (Siau and Bennett, 2006). For example, in models of traumatic nerve injury, which is often associated with paresthesias, dysesthesias, and ongoing pain, there are changes in the regulation of $[\text{Ca}^{2+}]_i$ in both putative nociceptive and non-nociceptive neurons in a pattern that appears to depend on whether or not the neurons were injured or were adjacent to those that were injured. That is, the duration of evoked Ca^{2+} transients were shorter in injured, but longer in adjacent putative nociceptive neurons (Fuchs et al., 2007). Similarly there was a decrease in resting $[\text{Ca}^{2+}]_i$ in injured putative non-nociceptive neurons with no change in resting $[\text{Ca}^{2+}]_i$ in putative nociceptive neurons (Fuchs et al., 2007). In

contrast, in a model of diabetic neuropathy, while there is an increase in the duration of the evoked Ca^{2+} transient in putative nociceptive neurons, there is also an increase in resting $[\text{Ca}^{2+}]_i$ (Kostyuk et al., 2001). In both models of peripheral neuropathy, there is evidence to suggest that the mechanisms contributing to the changes in the regulation of $[\text{Ca}^{2+}]_i$ contribute to changes in excitability (Tang et al., 2012). While there may be marked differences between peripheral nerve injury models with respect to the pattern of changes in the regulation of $[\text{Ca}^{2+}]_i$, there are only relatively subtle differences in the pain behavior associated with each model, highlighting the fact that the nervous system is able to achieve the same phenotype via multiple mechanisms.

One potential explanation for the differences between models with respect to the pattern of changes in the regulation of $[\text{Ca}^{2+}]_i$, is that each model impacts a different subpopulation of sensory neurons and as a result different subpopulations of neurons contribute to the observed pain behavior. For example, spontaneous activity in muscle afferents appears to play a particularly important role in pain behavior associated with traumatic nerve injury (Michaelis et al., 2000), while neurons innervating more superficial targets appear to play a more prominent role on diabetic neuropathy (Johnson et al., 2008). Furthermore, there are differences between subpopulations of sensory neurons with respect to the regulation of $[\text{Ca}^{2+}]_i$ (Lu et al., 2006). Consequently, the specific pattern of changes in the regulation of $[\text{Ca}^{2+}]_i$ may be a reflection of an interaction between the unique properties of specific subpopulations of sensory neurons and the relative impact of the nerve injury.

We reasoned that a chemotherapy model of peripheral neuropathy might enable us to begin to test this suggestion. Chemotherapeutic-induced peripheral neuropathy (CIPN) is associated with a unique distribution, in what is referred to as a “stocking-glove” pattern, with signs and symptoms of neuropathy largely restricted to the hands and feet. More interestingly,

CIPN also presents with what appears to be a differential impact on subpopulations of sensory neurons. Numbness and tingling appear to be associated with a loss of intra-epidermal nerve fiber density thought to reflect a selective dye-back of low threshold fibers, while the pain and hypersensitivity is thought to reflect the sensitization of nociceptive afferents (Tanner et al., 1998, Dougherty et al., 2004). Thus, we predicted, that this unique manifestation of CIPN would be reflected in a specific pattern of changes in the regulation of $[Ca^{2+}]_i$ in subpopulations of cutaneous neurons. To test this prediction, employed a combination of behavioral analysis and fura-2 based microfluorimetry to study the impact of paclitaxel-induced CIPN on different subpopulations of sensory neurons. An electronic von Frey device was used to assess the pattern of changes in mechanical sensitivity in the hindlimb. Retrograde tracers were used to identify subpopulations of cutaneous neurons innervating the glabrous and hairy skin of the hindpaw and skin of the thigh. Acutely dissociated DRG neurons were used to assess the impact of paclitaxel-induced CIPN on the regulation of $[Ca^{2+}]_i$ in subpopulations of neurons defined by target of innervation. Our results support the suggestion that the unique manifestation of CIPN is reflected in a specific pattern of changes in the regulation of $[Ca^{2+}]_i$ in subpopulations of cutaneous neurons and argue against a prevailing hypothesis that nerve length can account for the manifestation of CIPN.

2.2 METHODS

2.2.1 Animals

Adult (250-320g) male Sprague-Dawley rats (Harlan, Indianapolis, IN) were used for all experiments. Rats were housed two per cage in a temperature and humidity controlled, Association for Assessment and Accreditation of Laboratory Animal Care International (AAALAC) accredited animal housing facility on a 12h:12h light:dark schedule with food and water available *ad libitum*. All procedures were approved by the University of Pittsburgh Institutional Animal Care and Use Committee and performed in accordance with National Institutes of Health guidelines for the use of laboratory animals in research.

2.2.2 Tissue Labeling

1,1'-dioctadecyl-3,3,3',3'-tetramethylindocarbocyanine perchlorate (DiI) was injected intradermally at three different locations, one per animal, so as to label subpopulations of cutaneous afferents identified based on the target of innervation. These sites included the glabrous skin of the hind paw, the hairy skin on the dorsal side of the hind paw, and the hairy skin of the upper inner thigh. DiI was injected with a 30 g needle under isoflurane (Abbott Laboratories, North Chicago, IL) anesthesia at 3-5 sites per target for a total volume of 10 μ L in the dorsal and ventral hindpaw and 20 μ L in the thigh.

2.2.3 Paclitaxel Treatment

One week following the DiI injection, rats were anesthetized with isoflurane and injected into the tail vein with 2 mg/kg paclitaxel or its vehicle (1:1:23, cremophor EL:ethanol:0.9% saline). The tail vein injection was repeated three more times every other day for a total of four injections.

2.2.4 Behavioral Assessment of Mechanical Hypersensitivity

All behavioral data were collected in the Rodent Behavior Analysis Core of the University of Pittsburgh Schools of Health Sciences. Rats were habituated to the testing procedure, equipment, and the experimenter for two to three days before the collection of baseline data. An electronic von Frey (IITC Plantar Test Analgesia Meter 2390; IITC Life Sciences Inc., Woodland Hills, CA) fitted with a rigid tip (1.0-mm tip diameter) was used to assess changes in mechanical threshold. For assessment of changes in mechanical threshold in the glabrous skin, rats were placed in acrylic clear boxes on an aluminum mesh, which were separated by opaque dividers and, the tip was applied to the center of the middle of the hind paw from below with steady vertical pressure until the paw was lifted off the mesh floor. For assessment of mechanical threshold on the dorsal side of the hindpaw, rats were gently restrained in cotton socks cut so that their hind legs and tail protruded from the back. This enabled application of the mechanical probe in a manner comparable to that used for the glabrous skin of the hindpaw, perpendicular to the plane of the skin. Mechanical threshold was assessed in a similar manner at mid-thigh following removal of the hair covering the thigh, and placement of a spot on the target for mechanical probing with a permanent marker. Mechanical sensitivity was assessed at each site

three times each day with an inter-stimulus interval of 5 minutes, and the average of the three measures for each paw or thigh was considered the withdrawal threshold. While the investigator collecting behavioral data was blinded to treatment group, the weight loss in the paclitaxel treated animals made blinding difficult through the entire testing period.

2.2.5 Sensory Neuron Isolation

Rats were deeply anesthetized with an intraperitoneal injection (1 ml/kg) of an anesthetic cocktail containing ketamine (55 mg/kg), xylazine (5.5 mg/kg) and acepromazine (1.1 mg/kg). L4 and L5 DRGs were removed bilaterally, enzymatically treated, and mechanically dissociated. DRG neurons were plated on laminin (Invitrogen, 1mg/ml) and poly-L-ornithine (Sigma-Aldrich, 1 mg/ml) coated glass cover slips as previously described (Lu et al., 2006). All subsequent experiments were performed within 8 h of tissue harvest. Only neurons containing the retrograde label DiI were included for further analysis.

2.2.6 Ca²⁺ Imaging

Prior to fluoremetric analysis, neurons were incubated with 2.5 μ M Ca²⁺ indicator fura-2 AM ester with 0.025 % Pluronic F-127 for 20 min at room temperature. Neurons were then incubated with FITC-conjugated IB4 (10 μ g/ml) for 10 min at room temperature, placed in a recording chamber and continuously superfused with a HEPES-buffered bath solution consistent of (in mM): 130 NaCl, 3 KCl, 2.5 CaCl₂, 0.6 MgCl₂, 10 4-(2-Hydroxyethyl)piperazine-1-ethanesulfonic acid, N-(2-Hydroxyethyl)piperazine-N'-(2-ethanesulfonic acid) (HEPES), 10 glucose, pH 7.4, osmolality 325 mOsm. Fluorescence data were acquired on a PC running

Metafluor software (Molecular Devices, Sunnyvale, CA) via an EMCCD camera (Photometrics, Tucson, AZ; model QuantEM 512SC). The ratio (R) of fluorescence emission (510 nm) in response to 340/380nm excitation (controlled by a DG-4 (Sutter Instrument, Novato, CA)) was acquired at 1 Hz during application of KCl or capsaicin, which were applied through a computer-controlled, piezo-driven perfusion system (switching time <20 ms; Warner Instruments, Hamden, CT, USA, Fast-Step Model SF-77B). $[Ca^{2+}]_i$ was determined from fura-2 ratio according to the equation $[Ca^{2+}]_i$ (nM) = $K_d (S_{f2}/S_{b2}) ((R-R_{min})/(R_{max}-R))$ following *in situ* calibration as described previously (Scheff et al., 2013), where K_d is the dissociation constant for fura-2 for Ca^{2+} at room temperature; S_{f2}/S_{b2} is the fluorescence ratio of the emission intensity excited by 380 nm signal in the absence of Ca^{2+} ; R_{min} and R_{max} are the minimal and maximal fluorescence ratios respectively.

2.2.7 Chemicals

Paclitaxel (Sigma-Aldrich, St Louis, MO, USA), was dissolved at 25 mg/mL in 1:1 Cremophor EL: ethanol and freshly diluted 1:12.5 in 0.9% sterile saline prior to injections. The retrograde tracer, DiI (Invitrogen, Carlsbad, CA, USA), was dissolved at 170 mg/mL in dimethylsulfoxide (DMSO, Sigma-Aldrich) and diluted 1:10 in 0.9% sterile saline. FITC-conjugated Isolectin B4 (IB4, Sigma-Aldrich) was dissolved in dH₂O as a stock solution of 1 mg/ml, and then diluted to a final concentration of 5 μ g/ml in HEPES bath solution the day of use. Fura-2 acetoxymethyl (AM) ester (TEF Laboratories, Austin, TX, USA) was dissolved in DMSO as a 2.5 mM stock solution and diluted to a final concentration of 2.5 μ M in HEPES bath solution. Pluronic F-127 (TEF Laboratories) was dissolved in DMSO as a 25% stock solution and diluted to 0.025% in

HEPES bath solution. Capsaicin (Sigma-Aldrich) was dissolved in ethanol as a 10 mM stock solution and diluted to 500 nM in HEPES bath solution.

2.2.8 Data Analysis

Neurons from a single field were studied on each coverslip. Resting Ca^{2+} was determined prior to stimulation and was taken as the average of measurements taken over the 30 second prior to evoking a Ca^{2+} transient with high K^+ (30 mM, 4 seconds). The magnitude of the evoked Ca^{2+} transient was determined as the difference between resting and the peak of the evoked Ca^{2+} transient. The duration of the evoked Ca^{2+} transient was determined as the time for the transient to decay to 50% of the peak (T50). For experiments involving the application of test compounds, a vehicle control group was always included. Data are expressed as mean \pm s.e.m. One and two-way ANOVA were used for analysis of more than two groups with the Holm-Sidak test used for post-hoc analysis. Statistical significance was assessed at $p < 0.05$. Group sizes were determined by a power analysis which was based on the variability in T50 observed in putative nociceptive glabrous skin neurons from three naïve rats. With a power of 0.8, alpha of 0.05, and the standard six groups included in most experiments, with groups defined by target of innervation and paclitaxel treatment, we estimated the need for a group size of 47 neurons to enable us to detect a difference between groups of 50%.

2.3 RESULTS

2.3.1 Paclitaxel-Induced Mechanical Hypersensitivity

The rat model of CIPN used in the present study has been well described (Polomano et al., 2001, Flatters and Bennett, 2006, Xiao et al., 2008, Boyette-Davis et al., 2011a). However, despite the fact that clinical manifestation of CIPN is largely restricted to the feet and hands (Dougherty et al., 2004, Boyette-Davis et al., 2013), and in particular, the glabrous skin of the feet and hands (Dougherty et al., 2004, Pachman et al., 2011), assessment of mechanical and thermal sensitivity has largely be restricted to the hindpaw (Flatters and Bennett, 2006, Xiao et al., 2008, Boyette-Davis et al., 2011a). We therefore sought to determine the extent to which the pattern of hypersensitivity in the rat model parallels that observed clinically. Consistent with previous results (Polomano et al., 2001, Flatters and Bennett, 2006), mechanical hypersensitivity was readily detectable on the glabrous skin of the hindpaw with a significant decrease in threshold observed by the second paclitaxel injection (Figure 1A). In contrast, however, no detectable change in threshold was observed on the hairy skin of the hindpaw (Figure 1B) or the inner thigh (Figure 1C).

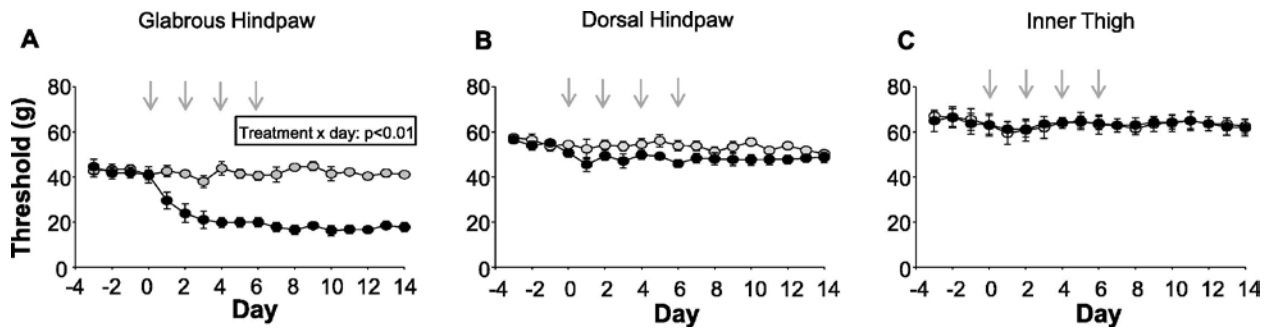


Figure 1. Paclitaxel-Induced Mechanical Hypersensitivity. Paclitaxel (2mg/kg per treatment, black circles) induced mechanical hypersensitivity in the glabrous skin of the hindpaw (A) but not in the hairy skin of the dorsal hindpaw (B) or inner thigh (C), as assessed with an electronic Von Frey device. No changes in mechanical threshold were observed in vehicle treated (grey circles) animals. Paclitaxel/vehicle were administered at the points indicated with gray arrows n = 7 per group.

2.3.2 The impact of target of innervation on resting and evoked intracellular calcium concentration $[Ca^{2+}]_i$ in putative nociceptive cutaneous neurons

Given evidence that dysregulation of $[Ca^{2+}]_i$ in subpopulations of nociceptive neurons may contribute to the manifestation of mechanical hypersensitivity (Kawano et al., 2009), we first sought to determine whether differences among subpopulations of nociceptive neurons defined by target of innervation may contribute to the selective manifestation of paclitaxel-induced hypersensitivity. Putative nociceptive neurons were identified based on cell body size (Lawson, 2002), IB4 binding (Fang et al., 2006) binding, and sensitivity to the algogenic compound, capsaicin (Holzer, 1991). Resting and evoked Ca^{2+} transients (magnitude and decay) were assessed as illustrated in Figure 2A. In putative nociceptive cutaneous neurons from naïve rats, there was a significant ($p < 0.01$, One-way ANOVA) difference between subpopulations defined by target of innervation in the resting $[Ca^{2+}]_i$, due to the level of Ca^{2+} in neurons innervating the

thigh, which was significantly lower than that in neurons innervating the hairy ($p < 0.01$) or glabrous ($p < 0.01$) skin of the hindpaw (Figure 2B). However, magnitude (Figure 2C) and duration (Figure 2D) of the high K^+ evoked transient were comparable between subpopulations ($p > 0.05$).

While there was no detectable influence of the paclitaxel vehicle on nociceptive threshold, even relatively simple solvents, such as DMSO can influence a variety of cellular processes. More importantly, there is evidence suggesting that the paclitaxel vehicle may be responsible for some of the side effects of the chemotherapy treatment (Gelderblom et al., 2001, Ahn et al., 2014). We therefore assessed the impact of vehicle on resting $[Ca^{2+}]_i$ and evoked transients in subpopulations of putative nociceptive neurons defined by target of innervation. Neurons from vehicle treated animals were harvested 14 days after the first IV administration. Data were analyzed with a two-way ANOVA. While there was a main effect associated with target of innervation ($p < 0.01$, Figure 2B) on resting $[Ca^{2+}]_i$, there was no detectable influence of vehicle on the resting $[Ca^{2+}]_i$ or the magnitude (Figure 2C) and duration (Figure 2D) of the evoked Ca^{2+} transient among subpopulations of cutaneous neurons. Data from naïve and vehicle treated animals was therefore pooled for subsequent analyses and are referred to as control neurons.

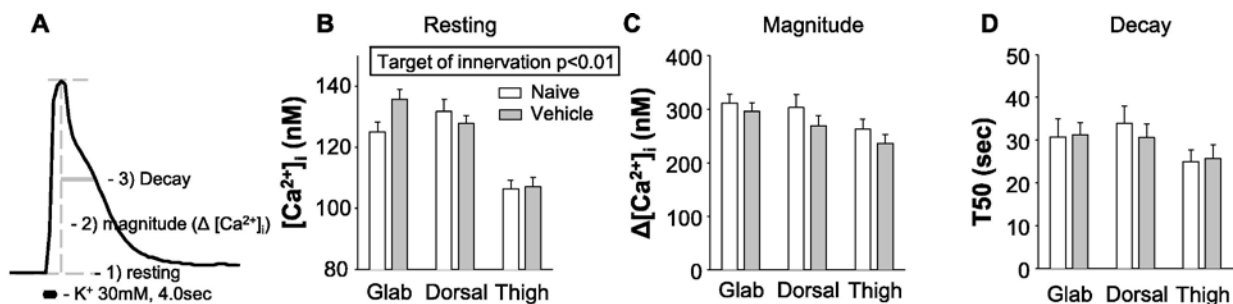


Figure 2. The impact of target of innervation on resting and evoked intracellular calcium concentration [Ca²⁺]_i in putative nociceptive cutaneous neurons. Resting and evoked Ca²⁺ transients from putative nociceptive DRG neurons defined by target of innervation from naïve rats or rats treated with the paclitaxel vehicle (cremophor EL: ethanol 1:1, diluted 1/12.5 with saline). A) Typical Ca²⁺ transient evoked with 30 mM K⁺ in a putative nociceptive neuron labeled from the glabrous skin. Features of the Ca²⁺ transient subsequently analyzed are indicated. Pooled data from naïve and vehicle treated rats were analyzed with a two-way ANOVA. B) While there was no detectable influence of vehicle on resting [Ca²⁺]_i in subpopulations of putative nociceptive neurons defined by target of innervation, there was a main effect of target of innervation on this parameter. There was no detectable influence of either vehicle treatment of target of innervation on either the magnitude (C) or decay (D) of the evoked Ca²⁺ transient. Glab (glabrous skin of the hindpaw), Dorsal (dorsal skin of the hindpaw) and Thigh (thigh skin of the hindleg) refer to targets of innervation. Numbers of neurons in each group are naïve glabrous = 38, vehicle glabrous = 53, naïve dorsal = 27, vehicle dorsal = 23, naïve thigh = 30, vehicle thigh = 32).

2.3.3 Paclitaxel attenuates the duration of the evoked Ca²⁺ transient in putative nociceptors

We next sought to determine whether changes in resting [Ca²⁺]_i or evoked Ca²⁺ transients in putative nociceptive cutaneous neurons could account for the pattern of changes in mechanical sensitivity. Data were again analyzed with a two-way ANOVA, in which the impact of target of innervation and paclitaxel treatment were compared. While the main effect ($p < 0.01$) associated

with target of innervation persisted on resting Ca^{2+} , there was no significant influence of paclitaxel treatment, or a significant interaction between paclitaxel treatment and target of innervation on this parameter (Figure 3A and B). There was no detectable influence of either paclitaxel or target of innervation, or an interaction between the two, on the magnitude of the evoked Ca^{2+} transient (Figure 3A and C). However, there was a significant interaction between target of innervation and paclitaxel treatment on the duration of the evoked Ca^{2+} transient (Figure 3A and D). Post-hoc analysis indicated that the duration was significantly shorter in neurons innervating the glabrous ($p < 0.01$) and hairy skin of the hindpaw ($p < 0.05$) obtained from paclitaxel compared to control rats (Figure 3D). To determine whether there were differences between groups of putative nociceptive cutaneous neurons defined by target of innervation with respect to the paclitaxel-induced decrease in the duration of the evoked Ca^{2+} transient, T50 data from paclitaxel treated rats were analyzed as a percent of that in control neurons. Pooled data (Figure 3E) were analyzed with a one-way ANOVA that indicated there was a significant difference between groups ($p < 0.01$). Post-hoc analysis showed that while there was no difference between hairy hindpaw and thigh skin neurons with respect to the paclitaxel-induced decrease in T50, the decrease in the duration of the evoked transient in putative nociceptive glabrous skin neurons was significantly greater than that in hairy hindpaw or thigh skin neurons (Figure 3E).

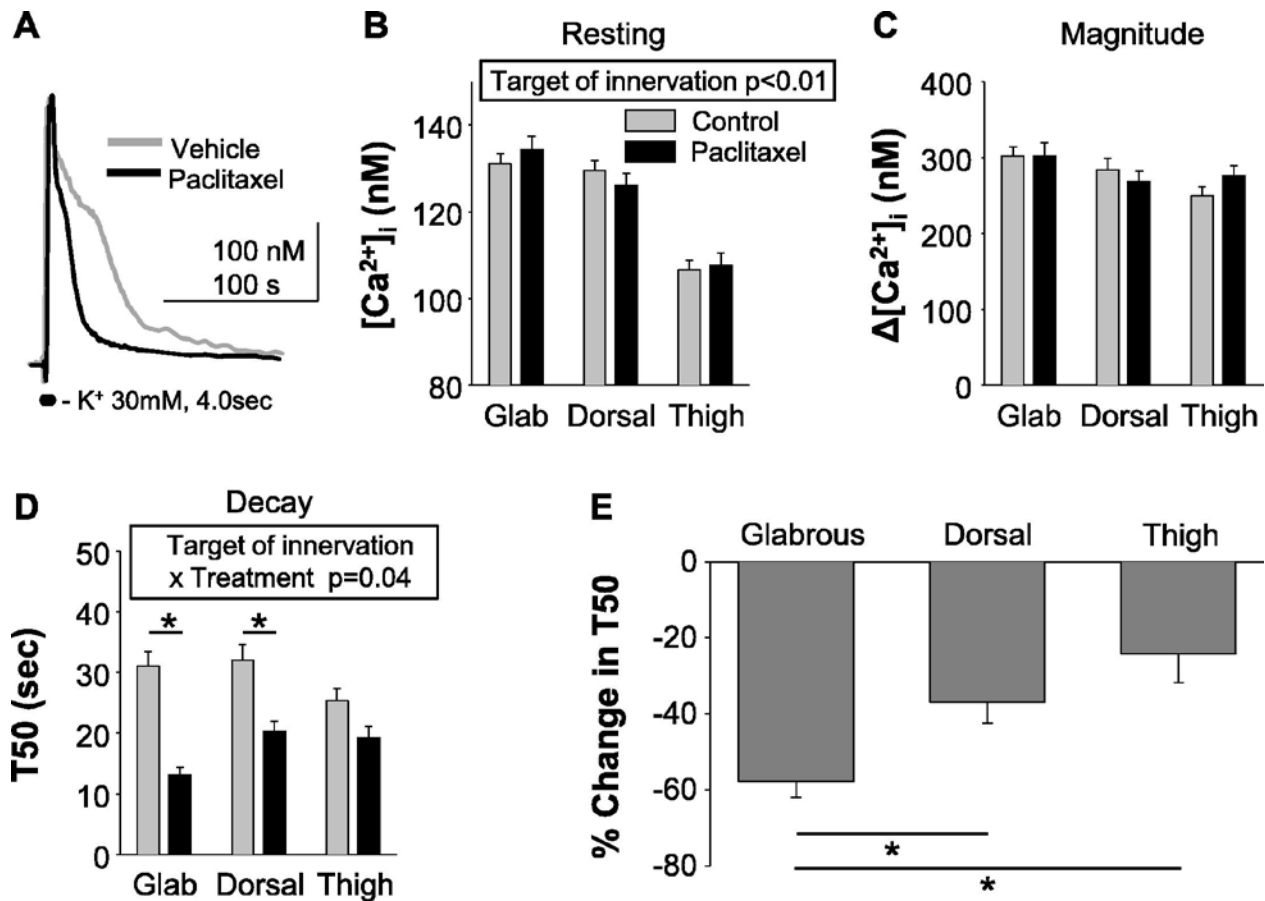


Figure 3. Paclitaxel attenuates the duration of the evoked Ca²⁺ transient in putative nociceptors. Resting and evoked Ca²⁺ transients from putative nociceptive DRG neurons defined by target of innervation from control (naïve and vehicle treated) rats or rats treated with paclitaxel. A) Typical high K⁺ (30 mM) evoked Ca²⁺ transients from putative nociceptive DRG neurons innervating glabrous skin of the hindpaw from rats treated with either vehicle or paclitaxel. Pooled data were analyzed as in Figure 2. B) While the main effect of target of innervation on resting [Ca²⁺]_i, persisted, there was no detectable influence of paclitaxel on this parameter. C) There was also no detectable influence of paclitaxel on the magnitude of the evoked Ca²⁺ transient. D) However, there was a significant interaction between target of innervation and paclitaxel treatment on the duration of the evoked Ca²⁺ transient. Post-hoc analysis confirmed that the decrease in the duration of the evoked Ca²⁺ transient in both glabrous and hindpaw hairy skin (Dorsal) neurons were significant. To determine whether there was a difference between groups defined by target of innervation with respect to the size of the paclitaxel-induced decrease in duration, data from paclitaxel treated neurons were analyzed as a percent change from control. These data (E), were analyzed with a one-way ANOVA, which confirmed that the difference between groups was significant (p < 0.01). Post-hoc analysis

confirmed the decrease in the glabrous neurons was significantly greater than that in neurons from either the dorsal hindpaw or thigh. Numbers of neurons in each group are control glabrous = 91, paclitaxel glabrous = 44, control dorsal = 50, paclitaxel dorsal = 33, control thigh = 62, paclitaxel thigh = 47; * $p < 0.05$).

2.3.4 Paclitaxel does not affect the resting or evoked Ca^{2+} transient properties in putative non-nociceptive sensory neurons.

While we were focused on mechanisms that may contribute to the paclitaxel-induced decrease in mechanical threshold, the first sign of CIPN is numbness and tingling, thought to reflect changes in non-nociceptive afferents (Dougherty et al., 2004). We therefore assessed the impact of paclitaxel on resting $[\text{Ca}^{2+}]_i$ and evoked Ca^{2+} transients in putative non-nociceptive cutaneous neurons defined by a relatively large cell body diameter, the absence of IB4 binding and insensitivity to capsaicin. Consistent with results from unlabeled DRG neurons (Lu et al., 2006), evoked Ca^{2+} transients in putative non-nociceptive cutaneous neurons were smaller and decayed more rapidly than those in putative nociceptive neurons (Figure 4A). Nevertheless, two-way ANOVA analysis of pooled data from control and paclitaxel-treated rats indicated that there were no significant interactions between target of innervation and paclitaxel treatment on resting Ca^{2+} (Figure 4B), the magnitude (Figure 4C), or the duration (Figure 4D) of the evoked transient. There was, however, a main effect of target of innervation on both the resting Ca^{2+} (Figure 4B) and the magnitude of the evoked Ca^{2+} transient (Figure 4C), which were significantly lower in thigh neurons than neurons innervating hindpaw hairy or glabrous skin.

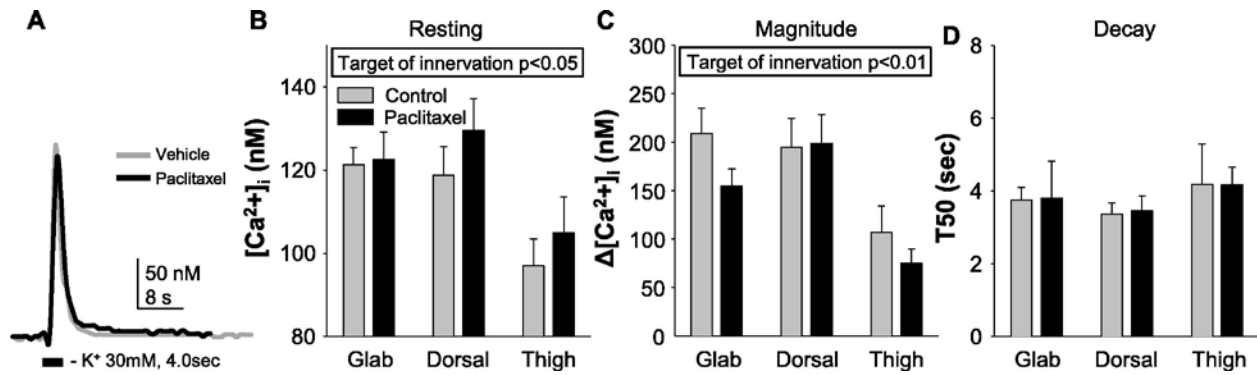


Figure 4. Paclitaxel does not affect the resting or evoked Ca^{2+} transient properties in putative non-nociceptive sensory neurons. Resting and evoked Ca^{2+} transients from putative non-nociceptive DRG neurons defined by target of innervation from control rats or rats treated with paclitaxel. A) Typical evoked Ca^{2+} transients from putative non-nociceptive DRG neurons innervating glabrous skin of the hindpaw from rats treated with either vehicle or paclitaxel. Pooled data were analyzed as described in Figure 2. B) While there was no detectable influence of paclitaxel treatment on resting $[Ca^{2+}]_i$, there was a significant effect of target of innervation on this parameter. C) There was also a significant main effect of target of innervation on the magnitude of the high K^+ evoked Ca^{2+} transient in putative non-nociceptive neurons. D) However, there was no detectable influence of either treatment or target of innervation on the duration of the high K^+ evoked Ca^{2+} transient in these neurons. Numbers of neurons in each group are control glabrous = 14, paclitaxel glabrous = 10, control dorsal = 15, paclitaxel dorsal = 8, control thigh = 9, paclitaxel thigh = 8).

2.4 DISCUSSION

The purpose of the present study was to begin to test the hypothesis that the unique manifestation of CIPN is due to unique properties of afferents defined by target of innervation, in particular, those involved in the regulation of $[Ca^{2+}]_i$. Towards this end, we provided further support for the validity of the rat paclitaxel model of CIPN, which was associated with mechanical hypersensitivity in the glabrous skin of the hindpaw, but not the hairy skin of the hindpaw or mid-thigh. Differences among subpopulations of sensory neurons from naïve animals defined by target of innervation were relatively small and included a lower resting $[Ca^{2+}]_i$ in both putative nociceptive and non-nociceptive neurons innervating the thigh, as well as a smaller magnitude of depolarization-evoked Ca^{2+} transient in putative non-nociceptive thigh skin afferents. And while paclitaxel had no detectable influence on resting $[Ca^{2+}]_i$, or the magnitude or duration of the depolarization-evoked Ca^{2+} transient in subpopulations of non-nociceptive afferents defined by target of innervation, it was associated with a significant decrease in the duration of the evoked transient in putative nociceptive afferents. This change was significantly larger in neurons innervating glabrous skin than those innervating hairy skin of the hindpaw or thigh. These results suggest that subpopulation and target of innervation are important factors determining the susceptibility and degree of dysregulation of $[Ca^{2+}]_i$, by paclitaxel treatment.

Our behavioral results indicate that the paclitaxel-induced mechanical hypersensitivity is associated with the type of target tissue (glabrous vs. hairy skin) rather than the axonal length. Previously, axonal length was thought to determine the presence of pain symptoms of paclitaxel-induced neuropathy due to the microtubule stabilizing action of paclitaxel presumably disrupting axonal transport and eventually leading to peripheral axon damage (Gornstein and Schwarz, 2014). Arguing against this proposal, however, is the observation that there are relatively minor

differences among chemotherapeutics with respect to the resulting CIPN phenotype despite the fact that the antineoplastic efficacy of different chemotherapeutics is due to completely different mechanisms such as proteasome inhibition, DNA alkylation, topoisomerase inhibition (Jaggi and Singh, 2012). Furthermore, our results are consistent with data obtained from chemotherapy patients, where painful symptoms of CIPN are confined in the glabrous surfaces and rarely occur in the hairy surfaces of hands and feet of most patients (Dougherty et al., 2004, Pachman et al., 2011). If target of innervation plays a more dominant role in the manifestation of CIPN than axon length, it will be necessary to re-evaluate several of the leading hypotheses concerning the mechanisms of CIPN.

While the differences between subpopulations of neurons defined by target of innervation were relatively small, the presence of differences among subpopulations of cutaneous neurons underscores the impact of target of innervation of afferent properties. Differences based on target of innervation are consistent with our own previous results (Gold and Traub, 2004, Harriott et al., 2006, Harriott and Gold, 2009, Vaughn and Gold, 2010) as well as the results of others (Yoshimura et al., 2003, Beyak et al., 2004, Malin et al., 2011), although differences appear to be most pronounced under pathological conditions, such as the presence of inflammatory mediators (Gold and Traub, 2004, Vaughn and Gold, 2010) or persistent inflammation (Harriott et al., 2006, Zhang et al., 2012b). Minimally, these data suggest that target of innervation must be taken into consideration when analyzing the properties of putative nociceptive and non-nociceptive afferents.

A paclitaxel-induced decrease in the duration of the evoked Ca^{2+} transient was surprising given the evidence for an increase in the duration of the evoked Ca^{2+} transient in putative nociceptive neurons from rats with diabetic neuropathy (Kostyuk et al., 2001), a neuropathic pain

syndrome that is also manifest in a stocking-glove distribution, as well as changes obtained with models of inflammatory pain, characterized by an increase in magnitude and duration of evoked Ca^{2+} transient (Lu and Gold, 2008, Scheff et al., 2013, Scheff and Gold, 2014). We predicted changes comparable to those observed in the persistent inflammation model based on previous results indicating that paclitaxel-induced neuropathic pain is associated with upregulation of proinflammatory cytokines and induction of TLR4-mediated signaling cascades (Ledeboer et al., 2007, Li et al., 2014). The difference between our results and the changes described in these other models could be due to the differences between models with respect to the site of release and/or the actions of specific combination of inflammatory mediators released (Ledeboer et al., 2007, Zhang et al., 2012a). More generally, however, the differences between models indicate that the pattern of changes in the regulation of $[\text{Ca}^{2+}]_i$ in sensory neurons are relatively specific to the site and nature of the nerve injury.

It is possible that the paclitaxel-induced changes in the regulation of $[\text{Ca}^{2+}]_i$ in putative nociceptive afferents are not directly responsible for the mechanical hypersensitivity observed. For example, the decrease in the duration of the evoked Ca^{2+} transient could be a compensatory response to the mitotoxic effects of paclitaxel. In this case, facilitating the decrease in the duration of the evoked Ca^{2+} transient may be beneficial for increasing the health and survival of these neurons. Alternatively, it is reasonable to speculate that a decrease in the evoked Ca^{2+} transient will increase the excitability of putative nociceptive cutaneous neurons given the importance of Ca^{2+} -dependent K^+ (BK) channels in the regulation of excitability of this population of afferents (Chen et al., 2009, Zhang et al., 2010). However, the observation that there was a significant decrease in the duration of the evoked Ca^{2+} transient in putative nociceptive neurons innervating the hairy skin of the hindpaw, a tissue in which we detected no

decrease in mechanical threshold, suggests that if there is a relationship between the decrease in the duration of the evoked Ca^{2+} transient and nociceptive threshold, it is not so simple. There are at least two potentially complicating factors in this relationship: 1) it is possible that because of the biophysical properties of the BK channel and/or the spatial distribution of the channel relative to Ca^{2+} sources in the terminal, the decrease in the evoked Ca^{2+} transient must reach a threshold before a decrease in BK activity is manifest, and 2) there is a differential distribution of Ca^{2+} -dependent channels in glabrous and hairy skin.

While it will be important to determine the mechanism(s) responsible for the paclitaxel-induced decrease in the duration of the evoked Ca^{2+} , available evidence suggests that this change is likely to be orchestrated by several different Ca^{2+} -regulatory mechanisms rather than a simple change in influx, release, extrusion, or re-uptake. For example, the persistent inflammation-induced increase in the magnitude and duration of the evoked Ca^{2+} transient (Lu and Gold, 2008), is associated with a decrease in voltage-gated Ca^{2+} current (Lu et al., 2010), a decrease in sodium/calcium exchanger (NCX) activity, secondary to selective trafficking of NCX to peripheral terminals (Scheff and Gold, 2014), and at least one more mechanism accounting for the increase in the magnitude of the evoked Ca^{2+} transient. With evidence that Ca^{2+} influx, re-uptake, release and extrusion mechanisms may all be functionally isolated, even in an isolated cell body (Scheff et al., 2013), a simple shift in the coupling of Ca^{2+} regulatory mechanisms could account for the paclitaxel-induced decrease in the duration of the evoked Ca^{2+} transient. Ongoing investigations are focused on teasing apart the relative contribution of the various Ca^{2+} regulatory mechanisms to the paclitaxel effects observed.

In conclusion, our results suggest that axon length alone does not account for the stocking-glove distribution of CIPN. Rather, our results are consistent with our central

hypothesis and suggest that the unique distribution of symptoms associated with CIPN are due to an interaction between the toxic effects of paclitaxel and unique properties of subpopulations of afferents defined by target of innervation. Identification of mechanisms responsible for the apparent vulnerability of glabrous skin neurons and/or the resistance of hairy skin neurons to the toxic effects of paclitaxel may suggest novel therapeutic approaches for the treatment, if not prevention of CIPN.

3.0 PACLITAXEL-INDUCED INCREASE IN NCX ACTIVITY IN SUBPOPULATIONS OF NOCICEPTIVE AFFERENTS: A PROTECTIVE MECHANISM AGAINST CHEMOTHERAPY-INDUCED PERIPHERAL NEUROPATHY?

3.1 INTRODUCTION

Chemotherapeutic-induced peripheral neuropathy (CIPN) is a painful condition mainly restricted to the hands and feet (Dougherty et al., 2004). We have recently shown that a rat model of CIPN is associated with a significant decrease in the duration of the depolarization-evoked Ca^{2+} transients in isolated cell bodies of putative nociceptive afferents, but no changes in the magnitude of the transient, or in resting levels of Ca^{2+} (Yilmaz and Gold, 2015). Moreover, the degree of this change in duration was significantly larger in neurons innervating the glabrous skin of the hindpaw, than those targeting the hindpaw hairy skin or the inner thigh where no change in transient duration was detected. Interestingly, paclitaxel-induced mechanical hypersensitivity was only detected in the glabrous skin (Yilmaz and Gold, 2015). These data indicate the presence of a subpopulation-specific dysregulation of Ca^{2+} caused by paclitaxel treatment in this model.

The purpose of the present study was to test the hypothesis that increased activity of the Na^+ - Ca^{2+} exchanger (NCX) is the underlying mechanism for the paclitaxel-induced changes in

the evoked Ca^{2+} duration. This hypothesis was based on several observations: 1) NCX is a major Ca^{2+} extrusion mechanism, but with a low affinity for Ca^{2+} , it is only activated with relatively high $[\text{Ca}^{2+}]_i$ such as during depolarization-induced Ca^{2+} transients (Blaustein and Lederer, 1999, DiPolo and Beauge, 2006). In the sensory neuron cell soma, NCX plays a major role in the regulation of the duration of the evoked Ca^{2+} with no influence on transient magnitude (Lu et al., 2006, Scheff et al., 2014). Consequently, NCX has the biophysical properties in DRG neurons to account for the selective paclitaxel-induced changes in the evoked Ca^{2+} transient. 2) Among sensory neurons, NCX is active only in putative nociceptive neurons (Lu et al., 2006, Scheff et al., 2014), the same subpopulation in which we observed the paclitaxel-induced decrease in the evoked Ca^{2+} transient duration (Yilmaz and Gold, 2015). 3) There is evidence that a change in NCX activity is associated with inflammatory hypersensitivity, albeit, a decrease in NCX activity (Scheff et al., 2014). Thus, given the often opposing cellular response to inflammation and nerve injury (Gold and Gebhart, 2010), it is possible that paclitaxel-induced neuropathy is associated with an increase in NCX activity.

To test this hypothesis, retrograde tracer-labeled, small-diameter, IB4+, capsaicin responsive DRG neurons from naïve, vehicle-treated, and paclitaxel-treated rats were studied with ratiometric Ca^{2+} imaging in combination with a variety of pharmacological manipulations. Our results suggest that the paclitaxel-induced decrease in the duration of the evoked Ca^{2+} transient is not due to an increase in NCX activity. However, both vehicle and paclitaxel treatments were associated with NCX sensitization. A compensatory Ca^{2+} regulatory mechanism was also present in afferents innervating target areas where there was no detectable evidence of a chemotherapy-induced change in mechanical sensitivity. Furthermore, paclitaxel treatment affects NCX subtypes differentially based on target of innervation.

3.2 METHODS

3.2.1 Animals

Adult (250-320g) male Sprague-Dawley rats (Harlan, Indianapolis, IN) were used for all experiments. Rats were housed two per cage in a temperature and humidity controlled, Association for Assessment and Accreditation of Laboratory Animal Care International (AAALAC) accredited animal housing facility on a 12h:12h light:dark schedule with food and water available *ad libitum*. All procedures were approved by the University of Pittsburgh Institutional Animal Care and Use Committee and performed in accordance with National Institutes of Health guidelines for the use of laboratory animals in research.

3.2.2 Tissue labeling

1,1'-dioctadecyl-3,3,3',3'-tetramethylindocarbocyanine perchlorate (DiI) was injected intradermally at three different sites, one location per animal, so as to label subpopulations of cutaneous afferents identified based on the target of innervation. These sites included the glabrous skin of the hind paw, the hairy skin on the dorsal side of the hind paw, and the hairy skin of the upper inner thigh. The hair covering the thigh was removed with an electrical shaver before retrograde labeling. DiI was injected with a 30 g needle under isoflurane (Abbott Laboratories, North Chicago, IL) anesthesia at 3-5 sites per target for a total volume of 10 μ L in the dorsal and ventral hindpaw and 20 μ L in the thigh.

3.2.3 Paclitaxel treatment

One week following the DiI injection, rats were anesthetized with isoflurane and received 2 mg/kg paclitaxel or its vehicle (1:1:23, cremophor EL:ethanol:0.9% saline) via the tail vein. The tail vein injection was repeated three more times every other day for a total of four injections.

3.2.4 Sensory Neuron Isolation

Rats were deeply anesthetized with an intraperitoneal injection (1 ml/kg) of an anesthetic cocktail containing ketamine (55 mg/kg), xylazine (5.5 mg/kg) and acepromazine (1.1 mg/kg). L4 and L5 DRGs were removed bilaterally, enzymatically treated, and mechanically dissociated. DRG neurons were plated on laminin (Invitrogen, 1mg/ml) and poly-L-ornithine (Sigma-Aldrich, 1 mg/ml) coated glass cover slips as previously described (Lu et al., 2006). All subsequent experiments were performed within 8 h of tissue harvest. Only neurons containing the retrograde label DiI were included for further analysis.

3.2.5 Ca²⁺ Imaging

Neurons were first incubated with 2.5 μ M Ca²⁺ indicator fura-2 AM ester with 0.01 % Pluronic F-127 for 20 min at room temperature. Neurons were then incubated with FITC-conjugated IB4 (5 μ g/ml) for 10 min at room temperature. Following labeling, neurons were placed in a recording chamber and continuously superfused with a HEPES-buffered bath solution (HBS) consisting of (in mM): 130 NaCl, 3 KCl, 2.5 CaCl₂, 0.6 MgCl₂, 10 HEPES, 10 glucose, pH 7.4, osmolality 325 mOsm. Fluorescence data were acquired on a PC running Metafluor software

(Molecular Devices, Sunnyvale, CA) via an EMCCD camera (Photometrics, Tucson, AZ; model QuantEM 512SC). The ratio (R) of fluorescence emission (510 nm) in response to 340/380nm excitation (controlled by a DG-4 (Sutter Instrument, Novato, CA)) was acquired at 1 Hz during application of KCl or capsaicin, which were applied through a computer-controlled, piezo-driven perfusion system (switching time <20 ms; Warner Instruments, Hamden, CT, USA, Fast-Step Model SF-77B). The concentration of intracellular Ca^{2+} ($[\text{Ca}^{2+}]_i$) was determined from fura-2 ratio according to the equation $[\text{Ca}^{2+}]_i \text{ (nM)} = K_d (S_{f2}/S_{b2}) ((R-R_{\min})/(R_{\max}-R))$ following *in situ* calibration as described previously (Scheff et al., 2013), where K_d is the dissociation constant for fura-2 for Ca^{2+} at room temperature (224 nM); S_{f2}/S_{b2} is the fluorescence ratio of the emission intensity excited with the 380 nm wavelength in the absence of Ca^{2+} to that in the presence of saturating Ca^{2+} ; R_{\min} and R_{\max} are the minimal and maximal fluorescence ratios, respectively. S_{f2}/S_{b2} , R_{\min} and R_{\max} were determined empirically with calibration runs as described previously (Kao, 1994), run periodically throughout the data collection period.

3.2.6 Chemicals

The retrograde tracer, DiI (Invitrogen, Carlsbad, CA, USA), was dissolved at 170 mg/mL in dimethylsulfoxide (DMSO, Sigma-Aldrich, St Louis, MO, USA) and diluted 1:10 in 0.9% sterile saline. Paclitaxel (Sigma-Aldrich), was dissolved at 25 mg/mL in 1:1 Cremophor EL (Sigma-Aldrich): ethanol and freshly diluted 1:12.5 in 0.9% sterile saline prior to injections. FITC-conjugated Isolectin B4 (IB4, Sigma-Aldrich) was dissolved in dH_2O as a stock solution of 1 mg/ml, and then diluted to a final concentration of 10 $\mu\text{g}/\text{ml}$ in HBS the day of use. Fura-2 acetoxymethyl (AM) ester (TEF Laboratories, Austin, TX, USA) was dissolved in DMSO as a 2.5 mM stock solution and diluted to a final concentration of 2.5 μM in HBS. Pluronic F-127

(TEF Laboratories) was dissolved in DMSO as a 20% stock solution and diluted to 0.01% in HBS. Capsaicin (Sigma-Aldrich) was dissolved in ethanol as a 10 mM stock solution and diluted to 500 nM in HBS. LiCl (Sigma-Aldrich) was used to replace NaCl in HBS. KB-R7943 mesylate (Tocris, Bristol, UK) was dissolved in DMSO as a 100 mM stock solution and diluted to 100 nM in HBS. SEA0400 (ChemScene, Monmouth Junction, NJ, USA) was dissolved in DMSO as a 100 mM stock solution and diluted to 1 μ M in HBS.

3.2.7 Data Analysis

Neurons from a single field were studied on each coverslip. Resting Ca^{2+} was determined prior to stimulation as the average of measurements taken over the 30 second prior to evoking a Ca^{2+} transient with high K^+ (30 mM, 4 seconds). The magnitude of the evoked Ca^{2+} transient was determined as the difference between resting and the peak of the evoked Ca^{2+} transient. The duration of the evoked Ca^{2+} transient was determined as the time for the transient to decay to 50% of the peak (T50). For experiments involving the application of test compounds, a vehicle control group was always included. Neurons with a small cell body diameter (<30 μm) (Lawson, 2002), responsive to capsaicin (500 nM) (Holzer, 1991), and labeled with the lectin IB4 (Fang et al., 2006), were studied and are referred to as putative nociceptors. While there are other subpopulations of putative nociceptors, IB4-negative nociceptors were not included in this study both because we previously failed to detect an influence of paclitaxel on the evoked Ca^{2+} transient in this subpopulation of neurons (Yilmaz and Gold, 2015), and because NCX is restricted to the subpopulation of small diameter, capsaicin responsive, IB4+ neurons (Scheff et al., 2014). Cell body diameter was determined with a calibrated eye-piece reticle. Capsaicin sensitivity was assessed at the end of every experiment and neurons were considered capsaicin

sensitive if application of capsaicin (500 nM, 1 second) resulted in an increase in $[Ca^{2+}]_i$ greater than 20% above baseline. IB4 binding was determined under epifluorescence illumination prior to the start of each experiment. Neurons in which the plasma membrane was clearly defined by epifluorescence were considered IB4+. Data are expressed as mean \pm s.e.m. One and two-way ANOVA were used for analysis of more than two groups with the Holm-Sidak test used for post-hoc analysis. Statistical significance was assessed at $p < 0.05$. The Chi-Square or Fisher exact tests were used to assess the presence of significant differences between groups with respect to the proportion or percentage of neurons with any evidence of NCX activity, or evidence of KB-R7943-sensitive or SEA0400-sensitive NCX activity. Group sizes were determined by power analysis which was based on the variability in the percent increase in T50 observed in putative nociceptive glabrous skin neurons from three naïve rats following block of NCX with Li^+ . This analysis was performed for both a three group experiment, with groups defined only by treatment (naïve, vehicle and paclitaxel) as well as a six group experiment with groups defined by treatment and target of innervation. With a power of 0.8 and $\alpha = 0.05$, we estimated the need for 20 neurons in the first set and 27 in the second.

3.3 RESULTS

3.3.1 NCX does not mediate the paclitaxel-induced attenuation of the depolarization-evoked Ca^{2+} transient duration in putative glabrous nociceptors.

To determine whether paclitaxel-induced attenuation of the evoked Ca^{2+} transients was due to increased NCX activity, we assessed NCX activity in glabrous skin neurons from naïve, vehicle- and paclitaxel-treated rats. We focused on IB4-binding, capsaicin-responsive, small diameter (<30 μm) lumbar DRG neurons that project to the glabrous skin of the hindpaw, because of our previous results indicating that the paclitaxel-induced attenuation of the depolarization-evoked Ca^{2+} transient was manifest in this subpopulation (Yilmaz and Gold, 2015). We blocked NCX activity by replacing Na^+ in HBS with Li^+ taking advantage of the fact that NCX activity requires presence of Na^+ ions in the extracellular environment (Yu and Choi, 1997), and minimal impact that replacing Na^+ with Li^+ has on the functioning of voltage-gated Na^+ channels (Gold and Thut, 2001). The relative increase in the duration of depolarization-evoked Ca^{2+} transient in the presence of Li^+ was assumed to reflect the loss NCX activity, and was therefore used as an indirect measure of NCX activity. Consequently, in neurons from paclitaxel-treated rats, an increase in NCX activity should be associated with a relatively larger increase in the duration of the evoked Ca^{2+} transient following NCX block. Consistent with our previous results (Yilmaz and Gold, 2015), the duration of the high K^+ (30 mM, 4 sec)-evoked Ca^{2+} transient in neurons from paclitaxel-treated rats was shorter than that neurons from vehicle treated rats (Figure 5A and 5B). Further, as expected, in the presence of Li^+ , the duration of the evoked Ca^{2+} transient was increased in neurons from both vehicle- and paclitaxel-treated rats (Figure 5A, solid lines). However, the relative increase in the duration of evoked Ca^{2+} transients was comparable ($p >$

0.05) in neurons from both groups of rats as illustrated when these data were analyzed as a percent change in duration (Figure 5C).

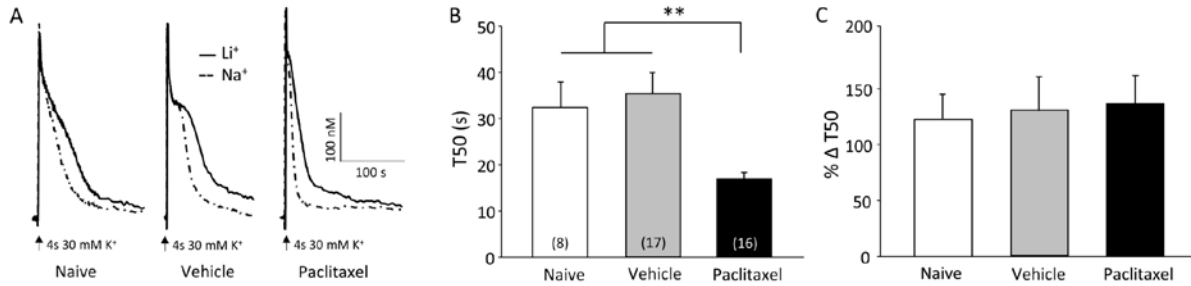


Figure 5. NCX does not mediate the paclitaxel-induced attenuation of the depolarization evoked Ca²⁺ transient duration in putative glabrous nociceptors. Paclitaxel-induced attenuation of the duration of the depolarization-evoked Ca²⁺ transient in putative glabrous nociceptors is not mediated by NCX. A) Ca²⁺ transients evoked with 4s application of 30 mM K⁺ in putative nociceptive neurons labeled from the glabrous skin from naïve (left) vehicle-treated (middle) and paclitaxel-treated (right) rats before (dotted traces) and after (solid traces) block of NCX by exchanging Na⁺ for Li⁺ in the bath solution. The duration of the evoked Ca²⁺ transient was quantified as the time to decay to 50 percent of the magnitude of the evoked Ca²⁺ transient (T50). B) Pooled T50 data from naïve (n = 8), vehicle-treated (n = 17 neurons) and paclitaxel-treated (n = 16 neurons) glabrous skin neurons in Na⁺ bath. C) Relative increase in the duration of evoked Ca²⁺ transients from the same group of neurons in (B) analyzed as a percent increase in T50 following block of NCX with Li⁺. * is p < 0.05.

3.3.2 NCX is sensitized by the vehicle of paclitaxel.

NCX activity not only depends on the extracellular Na⁺ concentration but also on [Ca²⁺]_i. Because NCX has a low affinity for Ca²⁺ (Blaustein and Lederer, 1999), the magnitude and the

duration of the evoked Ca^{2+} transient required to reach the threshold for engaging NCX activity are relatively large (Scheff et al., 2014). However, the duration of the evoked Ca^{2+} transient in putative nociceptors from paclitaxel-treated rats was shorter than that previously demonstrated to be required for NCX activation in glabrous skin neurons (Scheff et al., 2014). This raised the possibility that NCX was sensitized in glabrous skin neurons from paclitaxel treated rats. An increase in NCX activity in response to smaller and shorter duration increases in $[\text{Ca}^{2+}]_i$ could contribute to an overall decrease in the duration of the evoked transient, even if there was no difference in peak NCX activity in neurons from paclitaxel- and vehicle-treated rats. We tested this possibility with a stimulation-duration analysis of the activation of NCX, by application of 30 mM KCl for durations ranging between 0.1 to 2 s in the presence and absence of Li^+ to neurons from vehicle- and paclitaxel-treated rats. Consistent with our previous findings (Scheff et al., 2014), both the amplitude (Figure 6A) and duration (Figure 6B) of the depolarization evoked transient depends on the duration of KCl application. The amplitude saturates with a KCl application of ~2 seconds while the duration of the evoked transient appears to be bi-phasic, and has not fully saturated with even a 4 second application of KCl. A neuron was considered Li^+ -responsive, if the duration of the evoked Ca^{2+} transient increased $\geq 20\%$ in the presence of Li^+ . There was no difference in the proportion of Li^+ -responsive neurons from paclitaxel- (12/15 and 13/14 for 1 and 2 sec applications of 30 mM KCl, respectively) and vehicle- (12/12 and 10/10 for 1 and 2 sec applications of 30 mM KCl, respectively) treated rats. Similarly, in neurons stimulated with 4 sec of high K^+ (i.e., in figure 1), 1 out of 17 and 4 out of 21 neurons from paclitaxel and vehicle-treated rats, respectively, were unresponsive to Li^+ . Furthermore, there were no detectable differences between the Li^+ -responsive and non-responsive neurons from paclitaxel-treated rats with respect to the properties of the evoked Ca^{2+} transient. However, in

contrast to our previous results with glabrous neurons from naïve rats, where $[Ca^{2+}]_i$ above 325 nM for at least 12 seconds was required for NCX activation (Scheff et al., 2014), in the presence of Li^+ there was a ~2-fold increase in the duration of the evoked Ca^{2+} transient in response to any stimulus duration that was sufficient to drive an increase in $[Ca^{2+}]_i$ (Figure 6C, 6D, and 6E). This apparent sensitization of NCX was observed in neurons from both vehicle- and paclitaxel-treated rats.

Evidence of NCX activity induced with relatively small and brief Ca^{2+} transients in putatively nociceptive glabrous skin neurons suggested the possibility that the paclitaxel vehicle (Cremaphor EL and ethanol) was responsible for the sensitization of NCX. To test this possibility, we repeated the stimulation-duration experiment in glabrous neurons from naïve rats. The results of this experiment were comparable to our previous findings (Scheff et al., 2014), where an increase in NCX activity was only detected in neurons that had an increase in $[Ca^{2+}]_i$ above 325 nM that lasted longer than 11 seconds.

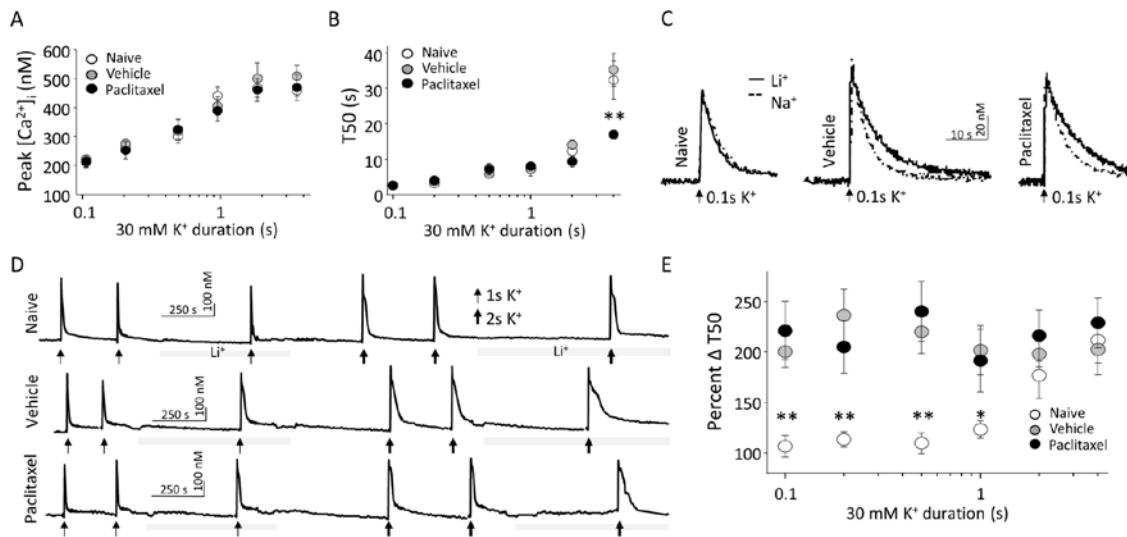


Figure 6. NCX is sensitized by the vehicle of paclitaxel. Paclitaxel vehicle sensitizes NCX. A) Peak evoked Ca^{2+} transients from naïve, vehicle-, and paclitaxel-treated rat putative nociceptor neurons as a function of 30 mM K^+ application duration (n for each 30 mM K^+ duration: 0.1s n = 4, 4, and 5; 0.2s n = 6, 7, and 10; 0.5s n = 6, 7, and 10; 1s n = 7, 12, and 15; 2s n = 7, 10, and 14; 4s n = 9, 17, and 21 neurons for naïve, vehicle, and paclitaxel, respectively). B) The T50 duration of the evoked Ca^{2+} transients of the same neurons plotted in (A). C) Ca^{2+} transients evoked with 0.1s application of 30 mM K^+ in putative nociceptive neurons labeled from the glabrous skin from naïve (left), vehicle-treated (middle), and paclitaxel-treated (right) rats in the before (dotted traces) and after (solid traces) block of NCX with Li^+ bath solution. D) Ca^{2+} transients evoked in the same neurons as in A, with 1 and 2 s applications of 30 mM K^+ , before and after block of NCX with Li^+ bath. E) Pooled data from neurons stimulated with 30 mM K^+ as illustrated in A and B, analyzed as a percent increase in T50 following NCX block with Li^+ (Percent Δ T50), are plotted as a function of 30 mM K^+ application duration.

3.3.3 The impact of paclitaxel on NCX activity is dependent on target of innervation.

The observation that NCX was sensitized in neurons from vehicle-treated rats, in the absence of any detectable influence of the paclitaxel vehicle on the duration of the depolarization-evoked

Ca²⁺ transient in these neurons (as compared to neurons from naïve rats (Figure 1 and (Yilmaz and Gold, 2015)) suggests that there are at least two Ca²⁺ regulatory mechanisms that are altered in neurons from vehicle treated rats: 1) the apparent increase in NCX activity and 2) another mechanism that compensates for the increase in NCX activity. Because we also previously failed to detect an influence of paclitaxel or its vehicle on depolarization-evoked Ca²⁺ transients in putative nociceptive neurons innervating the inner thigh (Yilmaz and Gold, 2015), the presence of compensatory changes in glabrous skin neurons that were undetected with a depolarizing stimulus alone raised the possibility that compensatory mechanisms contributed to the negative results in thigh neurons as well. To test this possibility, we repeated the Li⁺ application experiments with neurons labeled from the hairy skin of the hindpaw and the inner thigh.

The fraction of Li⁺-responsive neurons was significantly ($p < 0.05$, Chi-square test) lower in thigh skin neurons (7/15 neurons from vehicle-treated rats and 13/20 neurons from paclitaxel-treated rats) than that in glabrous skin neurons. However, the fraction of Li⁺-responders in hairy hindpaw neurons (16/22 neurons from vehicle-treated rats and 15/18 neurons from paclitaxel-treated rats) was not significantly ($p > 0.05$, Chi-square test) different from that in either thigh or glabrous skin neurons (Figure 7A). Moreover, of the Li⁺-responders, there was a significant interaction ($p < 0.05$) between treatment (paclitaxel vs vehicle) and target of innervation (thigh, hairy hindpaw and glabrous skin), where post-hoc analysis confirmed that the paclitaxel-induced increase in NCX activity in thigh neurons was significantly greater than that in neurons innervating either the hairy hindpaw ($p < 0.05$) or glabrous skin ($p < 0.01$). To determine whether the relative increase in evoked transient duration observed in thigh neurons was different than that in the hairy hindpaw or glabrous skin neurons, duration data for the paclitaxel groups from each target of innervation were analyzed as a percent increase over the mean change

in duration in the respective vehicle groups. Statistical analysis of these data confirmed that this difference based on target of innervation was significant ($p < 0.01$, one-way ANOVA), where post-hoc analysis confirmed that the increase in duration in thigh neurons was significantly greater than that in either hairy hindpaw ($p < 0.05$) or glabrous skin neurons ($p < 0.01$) (Figure 7B). This indicated that in contrast to glabrous skin neurons, paclitaxel was associated with an increase in NCX activity in thigh neurons.

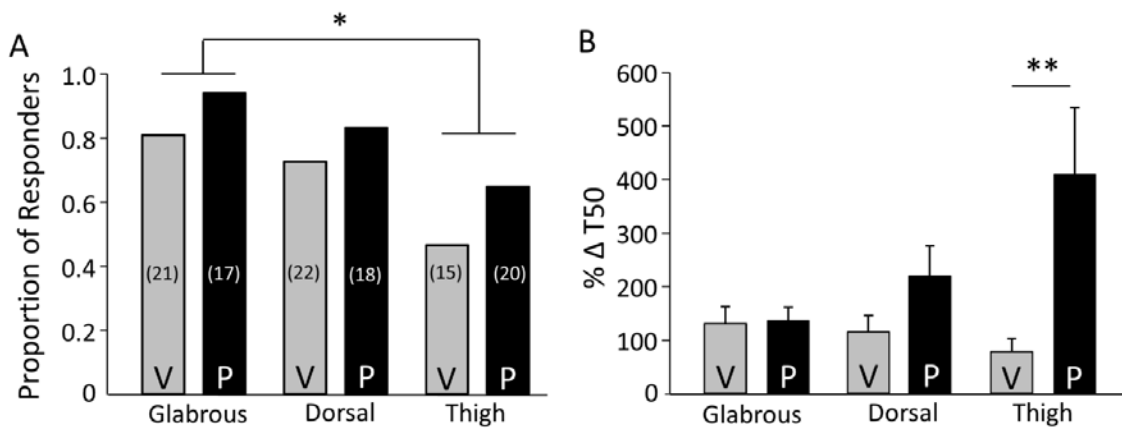


Figure 7. The impact of paclitaxel on NCX activity is dependent on target of innervation. Effect of paclitaxel on NCX depends of target of innervation. A) Putative nociceptive neurons from vehicle (V) and paclitaxel (P) treated rats retrogradely labeled from the glabrous skin (Glabrous), the dorsal skin of the hindpaw (Dorsal), and the inner thigh skin (Thigh), were analyzed as a function of whether or not Li^+ was associated with an increase in the duration of the evoked Ca^{2+} . The proportion of Li^+ responsive neurons in each group is plotted. The total number of neurons studied in each group is indicated in parenthesis. B) Li^+ -induced increase in the duration of the Ca^{2+} transient evoked with a 4 s application of 30 mM K^+ was analyzed as a percent increase T50. Pooled data are from the Li^+ -responsive neurons plotted in A. Data from the glabrous skin neurons from Figure 1C have been replotted here to facilitate comparisons between groups. * is $p < 0.05$

3.3.4 Paclitaxel-induced increase in NCX activity in thigh neurons is not due to NCX3 activity.

We sought to confirm our Li⁺ results with another NCX blocker both because Li⁺ influences a number of cellular processes in addition to blocking NCX and because of previous evidence that all three NCX isoforms are expressed in sensory neurons (Scheff et al., 2014). Based on previous evidence that NCX3 accounts for the majority of depolarization-evoked NCX activity in glabrous skin neurons, we used the NCX3 preferring blocker, KB-R7943 (Iwamoto and Shigekawa, 1998, Scheff et al., 2014). In this set of experiments, we focused on glabrous skin neurons and thigh neurons, in which there was no effect of paclitaxel on the Li⁺-induced increase in the evoked Ca²⁺ transient duration and the largest paclitaxel-induced change in the response to Li⁺ was observed, respectively. As with Li⁺, neurons were again subgrouped based on the impact of KB-R7943 on the duration of the depolarization (4 seconds of 30 mM K⁺) evoked Ca²⁺ transient, where those in which the duration of the evoked Ca²⁺ transient was $\geq 20\%$ were considered KB-R7943 responders (Figure 8A). Of the 10 glabrous skin neurons from naïve rats tested, 8 were KB-R7943 responders. A similar proportion of glabrous skin neurons from paclitaxel-treated rats (15/16) were KB-R7943 responders. However, the proportion of KB-R7943 responders from vehicle-treated rats (9/18) was significantly ($p < 0.01$) lower than that in the paclitaxel group (Figure 8B). In thigh neurons, paclitaxel treatment was associated with a significant ($p < 0.01$, Chi Square test) increase in the proportion of KB-R7943 responders (21/23) relative to that observed in neurons from either naïve (4/8) or vehicle-treated (10/19) rats (Figure 8B). This suggested at least some of the paclitaxel-induced increase in NCX activity in thigh neurons was due to an increase in a KB-R7943 sensitive NCX isoform (i.e., NCX3).

To further assess the contribution of a KB-R7943-sensitive NCX isoform to the paclitaxel-induced increase in NCX activity in thigh neurons, we analyzed the KB-R7943-induced increase in the Ca^{2+} transient duration of responders. Strikingly, the KB-R7943-induced increase in transient duration was comparable ($p > 0.05$) in glabrous and thigh skin neurons from naïve, vehicle-, and paclitaxel-treated rats (Figure 8A and 8C) suggesting that the majority of NCX activity in these neurons was KB-R7943-insensitive. To confirm this impression, KB-R7943 data were analyzed as a percentage of the mean response (increase in transient duration) to Li^+ . Analysis of these data revealed a significant interaction between target of innervation and treatment, where post-hoc analysis confirmed that there was a significant reduction in the KB-R7943 sensitive fraction of the Li^+ -induced increase in the duration of the evoked Ca^{2+} transient (Figure 8D). Finally, the NCX1 preferring blocker, SEA0400 was used to determine whether the apparent paclitaxel-induced increase in KB-R7943 insensitive NCX activity in thigh neurons was due to an increase in NCX1 activity. Thigh neurons from vehicle- and paclitaxel-treated rats were studied before and after application of SEA0400 (1 μM) (Figure 8E). Nine out of 10 thigh neurons tested from paclitaxel-treated rats were SEA0400 responders, however only two out of 10 thigh neurons from vehicle-treated rats were SEA0400 responders (Figure 8F, $p < 0.01$, Fisher Exact test). Analysis of the pooled transient duration data of the responders indicated that the paclitaxel-induced increase in KB-R7943-insensitive NCX activity in thigh neurons is associated, at least partially, with an increase in SEA0400-sensitive NCX activity, which accounted for 42 ± 24 percent of the Li^+ -induced increase in the duration of the evoked transient.

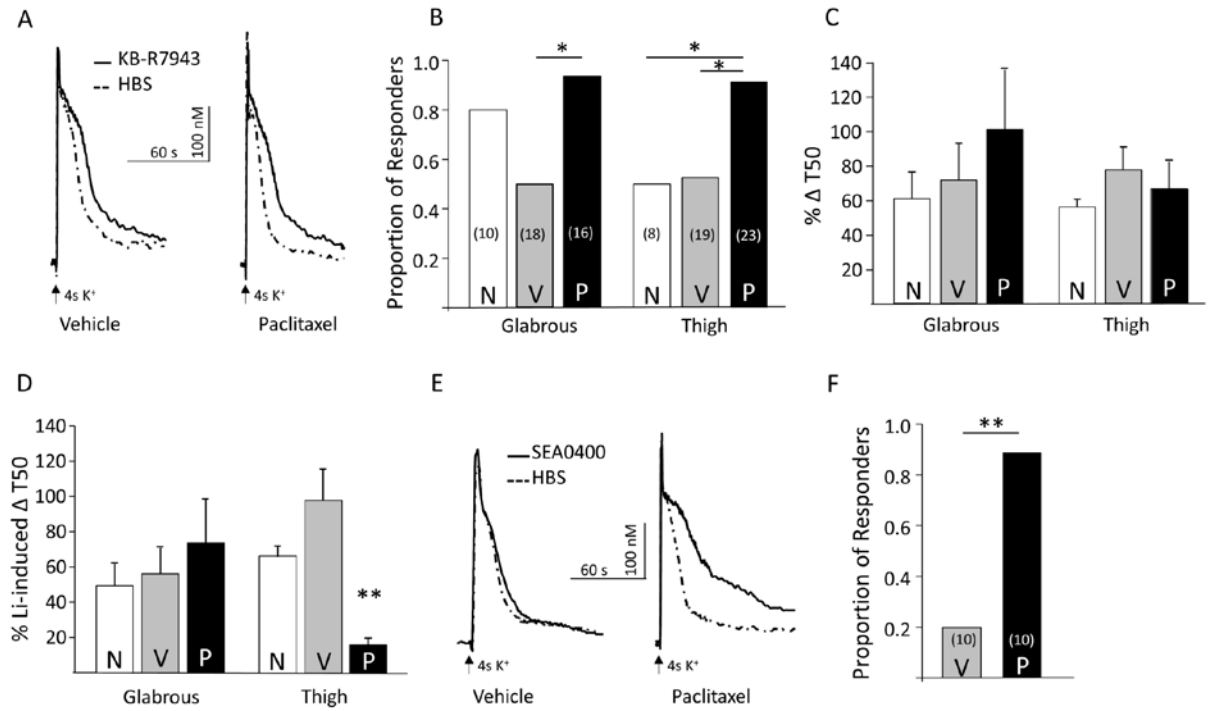


Figure 8. Paclitaxel-induced increase in NCX activity in thigh neurons is not due to NCX3 activity. The paclitaxel-induced increase in NCX activity in thigh neurons is KB-R7943 resistant and SEA0400 sensitive. A) Ca^{2+} transients evoked with 4s application of 30 mM K^+ in putative nociceptive neurons labeled from the thigh skin from vehicle-treated (left) and paclitaxel-treated (right) rats before (dotted traces) and after (solid traces) block of NCX with KB-R7943 (100 nM). B) Putative nociceptive neurons from vehicle (V) and paclitaxel (P) treated rats retrogradely labeled from the glabrous skin (Glabrous) and the inner thigh skin (Thigh), were analyzed as a function of whether or not KB-R7943 was associated with an increase in the duration of the evoked Ca^{2+} . The proportion of KB-R7943-responsive neurons in each group is plotted. The total number of neurons studied in each group is indicated in parenthesis. C) KB-R7943-induced increase in the duration of the Ca^{2+} transient evoked with a 4 s application of 30 mM K^+ was analyzed as a percent increase T50. Pooled data are from the KB-R7943-responsive neurons plotted in B. D) To estimate the fraction of total NCX activity sensitive to KB-R7943, increase in T50 associated with KB-R7943 was analyzed as a percentage of the average increase in T50 in response to Li^+ (% Li^+ -induced ΔT50). Pooled data from C analyzed in this way are plotted in D). E) Ca^{2+} transients evoked with 4s application of 30 mM K^+ in putative nociceptive neurons labeled from the thigh skin from vehicle-treated (left), and paclitaxel-treated (right) rats before (dotted traces) and after (solid traces) application of the putative NCX1 preferring blocker SEA0400. F) The proportion of SEA0400-responsive thigh neurons from paclitaxel (P) treated

rats was significantly greater than that in neurons from vehicle (V) treated rats. The number in parentheses is the total number of neurons studied from each group.* is $p < 0.05$, ** is $p < 0.01$.

3.4 DISCUSSION

The purpose of this study was to test the hypothesis that the paclitaxel-induced decrease in the duration of the evoked Ca^{2+} transient in putative nociceptive glabrous skin neurons is due to an increase in activity of NCX. Because we observed the paclitaxel-induced decrease in the duration of the Ca^{2+} transient evoked with a four second application of high K^+ , this stimulus duration was used to estimate the total NCX activity. With this stimulus duration, we failed to detect a difference in the relative levels of NCX activity between neurons from paclitaxel or vehicle-treated animals. Furthermore, there was no evidence of a paclitaxel-selective sensitization of NCX that was assessed with shorter duration applications of high K^+ . In contrast to glabrous skin neurons from naïve rats in which a relatively large and long lasting increase in $[\text{Ca}^{2+}]_i$ was needed to evoke NCX activity, there was evidence of NCX activity in neurons from both vehicle and paclitaxel-treated rats in response to evoked transients that were significantly smaller and of shorter duration. There were also differences between thigh, hairy hindpaw and glabrous skin with respect to the proportion of neurons with detectable NCX activity. Interestingly, there was a paclitaxel-induced increase in the proportion of thigh neurons with evidence of NCX activity. Even more interestingly, there was also a paclitaxel-induced increase in the impact of Li^+ on thigh neurons that was associated with no change in the actions of KB-R7943, but an increase in the impact of the NCX1-preferring blocker, SEA0400. Taken together, while these observations argue against our initial hypothesis, they highlight the potential confounding influence of the chemotherapeutic vehicle on cellular properties that may not only contribute to the manifestation of CIPN, but also potentially mask the underlying mechanism(s). They also suggest the

emergence of potential compensatory mechanisms in subpopulations of neurons that serve to protect them from the deleterious consequences of chemotherapeutics.

Our results argue against an increase in NCX activity as the mechanism of the paclitaxel-induced decrease in the duration of the evoked Ca^{2+} transient in glabrous skin neurons. Nevertheless, this conclusion is made with caution because of limitations associated with assumptions implicit in the indirect assessment of NCX activity. These include the specificity of the reagents used to block NCX activity, that a block of NCX will necessarily increase the duration of the evoked Ca^{2+} transient, and that it is possible to manipulate a Ca^{2+} regulatory mechanism, such as NCX, without affecting other mechanisms. While it is clear that these assumptions reflect an over-simplification of a very complex system, we suggest that the limitations associated with these assumptions are unlikely to significantly influence the interpretation of our results. For example, consistent results were obtained with Li^+ and the NCX3-prefering blocker KB-R7943, arguing against a contribution of NCX-independent mechanisms contributing to the effects of Li^+ . Similarly, that it was possible to detect a relative increase in NCX activity in thigh neurons suggests that the failure to detect a change in NCX activity in glabrous skin neurons was not due to a limitation in the sensitivity of this indirect assay. The changes detected in thigh neurons also argue against the possibility that the vehicle effects occluded our ability to detect a change in NCX activity in glabrous skin neurons.

If a change in NCX activity is not the underlying reason for paclitaxel-induced decrease in the Ca^{2+} transient duration, it is worth considering other Ca^{2+} regulatory mechanisms that may contribute to this change. It is possible to rule out several regulatory mechanisms, however, because of evidence that they influence resting $[\text{Ca}^{2+}]_i$ and/or the magnitude of the evoked Ca^{2+} transient. For example, the high affinity/low efficacy plasma membrane calcium ATPase

(PMCA) is the major regulator of resting Ca^{2+} level in many cells types (Carafoli, 1991) including putative nociceptive DRG neurons (Gemes et al., 2012), and therefore is unlikely to mediate the selective paclitaxel-induced change in the duration of the evoked transient. Similarly, because voltage-gated Ca^{2+} channels (VGCCs) and Ca^{2+} -induced Ca^{2+} release (CICR) machinery contribute to the magnitude of the evoked Ca^{2+} transient, neither is likely to underlie the paclitaxel-induced decrease of the Ca^{2+} transient duration. This leaves mitochondria and sarco-endoplasmic reticulum calcium ATPase (SERCA), which have both been shown to contribute to the regulation of the evoked Ca^{2+} transient duration in sensory neurons (Lu et al., 2006, Scheff et al., 2013). However, because previous results in unlabeled DRG neurons indicate that mitochondria can affect the magnitude of the evoked Ca^{2+} transients as well as the duration (Lu et al., 2006), future experiments should consider SERCA as a priority. Alternatively, because of the inter-dependence of Ca^{2+} regulatory mechanisms (Thibault et al., 2007, Garcia-Sancho, 2014, Moccia et al., 2015), a more likely explanation for the paclitaxel-induced decrease in the evoked transient duration is that it reflects changes in a combination of regulatory mechanisms. For example, reduced coupling of VGCCs to CICR machinery, thus reduced release of endoplasmic reticulum (ER) Ca^{2+} after influx through VGCCs, may result in transients that are shorter in duration without an impact on the magnitude.

Evidence of NCX activity in association with small amplitude brief duration Ca^{2+} transients in both vehicle- and paclitaxel-treated neurons indicates that the paclitaxel vehicle drives the sensitization of NCX. The presence of sensitized NCX in vehicle-treated neurons should have resulted in shorter duration-evoked transients in neurons from both vehicle and paclitaxel-treated rats, relative to that in neurons from naïve rats. However, the observation that evoked transient duration was comparable in neurons from vehicle-treated and naïve rats

(Yilmaz and Gold, 2015) indicates the presence of a second change in neurons from vehicle-treated rats, needed to compensate for the vehicle-induced increase in NCX activity. This would not be the first evidence of a vehicle effect, as it has been previously reported that cremophor EL is associated with anaphylactoid hypersensitivity reactions, ganglionopathy, axonopathy, and demyelination (Gelderblom et al., 2001, Mielke et al., 2006). Whether an increase in NCX activity contributes to any of these changes has yet to be determined. Furthermore, it is possible that one or both of these changes in Ca^{2+} regulation, contribute to the side effects associated with at least a taxol-based chemotherapy. In particular, while we failed to detect an influence of vehicle on nociceptive threshold, it is possible that the changes associated with vehicle treatment contribute to the manifestation of hypersensitivity in paclitaxel-treated animals. However, because a variety of chemotherapeutics administered in different vehicles produce a neuropathy with comparable symptoms and manifestation pattern, we suggest that changes associated with the paclitaxel vehicle are unlikely to be an important determinant of CIPN.

While the heterogeneity among subpopulations of sensory neurons has been well described, our results point to yet another manifestation of this phenomenon among subpopulations of sensory neurons based on target of innervation. First, there are differences between glabrous skin and inner thigh skin putative nociceptive neurons with respect to both the presence of NCX activity, and the NCX isoforms underlying this activity. Second, there is also a difference between these subpopulations with respect to the impact of paclitaxel on NCX activity. More importantly, however, are the implications of the apparently selective increase in NCX activity in thigh neurons. This observation suggests that in addition to the multiple vehicle-associated changes in glabrous skin neurons, there also needs to be (at least) two opposing changes in Ca^{2+} regulatory processes in putative nociceptors innervating the inner thigh skin to

account for the apparent absence of a paclitaxel-induced change in transient duration in these neurons (Yilmaz and Gold, 2015). Furthermore, given the absence of a detectable paclitaxel-induced change in the withdrawal threshold to noxious mechanical stimulation of the inner thigh, one, if not both of the changes in Ca^{2+} regulation may protect these neurons from the toxic effects of paclitaxel. This suggests an alternative explanation for the stocking glove distribution of CIPN, which is due to the failure of glabrous skin neurons to compensate for the toxic effects of chemotherapeutics, rather than the presence of a unique property of these neurons (such as their axon length), that confers a selective vulnerability. Identification of the protective mechanism(s) in thigh neurons may suggest novel approaches for the treatment, if not prevention of CIPN.

4.0 ROLE OF PACLITAXEL-INDUCED INCREASE IN MITOCHONDRIAL VOLUME ON CALCIUM DYSREGULATION IN SUBPOPULATIONS OF NOCICEPTIVE AFFERENTS: DIRECT AND INDIRECT MECHANISMS

4.1 INTRODUCTION

Chemotherapy-induced peripheral neuropathy (CIPN) is not only of the leading dose-limiting side effects of chemotherapy but the primary reason for therapy cessation (Wolf et al., 2008, Jaggi and Singh, 2012). CIPN generally starts with tingling and numbness in the distal appendages and progresses to a painful neuropathy, severity of which escalates with cumulative dosage (Quasthoff and Hartung, 2002, Jaggi and Singh, 2012).

We have recently demonstrated in a rat model of paclitaxel-induced CIPN, that the presence of mechanical hypersensitivity is associated with a dysregulation of intracellular Ca^{2+} in a subpopulation of putative nociceptive neurons. Specifically, we observed a significant decrease in the duration of the depolarization-evoked Ca^{2+} transient, with no changes in either the transient peak, or in resting Ca^{2+} (Yilmaz and Gold, 2015). Having recently described an inflammation-induced decrease in the activity of the Na^+ - Ca^{2+} -exchanger (NCX) that was responsible for the inflammation-induced *increase* in the duration of the evoked Ca^{2+} transient (Scheff et al., 2014) in the same population of neurons in which paclitaxel produced a *decrease*

in the evoked transient duration, our initial hypothesis was that an increase in NCX activity was responsible for the paclitaxel-induced changes. However, while paclitaxel does drive changes in NCX activity in a different subpopulation of neurons, we were able to rule out an increase in NCX activity as the mechanism underlying the paclitaxel-induced decrease in transient duration (Yilmaz and Gold, 2016). Thus, in the present study, we have pursued an alternative hypothesis regarding the mechanism(s) underlying the paclitaxel-induced decrease in the duration of the depolarization evoked Ca^{2+} transient.

Given the weight of evidence in support of mitotoxicity as a mechanism responsible for the numbness, tingling, and pain associated with CIPN (Bennett et al., 2014), in combination with the both a direct and indirect role for mitochondria in the regulation of intracellular Ca^{2+} , a role for mitochondria in the paclitaxel-induced dysregulation of intracellular Ca^{2+} would seem to be an even more compelling hypothesis than that in support of a role for NCX. Based on several different lines of evidence, Bennett and colleagues proposed that an increase in reactive oxygen species (ROS) combined with the chronic energy deficit associated with chemotherapeutic-induced mitotoxicity are responsible for both spontaneous discharges in afferents with myelinated (tingling) and unmyelinated (pain) axons, and degeneration of peripheral afferent terminals (numbness) (Bennett et al., 2014). Mitotoxicity has been documented in several different animal models of CIPN, which is characterized by mitochondrial swelling, an increase in the percentage of vacuolated mitochondria, and reduced rates of ATP production and respiration along sensory axons (Flatters and Bennett, 2006, Xiao et al., 2011, Zheng et al., 2011, 2012). The morphological changes in mitochondria were observed in both small and large diameter sensory but not in motor fibers (Xiao et al., 2011). In addition, the highest level of paclitaxel accumulation was detected in dorsal root ganglia (DRG) (Xiao et al., 2011), raising the

possibility that mitochondria damage is initiated at the sensory neuron cell body. Because longer nerves would be particularly vulnerable to the deleterious impact of mitochondria damage, mitotoxicity has also been suggested to account for the “stocking glove” distribution of CIPN (Gornstein and Schwarz, 2014).

Mitochondria are able to attenuate increases in intracellular Ca^{2+} directly via the mitochondrial uniporter (MCU) and indirectly via the regulation of primary active transporters including the plasma membrane Ca^{2+} ATPase (PMCA) and sarco-endoplasmic reticulum Ca^{2+} ATPase (SERCA), as well as secondary active transporters such as NCX. Thus, an increase in mitochondria and/or mitochondrial activity could account for the paclitaxel-induced decrease in the evoked Ca^{2+} transient. The problem with this suggestion, however, is that if mitochondria are damaged, there should be an attenuation of mitochondria-dependent Ca^{2+} uptake which should result in an evoked Ca^{2+} transient with a longer, not a shorter duration.

We suggest, however, that it is possible for chemotherapeutics to contribute to both gain- and loss-off mitochondrial function, if the changes in mitochondria occur in different subpopulations of neurons. Consistent with this suggestion is the observation that despite being referred to as a “stocking-glove” distribution, more detailed analysis indicates that CIPN symptoms are preferentially localized in the glabrous skin of the hands and feet (Dougherty et al., 2004). We have recently demonstrated this far more restricted manifestation of CIPN in a rat model of paclitaxel-induced CIPN, where mechanical hypersensitivity was detected in the glabrous skin of the hindpaw but not in the dorsal skin of the hindpaw or the inner thigh (Yilmaz and Gold, 2015). Minimally, this observation argues against the axon length-dependence of the manifestation of CIPN, but also supports the suggestion that there is a sensory neuron subpopulation specific vulnerability to the actions of chemotherapeutics.

Furthermore, we and others have not only documented differences among sensory neuron subpopulations with respect to both the magnitude and the duration of the depolarization-evoked Ca^{2+} transients and the underlying Ca^{2+} regulatory pathways (Lu et al., 2006) but there are now a number of lines of evidence supporting the presence of a sensory neuron subpopulation specific response to injury (Gold and Traub, 2004, Harriott et al., 2006, Vaughn and Gold, 2010). Most relevant in this regard, the paclitaxel-induced reduction in the duration of the depolarization-evoked Ca^{2+} transient in putative nociceptive afferents was significantly larger in neurons innervating the glabrous skin of the hindpaw in comparison to innervating the hairy skin of the hind paw or the inner thigh (Yilmaz and Gold, 2015). Similarly, while target of innervation was not determined, morphological evidence of mitotoxicity was only observed in 25 to 40% of axons (Flatters and Bennett, 2006, Xiao et al., 2011). Thus, we hypothesize that CIPN is due to both increases and decreases in mitochondria function, with changes manifest in distinct subpopulations of afferents.

To begin to test this hypothesis, we used behavioral approaches, fluorescent immunohistochemistry, live confocal microscopy, and Ca^{2+} imaging in combination with pharmacological manipulations to study paclitaxel-induced changes in retrograde tracer-labeled, small-diameter, IB4+, capsaicin-responsive DRG neurons from naïve, vehicle-treated, and paclitaxel-treated rats. Our results suggest that the paclitaxel-induced decrease in the duration of the evoked Ca^{2+} transient in putative nociceptive glabrous skin neurons is indeed mediated by an increase in mitochondria function, facilitating an increase in the clearance of Ca^{2+} from the cytosol via direct and indirect mechanisms.

4.2 METHODS

4.2.1 Animals

Adult (250-320g) male Sprague-Dawley rats (Envigo, Indianapolis, IN)) were used for all experiments. Because preliminary results suggest that there is a sex difference in the development of chemotherapy-induced mechanical sensitivity in rats, female rats were not included in this study. Rats were housed two per cage in a temperature and humidity controlled, Association for Assessment and Accreditation of Laboratory Animal Care International (AAALAC) accredited animal housing facility on a 12h:12h light:dark schedule. Food and water were available *ad libitum*. All procedures were approved by the University of Pittsburgh Institutional Animal Care and Use Committee and performed in accordance with National Institutes of Health guidelines for the use of laboratory animals in research.

4.2.2 Retrograde labeling

1,1'-dioctadecyl-3,3,3',3'-tetramethylindocarbocyanine perchlorate (DiI) or 3,3'-Dioctadecyloxycarbocyanine Perchlorate (DiO) was injected intradermally at one of three different locations so as to identify subpopulations of cutaneous afferents based on the target of innervation. These sites included the glabrous skin of the hind paw, the hairy skin on the dorsal side of the hind paw, and the hairy skin of the upper inner thigh. The hair covering the thigh was removed with an electrical shaver before retrograde labeling with DiI or DiO. The retrograde tracer was injected bilaterally under isoflurane (Abbott Laboratories, North Chicago, IL)

anesthesia with a 30 g needle at 3-5 sites per target for a total volume of 10 μ L in the dorsal and glabrous hindpaw and 20 μ L in the thigh. Only one tracer was injected into each animal.

4.2.3 Paclitaxel treatment

One week following the DiI or DiO injection, rats were anesthetized with isoflurane and injected into the tail vein with 2 mg/kg paclitaxel or its vehicle (1:1:23, cremophor EL:ethanol:0.9% saline). The tail vein injection was repeated three more times every other day for a total of four injections.

4.2.4 Behavioral Assessment

All behavioral data were collected in the Rodent Behavior Analysis Core of the University of Pittsburgh, School of Health Sciences by an experimenter blinded to the test group. Rats were habituated to the testing procedure, equipment, and the experimenter for two to three days before the collection of baseline data. For the cold hypersensitivity test, rats were placed individually in acrylic clear boxes (10 cm x 20 cm), separated by opaque dividers. The boxes were set on a 1/8 inch-thick glass platform. The barrel of a 3 mL syringe filled with powdered dry ice, was placed on the surface of the glass platform precisely beneath the footpad of the hindpaw. Paw withdrawal latency was recorded three times per paw, with an interval of at least five minutes for each paw. The cold hypersensitivity test was conducted three times per week.

For assessment of changes in mechanical sensitivity in the glabrous skin, the same clear acrylic boxes were used, except for this test, the boxes were placed on an aluminum mesh. Four g and 15 g von Frey filaments were applied to the center foot pad of the hind paw at a right angle

from below the mesh as previously described (Flatters and Bennett, 2006). Each filament was applied five times per paw (10 times total per rat), at a frequency of 3-5 min. Paw withdrawal response probability was calculated as, $P = \text{number of withdrawal responses} / 10 \text{ trials}$. Mechanical assessments were conducted once per week on a day that the rats were not tested for cold sensitivity.

4.2.5 Sensory Neuron Isolation

Rats were deeply anesthetized with an intraperitoneal injection (1 ml/kg) of an anesthetic cocktail containing ketamine (55 mg/kg), xylazine (5.5 mg/kg) and acepromazine (1.1 mg/kg). L4 and L5 DRGs were removed bilaterally, enzymatically treated, and mechanically dissociated. DRG neurons were plated on laminin (Thermo-Fisher, 1mg/ml) and poly-L-ornithine (Sigma-Aldrich, 1 mg/ml) coated glass coverslips as previously described (Lu et al., 2006). For immunocytochemistry experiments, chamber slides (EMD Millipore, Billerica, MA, USA) were used instead of glass coverslips. All subsequent experiments were performed within 8 h of tissue harvest.

4.2.6 Fura-2 and Rhod-2 Ca^{2+} Imaging

Fura-2 was used to monitor changes in free cytosolic Ca^{2+} , and Rhod-2 was used to monitor relative changes in mitochondrial Ca^{2+} (Davidson and Duchon, 2012). Cells were loaded with Fura-2 AM ester (2.5 μM) with 0.025 % Pluronic F-127 for 20 min at room temperature. They were loaded with Rhod-2 AM ester (500 nM) in combination with Fura-2 AM ester + Pluronic F-127 for 20 min at room temperature. Following loading with Ca^{2+} indicators, neurons from

DiI-labeled rats were then incubated with FITC-conjugated IB4 (10 $\mu\text{g/ml}$) for 10 min at room temperature. They were then placed in a recording chamber and continuously superfused with a 4-(2-Hydroxyethyl)piperazine-1-ethanesulfonic acid, N-(2-Hydroxyethyl) piperazine-N'-(2-ethanesulfonic acid) (HEPES)-buffered bath solution (HBS) consisting of (in mM): 130 NaCl, 3 KCl, 2.5 CaCl_2 , 0.6 MgCl_2 , 10 HEPES, 10 glucose, pH 7.4, osmolality 325 mOsm. Fluorescence data were acquired on a PC running Metafluor software (Molecular Devices, Sunnyvale, CA) via an EMCCD camera (Photometrics, Tucson, AZ; model QuantEM 512SC). For Fura-2 imaging, the ratio (R) of fluorescence emission (510 nm) in response to 340/380nm excitation (controlled by a DG-4 (Sutter Instrument, Novato, CA)) was acquired at 1 Hz during application of KCl or capsaicin, which were applied through a computer-controlled, piezo-driven perfusion system (switching time <20 ms; Warner Instruments, Hamden, CT, USA, Fast-Step Model SF-77B). $[\text{Ca}^{2+}]_i$ was determined from Fura-2 ratio according to the equation $[\text{Ca}^{2+}]_i$ (nM) = $K_d (S_{f2}/S_{b2}) ((R-R_{\min})/(R_{\max}-R))$ following *in situ* calibration as described previously (Scheff et al., 2013), where K_d is the dissociation constant for Fura-2 for Ca^{2+} at room temperature; S_{f2}/S_{b2} is the fluorescence ratio of the emission intensity excited with the 380 nm wavelength in the absence of Ca^{2+} to that in the presence of saturating Ca^{2+} ; R_{\min} and R_{\max} are the minimal and maximal fluorescence ratios, respectively. S_{f2}/S_{b2} , R_{\min} and R_{\max} were determined empirically with calibration runs as described previously (Kao, 1994), run every ~six weeks throughout the data collection period. The signal intensity of Rhod-2 at 580 nm in response to excitation at 555 nm was acquired simultaneously with Fura-2 acquisition with a custom dichroic and band pass emission filter. Rhod-2 intensity values were plotted as a change in fluorescence over baseline ($\Delta F/F$).

Neurons from a single field were studied on each coverslip. Resting Ca^{2+} or Rhod-2 intensity were determined prior to stimulation, where the average of the 30 seconds just prior to stimulation (with high K^+ (30 mM)) was used for this value. The magnitude of the evoked Ca^{2+} transient was determined as the difference between resting and the peak of the evoked Ca^{2+} transient. The duration of the evoked Ca^{2+} transient was determined as the time for the transient to decay to 25%, 50%, 75%, and 90% of the peak (T25, T50, T75, and T90, respectively). For experiments involving the application of test compounds, a vehicle control group was always included. Neurons with a small cell body diameter ($< 30 \mu\text{m}$), responsive to capsaicin (500 nM), and labeled with the lectin IB4, determined under epifluorescence illumination, were referred to as putative nociceptors. Cell body diameter was determined with a calibrated eye-piece reticle. Capsaicin sensitivity was assessed at the end of every experiment and neurons were considered capsaicin sensitive if application of capsaicin resulted in an increase in $[\text{Ca}^{2+}]_i$ greater than 20% above baseline. Neurons in which the plasma membrane was clearly defined by epifluorescence were considered IB4+.

4.2.7 Live cell confocal microscopy

All live cell confocal imaging experiments were carried using a Nikon A1R upright confocal microscope system, controlled with the Nikon (NIS) Elements software. Dissociated neurons were loaded with one or when appropriate in various combinations with Mitotracker Green (200 nM in HBS), Mitotracker Deep Red (200 nM in HBS), TMRM (50 nM in HBS), and/or Mitosox (250 nM in HBS) in the dark for 30 min at room temperature. At the same time, they were labeled with IB4-AF647 (1 $\mu\text{g}/\text{mL}$ in HBS). Neurons were then washed 10 min in HBS and placed in a live cell chamber on the microscope stage containing HBS. All experiments were

carried out at room temperature. For Mitotracker green density studies, images were collected with a 60x water immersion objective in a series of 3 μm -thick z-planes extending through the entire neuron at a 512 x 512 pixel resolution and a 1/2 frame/sec rate. For all other experiments, images were collected with a 60x water immersion objective as a single 3 μm z-plane at the center of the retrograde tracer-labeled neuron at a 2048 x 2048 pixel resolution and a 1/8 frame/sec rate. Excitation/detection settings were determined with preliminary experiments using neurons from naïve rats with each fluorophore to yield an image that was not saturated. The same settings were applied for all conditions (naïve, vehicle, paclitaxel). For all experiments neurons from paclitaxel-, and vehicle-treated rats, as well a naïve rats were tested the same day. The quantitative measurement of the fluorescence signal was performed using Nikon (NIS) Elements and ImageJ software.

4.2.8 Fluorescent Immunocytochemistry

Neurons plated on chamber slides were fixed with 4% paraformaldehyde (PFA) in PBS for 30 min at room temperature and then washed three times in PBS. Slides were blocked with the blocking buffer (0.2% Triton X-100, 3% normal donkey serum in PBS) for one hour at room temperature and incubated with anti-Tom20 primary antibody (Amoscato et al., 2014, Khare et al., 2016) at a 1:2000 dilution in the blocking buffer overnight at 4°C. Slides were washed three times for 10 min each in Tris-buffered saline with Tween 20 (TBST) at room temperature and then incubated with an AF488-conjugated donkey anti-rabbit secondary antibody at 1:200 dilution in the blocking buffer for one hour at room temperature. Slides were washed two times 10 min each in TBST and incubated in TBST containing 1 $\mu\text{g}/\text{mL}$ AF647-conjugated IB4 and 1:1000 DAPI. Slides were washed one last time in TBST for 10 min and subsequently mounted

with coverslips using Fluoromount. The Tom20 images were collected with a 100x oil immersion objective in a series of 0.125 μm -thick z-planes extending through the entire neuron at a 2048 x 2048 pixel resolution and a 1/8 frame/sec rate using Nikon (NIS) Elements software. The same settings were applied for all neurons. The images in the stacks were deconvolved using the blind configuration for 20 iterations with Nikon (NIS) Elements software. Following deconvolution, the same 3D threshold setting was applied to all neurons. Data responding to volume and number of the mitochondria were transferred to a spreadsheet and used for further analyses.

4.2.9 Chemicals

Paclitaxel (Sigma-Aldrich, St Louis, MO, USA), was dissolved at 25 mg/mL in 1:1 Cremophor EL: ethanol and freshly diluted 1:12.5 in 0.9% sterile saline prior to injections. DiI (Thermo-Fisher, Waltham, MA, USA), was dissolved at 170 mg/mL in anhydrous dimethyl sulfoxide (DMSO, Sigma-Aldrich) and diluted 1:10 in 0.9% sterile saline for a final concentration of 17 mg/mL. DiO (Thermo-Fisher), was dissolved at a concentration of 10% (wt/vol) in anhydrous DMSO and diluted 1:10 in 0.9% sterile saline for a final concentration of 1%. Both DiI and DiO were freshly prepared before injections. As DiO is more susceptible to precipitation after the addition of saline, a small amount of fresh DiO stock was diluted in saline immediately before injection for each paw. FITC-conjugated Isolectin B4 (IB4, Sigma-Aldrich) was dissolved in dH₂O as a stock solution of 1 mg/ml, and then diluted to a final concentration of 5 $\mu\text{g}/\text{mL}$ in HEPES bath solution (HBS) the day of use. Alexa Fluor 647-conjugated IB4 (Thermo-Fisher) was dissolved in dH₂O 0.5 mm stock solution and diluted to a final concentration of 1 $\mu\text{g}/\text{mL}$ in HBS. Fura-2 AM ester (TEF Laboratories, Austin, TX, USA) was dissolved in DMSO as a 2.5

mM stock solution and diluted to a final concentration of 2.5 μ M in HBS. Pluronic F-127 (TEF Laboratories) was dissolved in DMSO as a 25% stock solution and diluted to 0.025% in HBS. Rhod-2 AM ester (Thermo-Fisher) was dissolved in DMSO as a 5 mM stock solution and diluted to a final concentration of 500 nM in HBS. Capsaicin (Sigma-Aldrich) was dissolved in ethanol as a 10 mM stock solution and diluted to 500 nM in HBS. Carbonyl cyanide 3-chlorophenylhydrazone (CCCP) and Cyclopiiazonic acid (CPA) (both from Sigma-Aldrich) were dissolved in DMSO as 100 mM stocks and diluted to 10 μ M in HBS. Oligomycin A (Tocris, Bristol, UK) was dissolved in DMSO as a 10 mM stock and diluted to 10 μ M in HBS. Mitotracker Green FM and Mitotracker Deep Red FM (both from Thermo-Fisher) were dissolved in DMSO as 1 mM stocks and diluted to 200 nM in HBS. Mitosox (Thermo-Fisher) was dissolved in DMSO as a 1 mM stock and diluted to 250 nM. Tetramethylrhodamine Methyl Ester Perchlorate (TMRM, Thermo-Fisher) was dissolved in DMSO as a 10 mM stock and diluted to 50 nM. Rabbit polyclonal anti-Tom20 antibody (Santa Cruz, Dallas, TX, USA) was diluted in blocking buffer (0.2% Triton X-100, 3% normal donkey serum in phosphate buffer solution (PBS)) to 1:2000. Alexa Fluor 488-conjugated donkey anti-rabbit antibody (Jackson Immuno Research, West Grove, PA, USA) was diluted 1:200 in blocking buffer. 2-(4-Amidinophenyl)-6-indolecarbamide dihydrochloride, 4',6-Diamidino-2-phenylindole dihydrochloride (DAPI, Thermo-Fisher) was diluted in TBST to 1:1000.

4.2.10 Statistical Analysis

Data are expressed as mean \pm s.e.m. Potential differences between two groups were assessed with T-tests, while experiments with more than two groups were analyzed with one and two-way ANOVAs with the Holm-Sidak test used for post-hoc comparisons. Statistical significance was

assessed at $p < 0.05$. Group sizes for the behavioral endpoints were determined by power analysis, which was based on the variability in responses to the mechanical and cold stimulations from three control animals. This analysis was performed for groups defined by treatment (vehicle and paclitaxel) over time. With a power of 0.8, alpha of 0.05, we estimated the need for a group size of 5 rats for the cold test and 6 rats for the mechanical test. Group sizes for all other experiments were determined by power analyses that were based on the variability of the respective endpoint (such as $\Delta T50$ or staining intensity) observed in putative nociceptive glabrous skin neurons from three naïve rats. These analyses were performed for two groups defined by treatment (vehicle and paclitaxel) for Rhod-2, Tom20, and SERCA experiments. With a power of 0.8 and alpha of 0.05, we estimated the need for nine, 13, and 24 neurons, respectively. Analyses for TMRM and Mitosox experiments were performed for three groups defined by treatment (naïve, vehicle, and paclitaxel). With a power of 0.8 and alpha of 0.05, we estimated the need for 16 and 14 neurons, respectively. Analyses for CCCP and Mitotracker were performed for experiments with eight and nine groups, defined by target of innervation and treatment. With a power of 0.8 and alpha of 0.05, we estimated the need for 12 and 31 neurons, respectively.

4.3 RESULTS

4.3.1 The recovery of the paclitaxel-induced decrease in the duration of the depolarization evoked Ca^{2+} transient correlates with the resolution of paclitaxel-induced hypersensitivity.

We previously described the paclitaxel-induced decrease in the duration of the depolarization evoked Ca^{2+} transient in putative nociceptive neurons that were isolated during a period of peak mechanical hypersensitivity (i.e., one week after the last paclitaxel injection) (Yilmaz and Gold, 2015). To further assess the association between the paclitaxel-induced decrease in the transient duration and pain behavior, we assessed the resting and evoked Ca^{2+} transient in neurons from rats in which paclitaxel-induced hypersensitivity was no longer detectable. So that behavioral data could be collected in a blinded fashion, paclitaxel and vehicle treated rats were run in parallel. Cold sensitivity was detectable in paclitaxel-treated rats ($n = 6$) after the first day of treatment (Figure 9A), with withdrawal latencies significantly ($p < 0.01$) shorter than those in vehicle treated rats ($n = 6$). This difference persisted through day 28 post-treatment. For the same group of rats, paw withdrawal probability to 4 g and 15 g von Frey filaments also increased at a comparable time point to the cold hypersensitivity and resolved by day 39 (Figure 9B and 9C, $p > 0.05$). While we have observed a significant decrease in the duration of the evoked Ca^{2+} transient in putative nociceptive glabrous neurons from 27 different cohorts of rats one week after the last paclitaxel injection (Yilmaz and Gold, 2015, 2016), by six weeks after the last paclitaxel injection, there was no detectable difference between neurons from paclitaxel ($n = 12$ neurons from 4 rats) and vehicle ($n = 12$ neurons from 4 rats) treated rats with respect to the duration of evoked Ca^{2+} transients ($p > 0.05$, Figure 9D and 9E). Nor were there differences

between these groups with respect to resting $[Ca^{2+}]_i$, or the magnitude of the evoked Ca^{2+} transient.

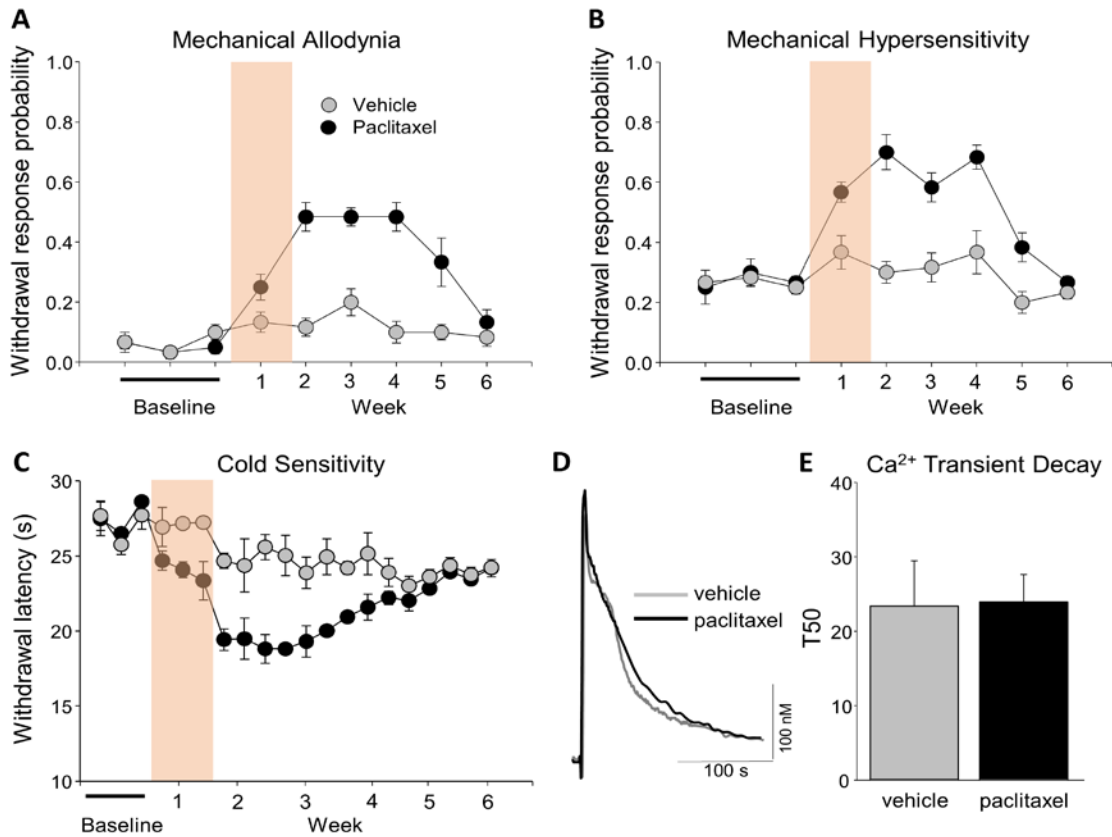


Figure 9. The recovery of the paclitaxel-induced decrease in the duration of the depolarization evoked Ca^{2+} transient correlates with the resolution of paclitaxel-induced hypersensitivity. Paclitaxel (black circles) administered at 2 mg/kg every other day for a total of 4 injections (pink column) induced mechanical allodynia (A), hyperalgesia (B), and cold sensitivity (C), as assessed with 4 g and 15 g Von Frey filaments, and the dry ice test, respectively. No changes in nociceptive behavior were observed in vehicle treated (grey circles) animals. Following resolution of behavioral sensitivity (at week 6), acutely dissociated DRG neurons retrogradely labeled from the glabrous skin of the hindpaw were studied with Ca^{2+} imaging. High K^+ (30 mM, 4 sec) evoked transients in putative nociceptive neurons (IB4+, capsaicin sensitive, small diameter) from vehicle- (grey trace) and paclitaxel-treated (black trace) rats were comparable (D). Pooled data (E) confirmed the absence of a significant difference in the duration of evoked Ca^{2+} transients, quantified as the time to decay 50 percent of the magnitude of the evoked Ca^{2+} transient. The number of neurons in each group is in parenthesis in each bar.

4.3.2 Mitochondrial $[Ca^{2+}]_i$ buffering is increased in putative nociceptive glabrous skin neurons from paclitaxel-treated rats.

Evoked Ca^{2+} transients in putative nociceptive neurons is generally bi-phasic, with a rapidly decaying phase followed by a more slowly decaying phase the results in the emergence of a “shoulder” at 30-40% of the peak increase (Figure 10A). Mitochondrial “buffering” of Ca^{2+} is thought to contribute to this unique decay profile: The initial decay of the evoked transient is due to the rapid uptake of cytosolic Ca^{2+} by mitochondria via the mitochondrial Ca^{2+} uniporter (MCU), while the “shoulder” is due to the slow release of Ca^{2+} from mitochondria via the mitochondrial Na^+/Li^+-Ca^{2+} -exchanger (NLCX) (Werth and Thayer, 1994, Rizzuto et al., 2012). One prediction of this model is that if mitochondrial Ca^{2+} uptake is increased, the rapid phase would make up a greater proportion of the transient and the slow-decaying phase would become even slower. To test this prediction, we performed a more detailed analysis of the evoked Ca^{2+} transient decay in glabrous putative nociceptive skin neurons from vehicle- and paclitaxel-treated rats. Results of this analysis indicate that while there was no detectable influence of paclitaxel on the relative contribution of rapid component of the overall decay of the evoked Ca^{2+} transient, the duration of the evoked transient was significantly shorter throughout the decay of the evoked transient in neurons ($n = 18$) from paclitaxel treated rats compared to neurons from vehicle treated rats ($n = 18$, Figure 10B).

To more directly assess the contribution of mitochondria to the decay of the evoked Ca^{2+} transient we assessed the impact of pharmacologically blocking mitochondrial Ca^{2+} buffering in neurons from vehicle- and paclitaxel-treated rats on the evoked Ca^{2+} transient. Furthermore, based on previous data indicating that the impact of paclitaxel is significantly greater in glabrous skin neurons, than in neurons innervating structures such as the dorsal skin of the hindpaw of the

inner thigh, where there was no detectable changes in mechanical sensitivity, we also assessed the impact of blocking mitochondrial Ca^{2+} uptake in neurons innervating these structures from vehicle- and paclitaxel-treated rats. Mitochondrial Ca^{2+} uptake depends on an intact mitochondrial membrane potential and uncouplers such as CCCP and FCCP are widely used to diminish the Ca^{2+} uptake into these organelles (Hajnoczky et al., 2006). To block mitochondrial Ca^{2+} uptake without ATP depletion due to the membrane potential loss-induced reversal of the ATP synthase (Hogan et al., 2014), we applied the uncoupler CCCP together with ATP synthase inhibitor oligomycin (Figure 10C). Application of CCCP/oligomycin caused an increase in the duration of evoked Ca^{2+} transient duration in all putative nociceptors (Figure 10D). However the CCCP/Oligomycin-induced increase in the transient duration was significantly ($p < 0.01$, two-way ANOVA, with the Holm-Sidak post-hoc test) larger in glabrous putative nociceptive neurons from paclitaxel-treated rats ($n = 13$) when compared to all other groups included in the analysis. These included unlabeled neurons from the same coverslips ($n = 15$), glabrous skin neurons from vehicle treated rats ($n = 13$), and dorsal skin neurons of the hindpaw ($n = 10$, and 11) or inner thigh neurons ($n = 12$ and 8) from vehicle- and paclitaxel-treated rats (Figure 10D). To determine whether there were differences between groups of putative nociceptive neurons defined by target of innervation with respect to the CCCP/Oligomycin-induced increase in the duration of the evoked Ca^{2+} transient, data from paclitaxel treated rats were analyzed as a fold change from respective vehicle neurons. Pooled data were analyzed with a one-way ANOVA that indicated there was a significant difference between groups ($p < 0.01$). Post-hoc analysis showed that while there was no difference among unlabeled, hairy hindpaw, and thigh skin neurons with respect to the CCCP/Oligomycin-induced increase in T50, the increase in the

duration of the evoked transient in putative nociceptive glabrous skin neurons was significantly greater than that in other neurons (Figure 10E).

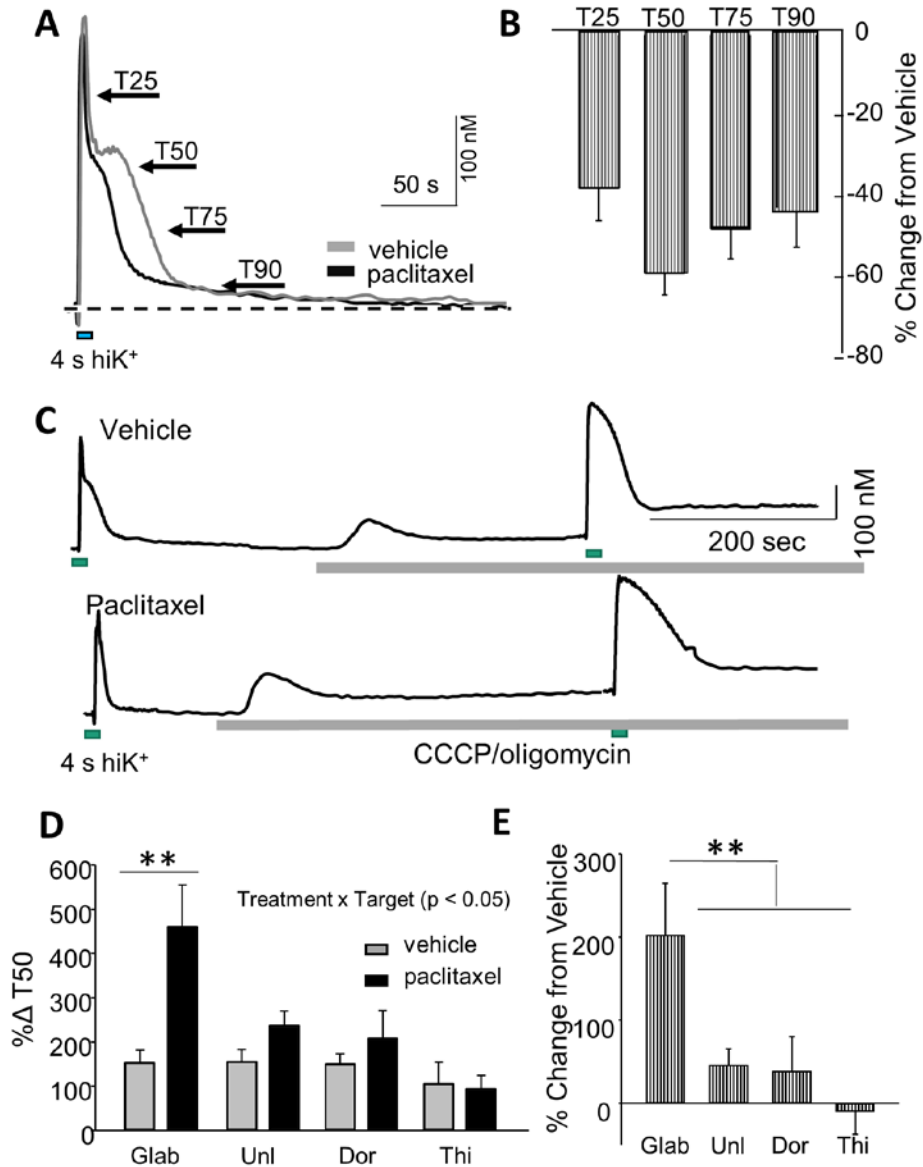


Figure 10. Mitochondrial [Ca²⁺]_i buffering is increased in putative nociceptive glabrous skin neurons from paclitaxel-treated rats. Consistent with previous results, and in marked contrast to the evoked Ca²⁺ transients 6 weeks after the last paclitaxel injection, the duration of the Ca²⁺ transient evoked with high K⁺ (30 mM, 4 sec (hiK⁺)) was significantly shorter in putative nociceptive neurons from paclitaxel treated rats, one week after the last

paclitaxel injection (A). This appeared to be true throughout the transient decay. When analyzed as the time to decay 25 (T25), 50 (T50), 75 (T75), and 90 (T90) percent of the peak of the evoked Ca^{2+} transient (as indicated in A), pooled data confirmed that the duration was significantly reduced at each of these time points compared to neurons from vehicle treated rats ($p < 0.01$, two-way ANOVA). Data plotted were calculated as a percent change from neurons from vehicle treated rats (B). (C) Representative hiK⁺ evoked Ca^{2+} transients from putative nociceptive glabrous skin neurons from vehicle (top) and paclitaxel (bottom) treated rats before and after application CCCP (10 μM) and oligomycin (10 μM). (D) The increase in the duration of the evoked Ca^{2+} transient in the presence of CCCP/oligomycin, was analyzed as a percent change from baseline at T50. Analysis of pooled data from putative nociceptive glabrous skin (Glab), unlabeled (Unl), dorsal hindpaw skin (Dor), and inner thigh skin (Thi) neurons from vehicle (gray bars) and paclitaxel (black bars) treated rats revealed a significant interaction between paclitaxel treatment and target of innervation. (E) To determine whether the relative increase observed in glabrous skin neurons from paclitaxel treated rats was significant, data were analyzed as a percent change from vehicle. The difference between groups was significant ($p < 0.01$, one-way ANOVA). The number of neurons in each group is in parenthesis in each bar. ** is $p < 0.01$.

4.3.3 While there are differences between putative nociceptive and non-nociceptive DRG neurons with respect to resting mitochondrial Ca^{2+} levels, paclitaxel was not associated with an increase in mitochondrial Ca^{2+} uptake in putative nociceptive glabrous skin neurons.

Because our results with CCCP/Oligomycin suggested that a relative increase in the contribution of mitochondrial Ca^{2+} uptake contributed to the observed decrease in the duration of the evoked Ca^{2+} transient in putative nociceptive glabrous skin neurons, we next sought to determine whether this influence of mitochondria was due to an increase in the amount of Ca^{2+} taken up by mitochondria. To address this issue, mitochondrial Ca^{2+} levels were assessed with Rhod-2

(Fonteriz et al., 2010). We first confirmed that depolarization-evoked Rhod-2 transients reflected changes in mitochondria Ca^{2+} levels by demonstrating that the evoked Rhod-2 transient could be blocked following treatment with CCCP/Oligomycin (Figure 11A). Interestingly, in neurons from naïve rats, resting Rhod-2 levels were significantly ($p < 0.05$) higher in putative non-nociceptive neurons ($n = 6$, large cell body diameter, IB4(-), capsaicin unresponsive), than in small diameter ($n = 17$) IB4(+) capsaicin(+) neurons (Figure 11B) and the magnitude of the depolarization evoked Rhod-2 transient was significantly smaller ($p < 0.01$) in putative non-nociceptive neurons (Figure 11C and 11D), although there was no difference between these two groups with respect to the duration ($p > 0.05$) of the depolarization evoked Rhod-2 transient (Figure 3E). More importantly, there was no detectable influence of paclitaxel on either resting Rhod-2 levels, on either the magnitude or duration of the depolarization-induced increase in Rhod-2 levels, in putative nociceptive glabrous skin neurons ($n = 14$), compared to neurons from vehicle treated rats ($n = 15$, Figure 11F, 11G, and 11H).

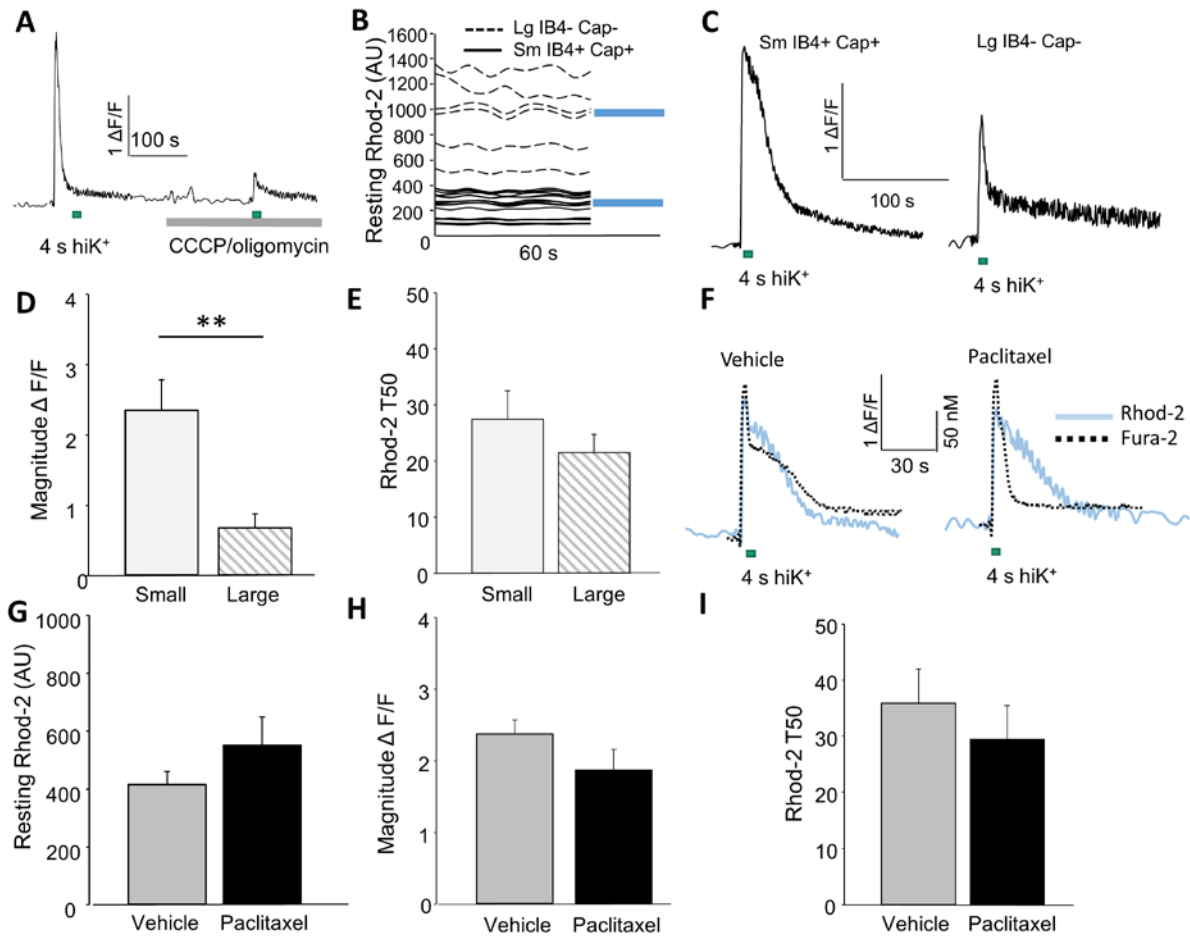


Figure 11. Paclitaxel was not associated with an increase in mitochondrial Ca^{2+} uptake in putative nociceptive glabrous skin neurons. (A) To confirm that Rhod-2 fluorescence reflected changes in mitochondrial Ca^{2+} levels, high K^+ (30 mM, 4 sec) was used to evoke a Ca^{2+} transient a naïve neuron before and after application of CCCP/oligomycin. Similar results were obtained in the 10 other neurons tested in this manner. (B) Distribution of resting Rhod-2 intensity levels in arbitrary units, in the absence of stimulation in small diameter IB4+ capsaicin responsive (sm IB4+ cap+, solid traces) and large diameter IB4- neurons unresponsive to capsaicin (lg IB4- cap-, dotted traces) from naïve rats. Solid bars indicate the mean of each group, which were significantly different ($p < 0.01$). (C) Typical high K^+ (30 mM, 4 sec) evoked increases in Rhod-2 fluorescence a small diameter IB4+ capsaicin+ neuron and a large diameter IB4- capsaicin- neuron from a naïve rat. Both the magnitude and the time-course of decay appear to be different. Pooled data confirmed this impression for magnitude (D) but not duration (E) when analyzed as a T50. However, the T25 and the T90 were different between these subpopulations of neurons. (F) Typical high K^+ (30 mM, 4 sec) evoked increases in Rhod-2 fluorescence (blue traces) recorded simultaneously

with Fura-2 (dotted black traces), in putative nociceptive glabrous skin neurons from vehicle (left) and paclitaxel (right) treated rats. Pooled resting (**G**), and evoked (magnitude (**H**) and T50 duration (**I**)) Rhod-2 data from glabrous skin neurons from vehicle and paclitaxel treated rats. Note the absence of a significant difference between groups, even for duration, in contrast to the significant decrease in the duration of the fura-2 signal in neurons from paclitaxel treated rats. The number of neurons in each group is in parenthesis in each bar. ** is $p < 0.01$.

4.3.4 Paclitaxel is associated with an increase in mitochondria in putative nociceptive glabrous skin neurons.

Our results with CCCP/Oligomycin and Rhod-2 raised the possibility that the apparent increase in mitochondrial Ca^{2+} buffering in neurons from paclitaxel treated rats was due to an increase in the number of mitochondria in these neurons. Three additional experiments were used to test this possibility. The first of these involved the use of mitotracker green, a fluorescent compound that binds to thiol groups on mitochondria, enabling an estimation of total mitochondria from the relative intensity of the mitrotracker fluorescence (Cottet-Rousselle et al., 2011). Putative nociceptive neurons targeting either the glabrous, dorsal hindpaw, or inner thigh skin from naïve, vehicle-, and paclitaxel-treated rats were studied. The neurons from each group were analyzed in parallel with the same confocal settings for image acquisition. The average fluorescence intensity per unit area was determined for each neuron, by dividing the cumulative intensity over the entire cell area, minus the area of the nucleus (Figure 12A). Representative images (Figure 12A) suggested that mitotracker levels were higher in glabrous neurons from paclitaxel treated rats (Figure 12A). Pooled data confirmed this impression, as the fluorescence per μm^2 in glabrous neurons from paclitaxel treated rats ($n = 50$) was significantly ($p < 0.01$, Holm-Sidak post-hoc test), higher than that in glabrous neurons from vehicle or naïve rats ($n = 26$ (naïve) and 41

(vehicle)), or from dorsal hindpaw (n = 20, 30, 36) or thigh skin (n = 23, 29, 31) neurons from naïve, vehicle treated, or paclitaxel treated rats, respectively (Figure 12B and 12C).

Because an increase in mitotracker fluorescence, may reflect an increase in the thiol groups the dye binds to rather than an increase in mitochondria number, we performed a second complimentary experiment using the antibody against the 20 kDa mitochondrial protein, translocase of outer membrane 20 (Tom20). Only small diameter IB4(+) glabrous skin neurons from naïve, vehicle-treated and paclitaxel-treated rats were studied. As with mitotracker, there appeared to be more Tom20 staining in neurons from paclitaxel treated rats, than from vehicle treated rats (Figure 12D). Pooled data again confirmed this impression, as the fluorescence per μm^2 , in neurons from paclitaxel treated rats (n = 19) was significantly higher than that in neurons from vehicle (n = 19) rats (Figure 12E, t-test, $p < 0.05$).

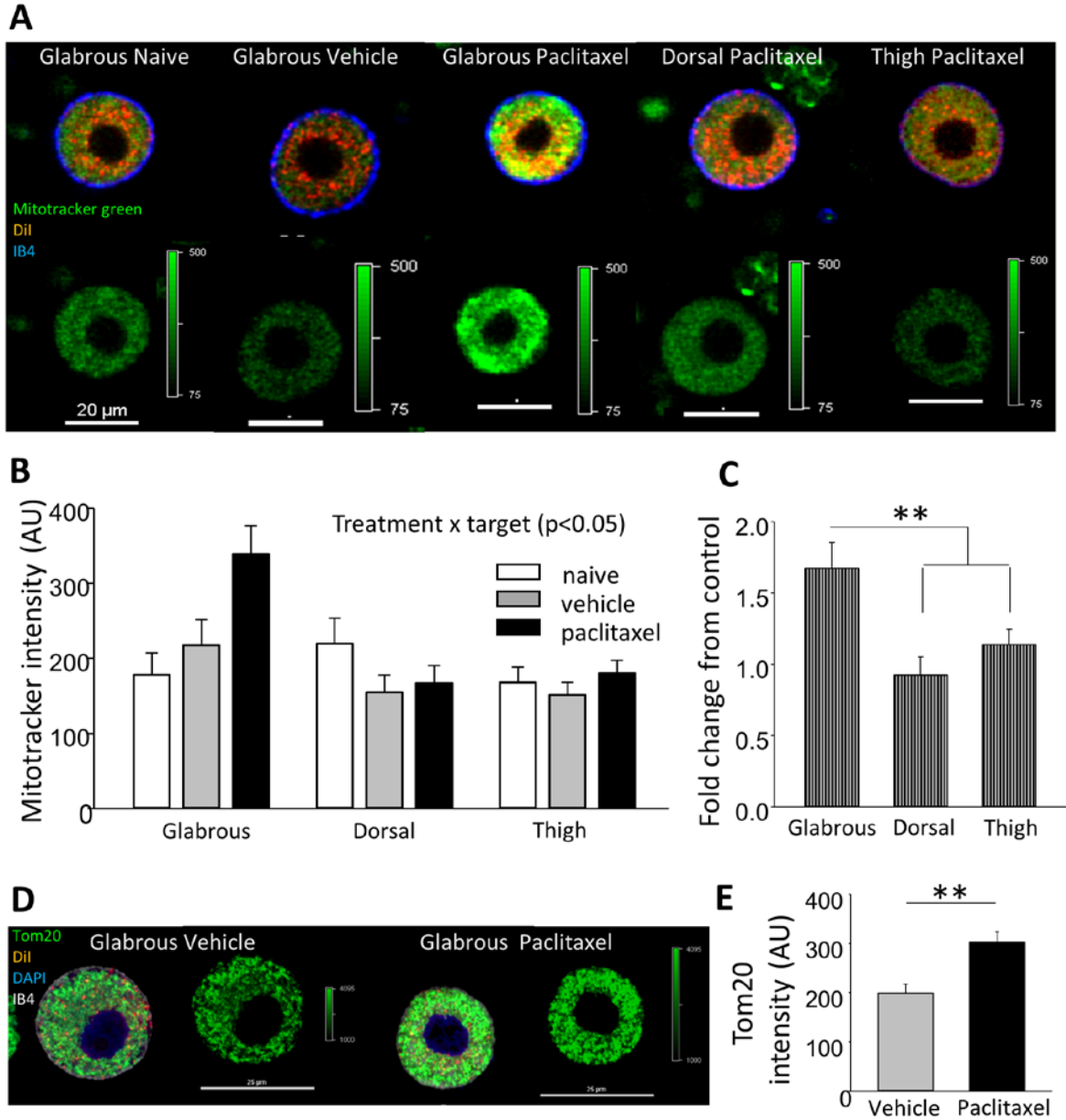


Figure 12. Paclitaxel is associated with an increase in the mitochondria in putative nociceptive glabrous skin neurons. (A) Live-cell confocal microscopy composite (top; green = mitotracker green, orange-red = DiI, blue = IB4) and mitotracker green (bottom) images of neurons from naïve, vehicle, and paclitaxel treated rats innervating the glabrous skin of the hindpaw, dorsal hindpaw, and inner thigh skin from paclitaxel treated rats. (B) Pooled mitotracker green intensity data from neurons from naïve (white bars), vehicle treated (gray bars), and paclitaxel treated (black bars) rats innervating the glabrous hindpaw, dorsal hindpaw, and inner thigh skin. There was a significant ($p < 0.05$, two-way ANOVA) interaction between paclitaxel treatment and target of innervation. (C) As

in Figure 3, to determine whether the change in mitotracker staining was significant between groups, data were analyzed as a percent change from control. In this case, because there were no detectable differences between neurons from naïve and vehicle treated rats, data from these two groups of neurons were pooled for each target of innervation. The difference between groups defined by target of innervation was significant ($p < 0.01$, one way ANOVA). Composite (top; green = Tom20, orange-red = DiI, DAPI = blue, light gray = IB4) and Tom20 (bottom) images (**D**) and pooled data (**E**) from glabrous skin neurons from vehicle and paclitaxel treated rats. Scale bars are $20\ \mu\text{m}$ for all neurons in (**A**) and $25\ \mu\text{m}$ for neurons in (**D**). The number of neurons in each group is in parenthesis in each bar. ** is $p < 0.01$.

Finally, to confirm that the increase in Tom20 staining was due to an increase in mitochondria, neurons from each group were analyzed with higher resolution imaging techniques combined with image deconvolution post-processing, to enable resolution of individual mitochondria in each neuron. With post-processing in which the same settings were used to analyze the Tom20 staining pattern, it was possible to estimate the relative volume, size, and number of mitochondria in each neuron. (Figure 13A). Pooled data indicate that total mitochondrial volume was increased in putative nociceptive glabrous skin neurons from paclitaxel-treated rats ($19.41 \pm 5.53\%$, $n = 9$) when compared to vehicle controls ($6.96 \pm 2.16\%$, $n = 11$; Figure 13B, $p < 0.05$). This increase in volume was not due to increase in number of mitochondria in neurons from paclitaxel treated rats, which was, in fact, significantly smaller in neurons from paclitaxel treated rats than vehicle treated rats (Figure 13C, $p < 0.05$). Rather, the difference in mitochondrial volume appeared to be due to formation of so called “megamitochondria” (Wakabayashi, 2002) which presented itself as large networks of interconnected mitochondria and thus fewer smaller mitochondria.

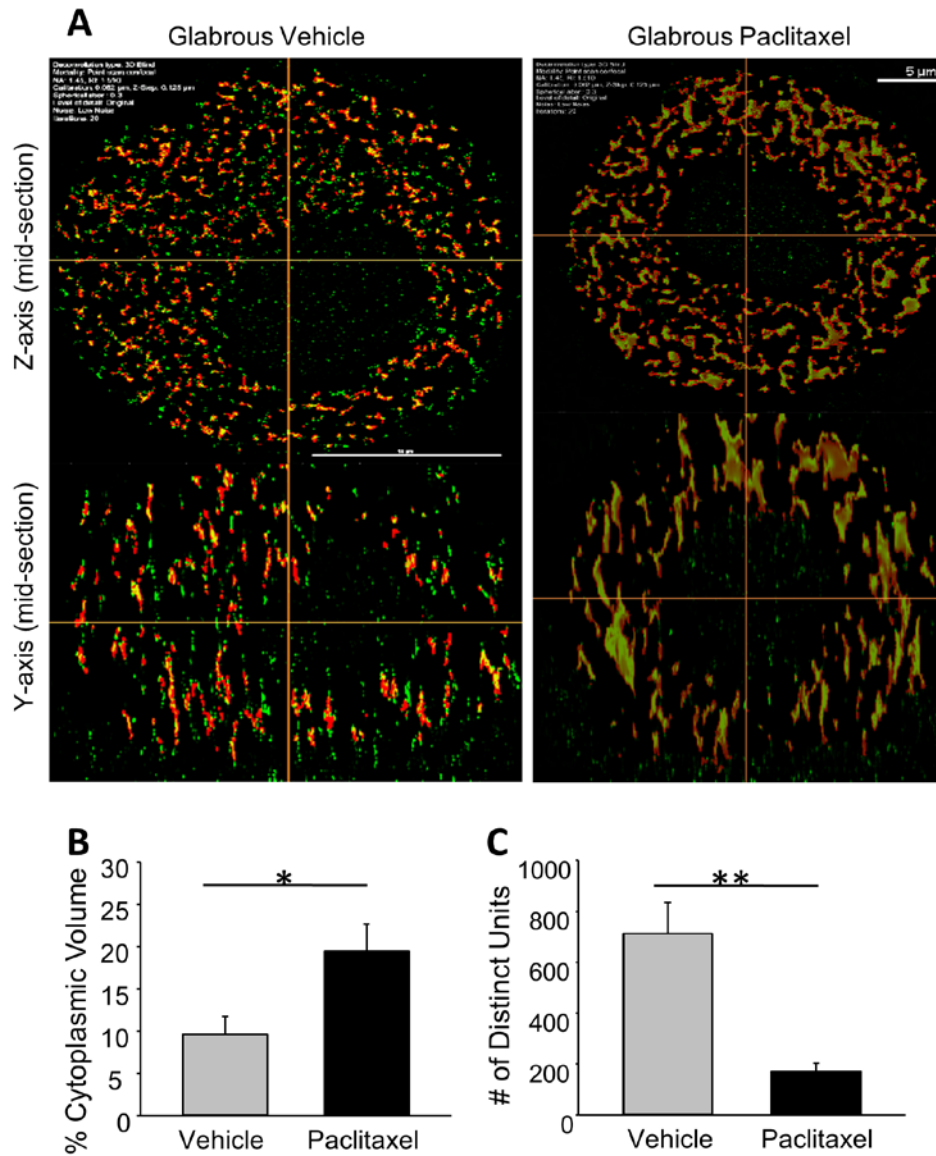


Figure 13. Paclitaxel is associated with an increase in the mitochondrial volume in putative nociceptive glabrous skin neurons. (A) Confocal images of Tom20 staining (top = mid-section on the z-axis, bottom – mid-section on the y-axis) in neurons from vehicle (left) and paclitaxel (right) treated rats. Images were post-processed with 20 deconvolution iterations, to enable resolution of individual mitochondria. Predicted mitochondria as determined with deconvolution are outlined in red. Pooled data from 8 neurons in each group analyzed as in A, for percent cytoplasmic volume comprised of mitochondria (B) and number of distinct mitochondria units (C). * is $p < 0.05$ and ** is $p < 0.01$.

4.3.5 Paclitaxel does not reduce the health and functionality of mitochondria in putative nociceptive glabrous skin neurons.

Studies have shown that bath application of paclitaxel to a variety of cell types is capable of causing damage to mitochondria (Andre et al., 2000, Goncalves et al., 2000). As noted above, there is also ample evidence that mitochondria in sensory neuron axons are damaged by paclitaxel treatment (Flatters and Bennett, 2006, Xiao et al., 2011). Therefore it is possible that the increase in mitochondrial volume in putative nociceptive glabrous skin neurons was a reflection of some of this damage, such as swelling. Two additional experiments were performed to address this possibility. First, we used confocal live imaging of neurons labeled with the mitochondrial membrane potential dependent dye TMRM. The intensity of TMRM staining correlates with the mitochondrial membrane potential; higher TMRM staining intensity is observed in mitochondria that are relatively hyperpolarized (Gerencser et al., 2012). Similarly, the mitochondrial membrane potential is indicative of mitochondrial functionality since the membrane potential is necessary for essential functions such as ATP synthesis and Ca^{2+} uptake (Hajnoczky et al., 2006, Gerencser et al., 2012). We first confirmed that TMRM staining reflected the mitochondrial membrane potential by demonstrating that TMRM staining is completely eliminated with CCCP/Oligomycin (Figure 14A). Interestingly, consistent with our Rhod-2 data, TMRM staining was significantly higher in putative non-nociceptive neurons than putative nociceptive neurons from naïve rats (Figure 14B and 14C, $p < 0.05$). More interestingly, and in contrast to the prediction that total TMRM fluorescence would be lower in neurons from paclitaxel treated rats because of the presence of unhealthy mitochondria, the TMRM fluorescence intensity was higher ($p < 0.05$, one way ANOVA, Holm-Sidak post-hoc) in neurons

from paclitaxel-treated rats ($n = 25$) than in naïve controls ($n = 18$). However, the difference between paclitaxel-treated and vehicle treated ($n = 20$) was not significant (Figure 14D).

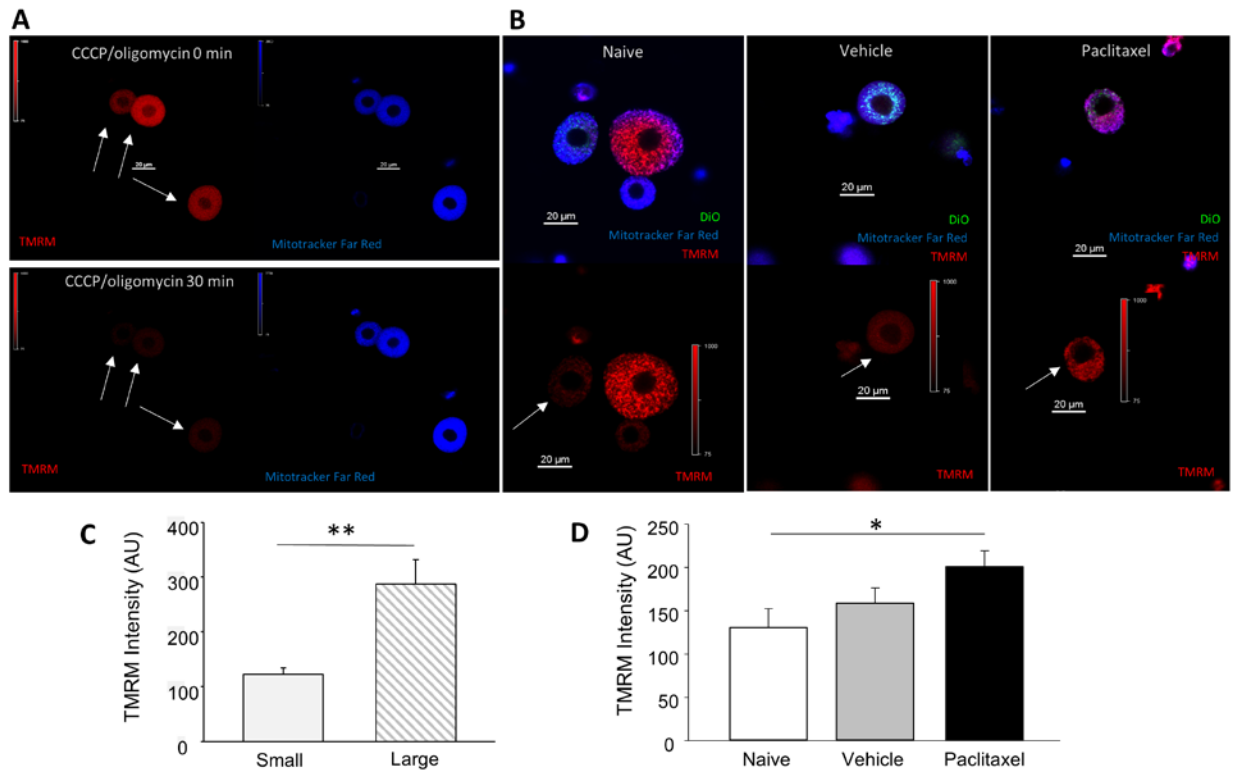


Figure 14. Paclitaxel does not reduce the functionality of mitochondria in putative nociceptive glabrous skin neurons. (A) To confirm TMRM fluorescence was associated with the mitochondrial membrane potential, TMRM was assessed before and after depolarizing mitochondria with CCCP/oligomycin with live cell confocal microscopy. Images with TMRM (left, red = TMRM) and mitotracker far red (right, blue = mitotracker far red) are from the same naïve neurons before (top) and 30 minutes after (bottom) the addition of CCCP/oligomycin. (B) Composite (top; red = TMRM, blue = mitotracker far red, green = DiO) and TMRM (bottom) live cell confocal microscopy images from naïve (left), vehicle treated (middle), paclitaxel treated (right) neurons. (C) Pooled TMRM intensity data from small diameter IB4+ and large diameter IB4- neurons from naïve rats. (D) Pooled TMRM intensity data from neurons from naïve (white bar), vehicle treated (gray bar) and paclitaxel treated (black bar) rats. The number of neurons in each group is in parenthesis in each bar. Scale bars are 20 μm for all panels, * is $p < 0.05$ and ** is $p < 0.01$.

Evidence suggests that 1–2% of oxygen consumed is converted into superoxide due to transfer of electrons that have leaked from the electron transfer chain to oxygen molecules during oxidative phosphorylation (Orrenius et al., 2007). Moreover, under certain conditions, such as cellular stress or mitochondrial damage, there is a surge in the number of leaked electrons, resulting in an increase in the generation of mitochondrial superoxide (West et al., 2011). Thus, to further assess the presence of a subpopulation of damaged mitochondria in neurons from paclitaxel treated rats, we tested in sister coverslips the mitochondrial superoxide indicator, MitoSox Red. While Antimycin A, which was used as a positive control for driving an increase in mitochondrial superoxide generation (Polster et al., 2014), produced an increase in MitoSox Red staining in DRG neurons (Figure 15A), there was no detectable difference between putative nociceptive neurons innervating the glabrous skin from naïve (n = 13), vehicle- (n = 14), and paclitaxel-treated (n = 14) rats, with respect to the intensity of MitoSox Red staining (Figure 15B, 15C, and 15D, $p > 0.05$).

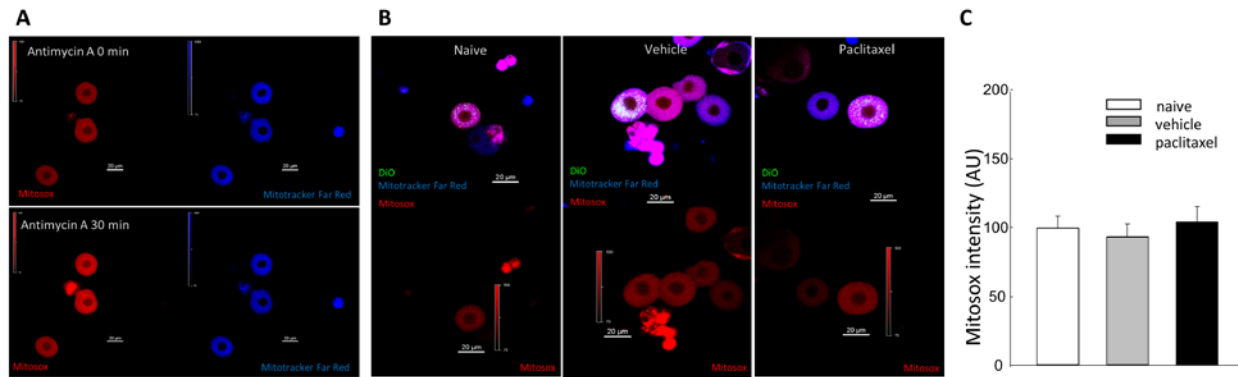


Figure 15. Paclitaxel does not reduce the health of mitochondria in putative nociceptive glabrous skin neurons. (A) To confirm that it was possible to detect an increase in mitosox staining in neurons in which there was an increase in superoxide, neurons were studied with live confocal imaging before (top) and after (bottom) a 30 min application of antimycin A to induce mitochondrial superoxide production. Mitosox Red (left, red = mitosox) and mitotracker far red (right, blue = mitotracker far red), were monitored in the same neurons. (B) Composite (top; red = mitosox, blue = mitotracker far red, green = DiO) and mitosox (bottom) images from neurons from naïve (left), vehicle treated (middle), paclitaxel treated (right) rats. (C) Pooled data from glabrous skin neurons from the three groups of rats shown in B. The number of neurons in each group is in parenthesis in each bar. Scale bars are 20 μ m for all panels.

4.3.6 Paclitaxel increases ATP-dependent Ca^{2+} uptake into endoplasmic reticulum.

There are two other major regulators of the duration of evoked Ca^{2+} transients, SERCA and PMCA (Lu et al., 2006, Gemes et al., 2012, Duncan et al., 2013). Interestingly, both of these proteins are membrane bound Ca^{2+} pumps that utilize the energy released from ATP hydrolysis to reduce the $[\text{Ca}^{2+}]_i$ (Demaurex et al., 2009). Moreover mitochondria can act as Ca^{2+} relay centers by quickly taking up the increased $[\text{Ca}^{2+}]_i$ and then releasing it through NLCX at specific domains near SERCA (Demaurex et al., 2009, Takeuchi et al., 2015). This relay process have been suggested to play a significant role in the refilling of intracellular Ca^{2+} stores, enabling Ca^{2+}

funneling to these stores even without detectable changes in $[Ca^{2+}]_i$ (Demaurex et al., 2009). Therefore it is possible that mitochondria also contribute to the attenuation of the evoked transient in neurons from paclitaxel treated rats via indirectly facilitating Ca^{2+} uptake via SERCA. We tested this possibility indirectly with Fura-2 imaging before and after blocking SERCA activity with the SERCA inhibitor CPA. Inhibition of SERCA resulted in significant increases in the duration of the evoked Ca^{2+} transient in neurons from both vehicle- and paclitaxel-treated rats (Figure 16A), suggesting SERCA contributes to the regulation of the duration of the evoked transient in putative nociceptive glabrous skin neurons. However, the relative increase in the Ca^{2+} transient duration after CPA application was significantly larger in neurons from paclitaxel-treated rats when compared to vehicle controls (Figure 16B, $n = 31$ (paclitaxel) $n = 27$ (vehicle) $p < 0.05$).

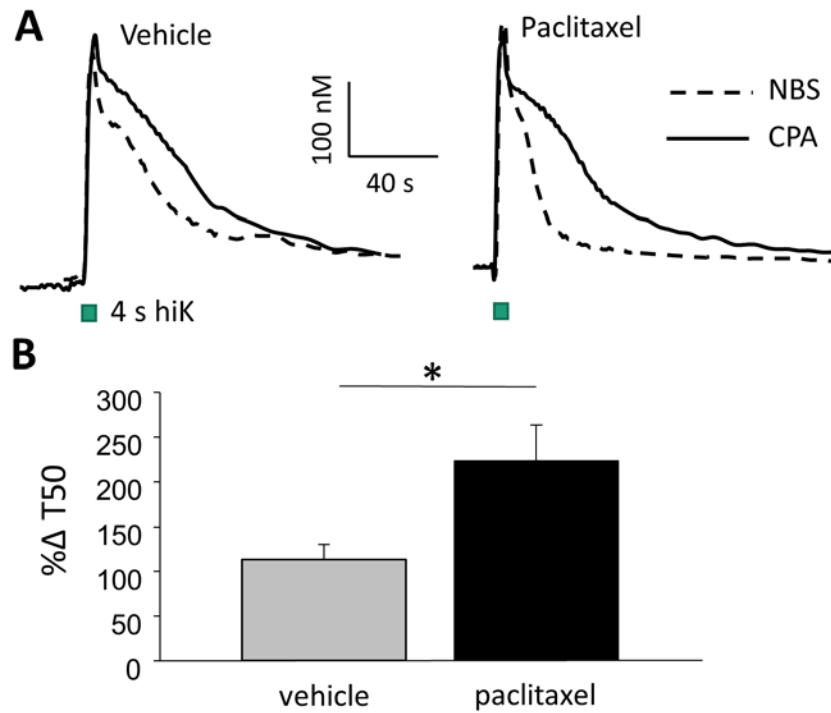


Figure 16. Paclitaxel increases ATP-dependent Ca^{2+} uptake into endoplasmic reticulum. (A) Fura-2 was used to assess high K^+ (30 mM, 4 seconds) evoked Ca^{2+} transients in glabrous skin neurons from vehicle and paclitaxel treated rats before and after blocking SERCA with CPA (10 μM). To assess the impact of CPA on the duration of the evoked Ca^{2+} transient, data obtained in the presence of CPA were analyzed as a percent change from baseline T50. (B) Pooled data from neurons analyzed in this way indicated that the relative increase in putative nociceptive glabrous skin neurons from paclitaxel treated rats was significantly greater than that in vehicle treated rats. The number of neurons in each group is in parenthesis in each bar. * is $p < 0.05$.

4.4 DISCUSSION

The purpose of this study was to begin to test the hypothesis that CIPN is due to both increases and decreases in mitochondria function, with changes manifest in distinct subpopulations of afferents. We started by further testing the association between the changes in Ca^{2+} regulation and the changes in nociceptive behavior: changes in Ca^{2+} regulation were no longer detectable at a time point when paclitaxel-induced hypersensitivity had fully resolved. A detailed time course analysis of depolarization-evoked Ca^{2+} transients revealed that while the duration of the evoked transient was significantly shorter throughout the decay in neurons from paclitaxel-treated rats, the overall shape of the transient, thought to reflect mitochondrial Ca^{2+} uptake and release, was unchanged. Nevertheless, the relative impact of pharmacologically blocking mitochondrial Ca^{2+} uptake resulted in a significantly larger increase in the duration of the evoked Ca^{2+} transient in putative nociceptive glabrous skin neurons from paclitaxel treated rats than that in glabrous skin neurons from vehicle treated or naïve rats, or from hindpaw hairy skin or inner thigh skin neurons from paclitaxel treated or control rats. However, there was no detectable difference in relative amount of Ca^{2+} taken up by mitochondria in neurons from paclitaxel-treated rats. In contrast, staining intensities of mitochondrial markers were significantly higher in putative nociceptive glabrous skin neurons from paclitaxel-treated rats than in neurons from control rats or those innervating hairy hindpaw or thigh skin. Higher resolution analysis of mitochondria in sensory neurons revealed an increase in mitochondrial volume. Furthermore, while there were differences between putative nociceptive and non-nociceptive neurons with respect to mitochondria resting membrane potential, there was no evidence of mitochondria with a low resting membrane potential in putative nociceptive glabrous skin neurons from paclitaxel treated rats. In addition, neurons from paclitaxel-treated rats had levels of mitochondrial superoxide

comparable to controls. Finally, in addition to an increase in a direct role for mitochondria in the attenuation of the evoked Ca^{2+} transient, we obtained evidence of an increase in an indirect role, with at least a significant increase in the contribution of SERCA to the regulation of the evoked Ca^{2+} transient in neurons from paclitaxel treated rats. Taken together our results support our initial hypothesis that CIPN is due to both increases and decreases in mitochondria function, with changes manifest in distinct subpopulations of afferents.

The resolution of the paclitaxel-induced decrease in the evoked Ca^{2+} transient duration in neurons from rats in which cold/mechanical hypersensitivity had also resolved does not mean that these two phenomena are causally linked. However, the persistence of the Ca^{2+} dysregulation in neurons from rats in which hypersensitivity had resolved would have suggested that the changes in Ca^{2+} regulation are not sufficient to maintain hypersensitivity. That said, given the importance of the tight regulation of $[\text{Ca}^{2+}]_i$ for numerous cellular processes and that the observation of the paclitaxel-induced decrease in the evoked Ca^{2+} transient duration is limited to a specific subpopulation of neurons, establishing a causal link between the decrease in the evoked Ca^{2+} transient and pain associated with CIPN will not be easy. A more detailed analysis of the time-course of the changes in Ca^{2+} regulation may help in this regard, if only to enable rejection of the hypothesis. The use of IB4-saporin, to eliminate the neurons in which the changes are manifest, as we have done previously (Scheff et al., 2014), would also help in this regard. It may also be possible to acutely manipulate Ca^{2+} levels in sensory neurons with Ca^{2+} ionophores, or Ca^{2+} uptake with blockers, as was done previously in a model of CIPN (Siau and Bennett, 2006). With respect to the specific role for mitochondrial Ca^{2+} , it would be possible to target the uniporter pharmacologically, where a block of MCU would be expected to normalize pain behavior. While genetic strategies may also enable a more targeted approach, we suggest

that the first step should be to determine where in the sensory neuron, the changes in Ca^{2+} regulation are manifest, and now that we have identified a potential mechanism underlying these changes, such experiments should be possible.

The time course of the paclitaxel-induced mechanical sensitivity observed in the present study was consistent with that previously described (Cata et al., 2008). However, there is evidence that mechanical hypersensitivity may persist for considerably longer (Flatters and Bennett, 2006). While additional factors may contribute to the relative duration of the hypersensitivity, we suggest one likely factor is the route of paclitaxel administration: it was administered I.V. in the present study and I.P. in the study in which a more persistent hypersensitivity was observed. Given the impact of route of administration on pharmacokinetic and pharmacodynamics of the drug administered (Turner et al., 2011), combined with evidence that the signs and symptoms of CIPN are dose and treatment duration dependent dosage (Quasthoff and Hartung, 2002, Jaggi and Singh, 2012), it will be important to determine whether the more persistent hypersensitivity reflects the same underlying mechanisms. In this regard, it was interesting to note that there was a difference in the resolution of cold and mechanical hypersensitivity, suggesting that there are sensory neuron subpopulation specific differences in the response to same dose and route of administered paclitaxel.

While we employed a variety of different analyses and approaches in this study, all were internally consistent and pointed to a direct role of mitochondria in the paclitaxel-induced decrease in the duration of the depolarization-evoked Ca^{2+} transient due to an increase in mitochondria size, and consequently buffering capacity, rather than a change in functionality. The CCCP/oligomycin data were consistent with an increase in the relative contribution of mitochondria to the control of the duration of the evoked Ca^{2+} transient in neurons from

paclitaxel treated rats. The results of the detailed analysis of the decay of the Ca^{2+} transient were consistent with an increase in the total mitochondrial buffering capacity rather than a shift in functionality, as changes to either uptake or release should have resulted in changes to the fast and/or slow components of the transient, and/or the relative proportion of the decay accounted for by either component. Consistent with this interpretation, the TMRM data argued against a change in mitochondrial resting membrane potential, where hyperpolarization could have contributed to faster Ca^{2+} uptake and/or a slower release. Conversely, the presence of even a subpopulation of damaged mitochondria with a low resting membrane potential should have resulted in a decrease in average TMRM signal. The absence of a change in mitochondrial resting membrane potential was confirmed with the Rhod-2 data, which indicated that there was no influence of paclitaxel on either the magnitude of the mitochondrial Ca^{2+} uptake, or the rate of release. These data also argue against paclitaxel-induced changes in either MCU or NCLX activity. Similarly, the absence of a detectable influence of paclitaxel on mitoxox staining, argues against the presence of even a subpopulation of injured mitochondria. On the other hand, the increase in mitotracker and Tom20 staining both point to an increase in mitochondria, where the higher resolution of the Tom20 data confirmed the increase in total mitochondria volume. Importantly, the presence of an increase in Tom20 in cutaneous afferent somata in situ, suggests that the changes observed in the present study are not an artifact of cell culture. Thus, in stark contrast to the chemotherapeutic-induced mitotoxicity described in sensory axons, the chemotherapeutic-induced changes in Ca^{2+} regulation in the cell body, appear to be due, at least in part, to an increase in otherwise healthy mitochondria.

It is known that mitochondria form a complex reticulum in many cell types (Sukhorukov et al., 2012, Schwarz, 2013, Glancy et al., 2015), however axonal mitochondria are separated from

this network and observed as individual entities of typically 1-3 μm in length (Schwarz, 2013). Our high resolution imaging results indicate a paclitaxel induced increase in mitochondrial volume that was reflected as an enlargement of the interconnected mitochondrial network and reduction of the number of individual smaller mitochondria. However, we cannot rule out the possibility that paclitaxel-induced increase in mitochondrial volume is due to an increase in the number of mitochondria in very close proximity that is below the resolution limit of imaging techniques employed. Additional higher-resolution techniques may be required to determine the nature of the paclitaxel-induced changes in mitochondrial volume.

There are several mechanisms that could account for the paclitaxel-induced increase in the total volume of mitochondria in putative nociceptors. First, it might be a reaction to a more distal insult associated with paclitaxel treatment, where an increase in density of mitochondria may enable the neurons to respond to the increased demands associated with injury. Similarly, if mitochondria in the axons are damaged, the increase in mitogenesis in the soma may enable the neuron to compensate for the loss of energy production. Such a mechanism has been described in the *Lep^r^{db/db}* diabetic neuropathy mouse model, where mitochondria are increased in DRG neurons and the dorsal root (Vincent et al., 2010), which was suggested to compensate for the decrease in ATP production (Vincent et al., 2010, Bennett et al., 2014). Moreover, a large network of mitochondria that are either interconnected or in close proximity that facilitates fusion/fission may be a mechanism to sustain mitochondrial health as fusion/fission kinetics of mitochondria are closely linked to mitochondrial health and function. Fusion is thought to protect mitochondrial function by providing an opportunity for mitochondria to mix their contents, which in turn enables efficient repairing and complementation of damaged components and functions and sharing a bigger pool of structural/functional proteins and metabolites

(Wakabayashi, 2002, Chen and Chan, 2009). Moreover, mitochondria resume normal structure and function after the response to an insult is resolved (Takeuchi et al., 2015).

Another mechanism that could account for the paclitaxel-induced increase in mitochondrial volume is a reduction in axonal transport (Gornstein and Schwarz, 2014), which may result in accumulation of mitochondria in the cell bodies. If paclitaxel treatment increases the volume of mitochondria by facilitating fusion, these organelles may also be too large or heavy to be transported along the axons.

There are at least two possibilities that can account for the apparent increase in healthy mitochondria observed in the present study in the face of all the previous data pointing to chemotherapy-induced mitotoxicity. First, it is possible that the increase in healthy mitochondria in the cell body and mitotoxicity along the axons occur in separate subpopulations of afferents. As noted previously, morphological evidence of paclitaxel-induced mitotoxicity was only present in 25 - 40 % of the small and large-diameter fibers (Flatters and Bennett, 2006, Xiao et al., 2011), and we have studied an even smaller proportion of the neurons contributing axons to the peripheral nerve. That we failed to detect a change in Ca^{2+} regulation or mitochondria in putative non-nociceptive afferents argues against a role for the changes observed in putative nociceptive glabrous skin neurons in either the numbness or tingling associated with CIPN. And to the extent to which numbness is due to the chemotherapeutic-induced decrease in intra-epidermal nerve fiber density and associated loss of Merkel cell innervation, the presence of mitotoxicity in myelinated fibers, puts this mechanism in the right population to mediate this effect. This begs the question, however, as to whether there is a subpopulation of nociceptive afferents in which mitotoxicity also accounts for the CIPN-induced pain, or whether the pain is due to the changes described in the present study.

The second possibility is that both the increase in mitochondrial volume and the mitotoxicity occur in the same subpopulation of neurons. The increase in mitochondrial volume may then be a consequence or/response to mitotoxicity in the axons as discussed above. This possibility would also beg the question as to which, if either of the two changes contribute to the pain associated with CIPN. Given the presence of Ca^{2+} -dependent K^+ channels in putative nociceptive glabrous skin neurons (Zhang et al., 2010), and the role for these channels in controlling the excitability of these neurons (Zhang et al., 2010), a paclitaxel-induced decrease in Ca^{2+} could contribute to an increase in neuronal excitability and pain secondary to the decrease in K^+ current. Minimally, however, the presence of both an increase in healthy mitochondria in the cell body and damaged mitochondria in the axons would suggest that the mitochondria damage is not initiated within the cell body as previously suggested (Xiao et al., 2011).

It is possible that paclitaxel influences SERCA activity via a mechanism independent of the changes in mitochondria. However, given that SERCA activity is ATP-dependent and that mitochondria and ER are structurally and functionally linked, especially in the context of Ca^{2+} regulation (Contreras et al., 2010, Rowland and Voeltz, 2012, Eisner et al., 2013, Marchi et al., 2014), we suggest that it is most-likely that the apparent increase in SERCA activity is secondary to the paclitaxel-induced increase in mitochondrial volume. This may be due to an associated increase in resting ATP levels and/or a more tightly coupled mitochondria and ER. Such an increase in ATP levels could also contribute to an increase in the excitability of putative nociceptive neurons secondary to an increased Na^+ - K^+ -ATPase-dependent membrane hyperpolarization. The increase in excitability would be due to the increase in voltage-gated Na^+ channels able to contribute to action potential generation following hyperpolarization-induced relief of channel inactivation.

Taken together, our study provides evidence that paclitaxel-induced decrease in evoked Ca^{2+} transient duration in glabrous putative nociceptors is mediated by mitochondria, whose structure and volume, but not health and functionality is greatly affected by this treatment. Our results argue against the notion that mitotoxicity is manifest throughout the sensory neuron, and raise the possibility that mitotoxicity is present in a subpopulation of neurons that do not contribute to the pain associated with CIPN. In addition, since these large mitochondrial networks are still functional, it may explain why clinical trials with acetyl-L-carnitine treatment that aimed to improve mitochondrial function resulted in worsening of the symptoms (Hershman et al., 2013). Moreover, our results suggest that SERCA activity also is important for paclitaxel-induced decrease in the evoked Ca^{2+} transient duration in putative nociceptors innervating the glabrous skin. Understanding the contribution of these changes in Ca^{2+} regulation as well as increased mitochondria volume to the pain associated with CIPN, may provide novel therapeutic strategies to limit the most debilitating side effects of some of the most effective cancer treatments.

5.0 DISCUSSION

5.1 SUMMARY OF THE DISSERTATION

5.1.1 The Goal of the Study

When I came to the pain research field I was intrigued by the observation that all classes of chemotherapeutics with different primary mechanisms lead to the development of CIPN, a condition with both loss- and gain-of-function symptoms and localized predominantly in soles and palms of patients. Activation of inflammatory pathways, selective damage to long axons, and mitotoxicity were proposed to underlie CIPN. There is evidence supporting the involvement, and to some degree, interdependence of these mechanisms in CIPN. However, each failed to account for all of the clinical features of this form of neuropathy. For example, the release of inflammatory mediators within DRG or spinal cord cannot explain numbness and tingling associated with CIPN and if only a mechanism of pain, it is unclear how the somatotopic manifestation of the pain is established or maintained. Similarly, while mitotoxicity could account for both the numbness and pain, this mechanism also fails to account for the somatotopic manifestation of CIPN. Even though there is evidence of the tremendous heterogeneity among sensory neurons regarding their resting properties, as well as the response to injury, the potential impact of target of innervation on CIPN has been overlooked. Moreover, regulation of Ca^{2+} in

primary afferents are of significant importance, not only in the presence of injury, but also its role in the manifestation of both positive and negative signs of neuropathic pain. Based on these lines of evidence in combination with the limitations associated with the current models of CIPN, I hypothesized that both the positive and negative signs of CIPN are due to subpopulation and target-of-innervation specific changes in Ca^{2+} regulation. Using a paclitaxel-induced peripheral neuropathy model, I set forth two specific aims to tackle this hypothesis. My first aim was to characterize paclitaxel-induced changes in Ca^{2+} regulation in different subpopulations of sensory neurons based on target of innervation. My second aim was to characterize the underlying mechanisms with paclitaxel-induced change in Ca^{2+} regulation in sensory neurons.

5.1.2 Summary of the Findings

I first showed that paclitaxel treatment was associated with mechanical hypersensitivity in the glabrous skin of the hindpaw, but not the hairy skin of the hindpaw or mid-thigh. This observation argued against the axon length hypothesis, as there should have been no difference between the glabrous and hair skin of the hindpaw with respect to the hypersensitivity detected. In contrast, it provided support for my hypothesis that painful symptoms of CIPN were due to intrinsic properties of the neurons targeting distinct areas. Further support for this hypothesis was provided by the observation that there was a significant decrease in the duration of the evoked Ca^{2+} transients in putative nociceptive afferents, which was significantly larger in neurons innervating glabrous skin than those innervating hairy skin targets. The observation that there was a correlation between the peak manifestation and recovery of hypersensitivity and the changes in Ca^{2+} regulation was consistent with the possibility that the changes in Ca^{2+} regulation contribute to the manifestation of the hypersensitivity.

The first mechanism I tested as the potential culprit for the paclitaxel-induced decrease in the transient duration in putative nociceptors was the Ca^{2+} extrusion via NCX. I hypothesized that an increase in NCX activity underlies the paclitaxel-induced change in the evoked transient because NCX is a major Ca^{2+} extrusion mechanism, is active solely in putative nociceptive DRG neurons, and contributes to the regulation of the duration but not the magnitude of the evoked Ca^{2+} transient. However, the paclitaxel-induced decrease in the duration of the evoked Ca^{2+} transient was not due to an increase in NCX activity. Nevertheless, both vehicle and paclitaxel treatments were associated with NCX sensitization and there was evidence of a compensatory Ca^{2+} regulatory mechanism in putative nociceptors innervating target areas where there was no detectable paclitaxel-induced mechanical hypersensitivity.

After ruling out NCX as the source of paclitaxel-induced decrease in the evoked Ca^{2+} transient duration, I determined whether mitochondria are directly and/or indirectly responsible for this change in the transient despite the evidence in the field suggesting paclitaxel treatment should lead to defective mitochondria. Our data argued against the notion that paclitaxel treatment is associated with defective mitochondria in all sensory neurons. Rather, the paclitaxel-induced decrease in the evoked Ca^{2+} transient duration appears to be due to an increase in both the direct and indirect involvement of mitochondrial in Ca^{2+} regulation.

Taken together, I have been able to implicate a novel mechanism of CIPN. I have also been able to uncover additional layers of sensory neuron heterogeneity based on both phenotypic characteristics and target of innervation.

5.2 COMPLEXITY OF Ca^{2+} REGULATION

There were several recurring themes that emerged at all stages of this work. One such theme was the complexity of Ca^{2+} regulation. The Ca^{2+} regulatory toolkit contains many components, all of which contribute to the Ca^{2+} maintenance and/or signaling. Moreover, some of these players have similar and overlapping functions and some of their activities are interrelated or even dependent upon the functions of the others. For example, NCX, PMCA, SERCA, and mitochondria are all working together to reduce the Ca^{2+} load following the Ca^{2+} influx through the VGCCs. Among these, mitochondria can also indirectly influence the activity/function of PMCA and SERCA by both providing ATP and by directing or diverting Ca^{2+} towards or away from these pumps. This complexity of Ca^{2+} regulation was reflected most prominently in subpopulation differences in Ca^{2+} transients in neurons from paclitaxel-treated rats; compensatory mechanisms for the vehicle-treated glabrous skin neurons as well as the paclitaxel-treated thigh skin neurons that had increased NCX activity with no detectable influence of paclitaxel on the duration of the depolarization-evoked Ca^{2+} transient in these neurons; paclitaxel-induced increase in direct Ca^{2+} uptake in mitochondria as well as indirect mitochondrial Ca^{2+} regulation via SERCA.

One problem with the complexity of Ca^{2+} regulation is the difficulty to identify differences due to potential compensatory actions of distinct regulatory components. In this regard, the main concern is that in the presence of a robust compensation, there is increased likelihood for false negatives or incorrect interpretations. For example, the virtual lack of effect of paclitaxel on Ca^{2+} transient in thigh neurons was not because there was no change in Ca^{2+} regulation but because the NCX-mediated change in Ca^{2+} regulation was compensated by

another mechanism. We could have missed this change and come to a very different conclusion about thigh neurons, if we did not include this group of neurons as a control group

Another problem with the complexity in Ca^{2+} regulation is due to difficulties to interpret results that are obtained with relatively non-specific approaches employed to study components of the Ca^{2+} regulatory toolkit. For example, Li^+ not only blocks all NCX isoforms that may be affected differently by the treatment, but there is also evidence that it can affect other Ca^{2+} regulatory components (Mo et al., 2012) or mechanisms (Mo et al., 2012) that may contribute to Ca^{2+} regulation. Similarly, the NCX3 preferring blocker KB-R7943 also has some affinity for MCU thus may affect mitochondrial Ca^{2+} uptake. Moreover, the mitochondrial uncoupler CCCP can also embed itself on the plasma membrane and cause membrane depolarization which may influence the regulation of intracellular Ca^{2+} . Therefore, using multiple approaches, such as following up CCCP/oligomycin experiments with Rhod-2 imaging, is one way to reduce the likelihood of data misinterpretation, since confirmation of the results with one approach can strengthen the interpretation of data or the lack thereof may imply an unspecific effect.

5.3 HETEROGENEITY OF NEURONS BASED ON PHENOTYPE AND TARGET OF INNERVATION

As discussed in the introduction, the heterogeneity of primary afferent neurons is well documented. For example our laboratory and others have described electrophysiological and biochemical differences among sensory neurons based on target of innervation (Yoshimura et al., 2003, Beyak et al., 2004, Gold and Traub, 2004, Harriott et al., 2006, Harriott and Gold, 2009, Vaughn and Gold, 2010, Malin et al., 2011). The results presented in this thesis work add to these observations by providing further evidence of differences in Ca^{2+} regulation. For example, both putative nociceptive and non-nociceptive neurons from naïve rats innervating the thigh skin exhibited a lower resting $[Ca^{2+}]_i$ compared to neurons innervating the glabrous or the dorsal skin of the hindpaw. In addition, putative non-nociceptive thigh skin neurons from naïve rats had a smaller magnitude of depolarization-evoked Ca^{2+} transient compared to those innervating other targets. Moreover there was evidence of different expression of NCX isoforms based on target of innervation. Previously, our group identified NCX3 to be the only active isoform in glabrous putative nociceptors, however we observed NCX1 activity in thigh putative nociceptors in this current study.

Another example of heterogeneity among subpopulations was the differences in mitochondria. There was no evidence of heterogeneity in mitotracker staining among subpopulations in naïve neurons. However, there was heterogeneity among neurons with respect to the staining intensity of TMRM, which was relatively higher in putative non-nociceptors when compared to putative nociceptors, independent of target of innervation. Similarly, Rhod2 staining was also consistently higher in putative non-nociceptors. These observations are likely linked since resting mitochondrial Ca^{2+} concentration is determined by the mitochondrial membrane

potential. In addition, ATP synthesis is directly linked to mitochondrial membrane hyperpolarization (Dimroth et al., 2000). It is possible that large diameter putative non-nociceptive neurons have higher energy needs due to relatively high levels of neural activity, as well as to keep up with maintenance of a larger cell. Therefore an increase in mitochondrial membrane potential may assure relatively high levels of ATP generation to meet the energy needs of these neurons

There is also documented heterogeneity among subpopulations defined by target of innervation with respect to the response to injury, inflammatory mediators (Gold and Traub, 2004, Vaughn and Gold, 2010) and persistent inflammation (Harriott et al., 2006, Zhang et al., 2012b). I have provided further evidence of heterogeneity in response to injury given the differences between glabrous and thigh skin putative nociceptive neurons with respect to the response to paclitaxel. These differences were specific to putative nociceptive neurons as they were not observed in putative non-nociceptors.

5.4 EXPERIMENTAL LIMITATIONS

5.4.1 Isolated Cell Body

Because the isolated sensory neuron cell body has many advantages for the study of Ca^{2+} regulatory pathways it was utilized throughout this project. These include: 1) the presence of many of the same molecular mechanisms that are expressed in free nerve endings both at the peripheral and central terminals (Baccaglini and Hogan, 1983, Malin et al., 2007). 2) The isolated cell body allows precise control of the extracellular environment, which is highly advantageous for studying physiological, pharmacological, and electrical properties of sensory neurons. 3) Isolated neurons are easy to prepare. 4) Isolated cell bodies can be readily characterized using a multi-criterion approach. 5) Isolated neuron facilitates identification of intrinsic changes in neurons that are not dependent on the influence of other cell types/mediators and 6) it allows studying distinct subpopulations of neurons innervating only the area of interest, which is a great benefit in a highly heterogeneous population of neurons.

Despite the many advantages of the isolated sensory neurons cell body for the study of Ca^{2+} regulation, it is important to be aware of the limitations of this model system. One major disadvantage is that the dissociation of neurons requires axotomy of both central and peripheral processes, thus introduces an injury and associated cellular cascades to every neuron. Even if the same molecules and proteins are present in the soma and the axons and terminals, the spatial distribution and local concentration of these molecules may differ based on location. Therefore, it will always be necessary to confirm that the interactions observed in the cell body are present in the neuronal compartment (axons and terminals) of interest. Moreover, there is always the possibility that the behavior of a cell in culture may be different than in an intact system. For

some treatment-induced changes, signals from neighboring cells or the extracellular environment may be key for their responses, which would be taken away in isolated preparations.

5.4.2 Generalizability of Paclitaxel Model to CIPN

All major classes of chemotherapeutics produce CIPN with the same general phenotype, suggesting that CIPN produced by one class of drugs potentially involves the same main players as CIPN produced by other chemotherapeutics. In fact, this was the case for studies characterizing chemotherapy-induced mitotoxicity along the sensory neurons axons: Initial observations with the paclitaxel model were later confirmed with oxaliplatin and bortezomib models showing that systemic chemotherapy treatment with any of these antineoplastic drugs resulted in mitotoxicity along sensory axons (Flatters and Bennett, 2006, Xiao et al., 2011, Zheng et al., 2011, 2012), supporting the notion of generalizability of findings with paclitaxel model to other CIPN models.

The behavioral phenotype we observed with the paclitaxel rat model is comparable to the clinical observations. The mechanical hypersensitivity in the rat was limited to the glabrous skin, which is analogous to the area where patients suffer from painful symptoms. Moreover, the hypersensitivity observed with the rat was also reversible after cessation of therapy, again resembling the clinical observations. An open question, however, is what underlies the negative symptoms of CIPN, such as numbness and tingling. Although my initial hypothesis was that both the positive and negative signs of CIPN are due to changes in Ca^{2+} regulation. Besides putative nociceptors, I also predicted that paclitaxel would induce changes in Ca^{2+} regulation in large diameter putative non-nociceptors. The lack of a change in Ca^{2+} regulation in large diameter neurons suggest another mechanism accounts for the impact of chemotherapy on this

subpopulation. Another interpretation would be that other chemotherapy-induced changes, such as mitotoxicity or inflammatory mediators cause numbness and tingling in the absence of Ca^{2+} dysregulation, whereas presence of the Ca^{2+} dysregulation causes pain. It would be difficult to test these possibilities due to lack of models to test some of the CIPN symptoms, such as tingling.

Patients often receive paclitaxel in combinations of two or more antineoplastic drugs. Since all classes of chemotherapeutics result in comparable CIPN phenotypes and based on studies showing comparable changes with different CIPN models, I would argue that using paclitaxel alone is not a major concern/limitation with the model employed. However we are aware that certain combinations of chemotherapy drugs may have additive or synergistic effects on underlying mechanisms. Our group recently started establishing a novel paclitaxel-carboplatin combination chemotherapy model.

Another concern regarding the rat model is the dosing and timing schedule of paclitaxel delivery. In this work, we used a single dosing and timing schedule, consisting of four paclitaxel injections every other day for a cumulative dose of eight mg/kg. This schedule is assumed to mimic a dosing/timing of human treatments that would result in CIPN. However, in the clinic there are multiple dosing and timing schedules of paclitaxel chemotherapy based on the patients' needs. This becomes important with evidence that there is a positive correlation between cumulative dose and severity of CIPN symptoms. Therefore, it is possible that there are additional paclitaxel-induced changes that occur with larger cumulative doses that we did not detect with the model we used.

A third concern is that all rats in this study were healthy young adult animals within a very specific age and weight range, whereas in the clinic cancer patients with a much wider variability for age and weight measures are treated with chemotherapy.

It is possible that physiological impact of age, weight, or cancer influences mechanisms responsible for the manifestation of CIPN. For example there is a positive correlation between age and production of proinflammatory cytokines and markers (Cevenini et al., 2010). Similarly, there is a correlation with body weight and inflammatory state as well as risk for cancer (Hursting, 2014), and studies draw a link between the inflammatory markers such as IL-6 and TNF α in the circulatory system and cancer susceptibility (Il'yasova et al., 2005, Song et al., 2013). If the inflammatory milieu impacts the manifestation and mechanisms of CIPN, it is therefore possible that the changes observed in the rat may not translate well to the patient care. Yet another concern is that almost all the data in this work was collected at a single timepoint, two weeks after the start of the paclitaxel treatment, which was the time of peak mechanical hypersensitivity. The only other timepoint that I assessed the paclitaxel-induced decrease in the depolarization-evoked Ca²⁺ transients was after the resolution of the paclitaxel-induced hypersensitivity, where the paclitaxel-induced change in Ca²⁺ transient duration was comparable to vehicle controls. However, I did not characterize any changes during the onset of CIPN. Therefore, it is not clear when paclitaxel-induced changes are initiated. Similarly, I did not characterize any changes during recovery, such as four weeks after the start of the treatment when the hypersensitivity started to dissolve, thus it is uncertain how long the changes in Ca²⁺ regulation are present.

5.4.3 Species Differences

We observed changes in a specific subpopulation of sensory neurons in the rat that responds to capsaicin and binds IB4. However, the subpopulations defined by IB4 and capsaicin sensitivity are very different in the rat and the mouse (Woodbury et al., 2004). Thus it is not clear whether and which subpopulation of mouse neurons express any subpopulation-specific changes that I observed with the rat model.

More importantly, while the behavioral phenotype observed in the rat model of CIPN is comparable to that observed in patients, there are important species differences between rats and humans to consider. As noted above, these include dosing, which are generally determined by surface area, which is dramatically different in the rat. However, human DRG neurons do not bind IB4 (Davidson et al., 2014), thus, similar to mice, it is not clear whether and which subpopulation of human neurons express the changes I observed with the rat putative nociceptors. Furthermore, evidence also exists for pharmacological or mechanistic species differences regarding primary afferent function between rats and humans (McIntyre et al., 2001, Serrano et al., 2012), likely accounting at least partially for the relatively high failure rates of translational studies. Therefore, attempts to test the validity of results presented in this dissertation in post-mortem human primary afferent neurons taken from control subjects and donors who underwent chemotherapy may provide answers about the presence, and if so, neuron subpopulation specificity, of comparable chemotherapy-induced changes.

5.4.4 Sex Differences

We used only male rats were in this dissertation. To date, the majority of CIPN animal model data in literature have been obtained using males. One reason behind using only males is to avoid potential complicating influences of the estrous cycle. Another reason is to reduce the number of animals for initial characterizations with the assumption that most biological processes will be conserved among the two sexes. This approach may be problematic, given the evidence of sex-differences in prevalence and mechanisms in certain pain conditions, such as inflammatory pain (Mogil and Bailey, 2010, Scheff and Gold, 2011, Mogil, 2012, McIlvried et al., 2015, McIlvried et al., 2016). Moreover, paclitaxel is most commonly used to treat breast, ovarian, and non-small cell lung cancers, therefore majority of patients receiving paclitaxel treatment are women. Consequently, it will be essential to characterize paclitaxel-induced changes using female rats.

5.5 FUTURE DIRECTIONS

5.5.1 Paclitaxel-Induced Changes in Ca²⁺ Regulation and Pain-Related Behavior

So far, I have only been able to establish the presence of a correlation between the changes in Ca²⁺ and mechanical/cold hypersensitivity induced by paclitaxel. In future studies, it will be necessary to determine whether there is a causal link between the two. Towards this goal, the first step would be to characterize the paclitaxel-induced mitochondrial changes in the axons and terminals of putative nociceptors innervating the glabrous skin. Based on the literature, mitochondria are defective in many axons. However, these axons were not defined by target of

innervation. Thus, it is possible that paclitaxel has an ill effect on mitochondria in axons of other sensory neurons, sparing the ones innervating the glabrous skin of the hindpaw. This may be assessed by examination of mitochondria in glabrous and control skin nerve terminals, as well as mitochondria along the retrogradely labeled axons using electron microscopy. If the paclitaxel-induced changes in the somata are also observed in the axons and terminals of the neurons innervating the glabrous skin, targeting mitochondrial Ca^{2+} buffering may provide answers as to whether a mitochondrial change in the entirety of these afferents is mediating pain-related symptoms of paclitaxel treatment. One way to test this would be blocking the protein responsible for mitochondrial Ca^{2+} intake, the mitochondrial Ca^{2+} uniporter (MCU). This can be accomplished by injecting the MCU inhibitor Ru360 directly into the glabrous hindpaw skin of paclitaxel-treated rats and test for the behavioral endpoints.

5.5.2 Compensatory Mechanisms

The presence of a compensatory mechanism opposing the increased NCX activity in putative nociceptors innervating the thigh skin raised the question as to whether the painful symptoms are due to the absence of this compensatory change in putative nociceptors innervating the glabrous skin. It was beyond the focus of this work to characterize such compensatory mechanisms in thigh neurons, especially without a clear causal link between changes in Ca^{2+} regulation and pain-related behavior induced by paclitaxel. However, if a compensatory change in Ca^{2+} regulation is protective for the neurons projecting to the thigh skin, then activating this mechanism in neurons innervating the glabrous skin may provide a new avenue for pain treatment in CIPN patients. Thus, characterization of such mechanisms with future studies may be useful for new clinical approaches.

Based on what we know about Ca^{2+} regulatory toolkit in primary afferents, characterization of this compensatory mechanism would start with the regulators that affect the duration of the depolarization-evoked Ca^{2+} transients, such as SERCA and PMCA, testing the hypothesis that the decrease in the activity of one or more of these regulators may oppose the decrease in the duration that is caused by increased NCX activity in neurons innervating the thigh skin. We have evidence that mitochondria and SERCA do not mediate this compensatory change in putative nociceptors innervating the thigh skin. However it is possible that NCX activity is increased in these neurons as a response to dysfunctional mitochondria. Therefore if PMCA and any other potential pathway is eliminated, the electron microscopy studies suggested previously may also clarify aspects of our observation in thigh neurons regarding the paclitaxel-induced increase in NCX activity.

5.5.3 Clinical Implications

Currently there is no effective treatment for CIPN. Steroids, topical creams, anti-seizure medications, antidepressants, and even opioids have limited efficacy to alleviate painful symptoms of CIPN. Many adjuvant therapies involving Ca^{2+} , Mg^{2+} , vitamin B, glutathione, acetyl-L-carnitine, selenium, and vitamin E supplementation were shown to be ineffective in preventing or treating CIPN (Wolf et al., 2008, Hershman et al., 2014, Pachman et al., 2014, Schneider et al., 2015). Among these, glutathione, acetyl-L-carnitine, selenium and vitamin E are used with the expectations that their antioxidant properties will help prevent or treat neuronal damage exerted by antineoplastic drugs due to oxidative stress. Our results may explain why these treatments are not effective; paclitaxel-induced mitochondrial Ca^{2+} regulation changes we

have observed are localized in a specific subpopulation of neurons and these neurons do not appear to exhibit signs of increased oxidative stress.

Despite the success of interventions designed to increase mitochondrial function in alleviating chemotherapy-induced mechanical hypersensitivity in preclinical studies (Ghirardi et al., 2005a, Ghirardi et al., 2005b), differences in preclinical and clinical endpoints may also account for the failure of these interventions to translate. Whereas research in preclinical studies, including the experiments in this dissertation, have been focused mainly on chemotherapy-induced mechanical or cold hypersensitivity, the main complaint in the clinic is ongoing rather than evoked pain. This raises the possibility that mitochondrial dysfunction is the underlying mechanism for evoked pain. And while a stretch, it would also then be possible that the mitochondrial gain-of-function described here, is important for ongoing painful symptoms of CIPN. However, this possibility needs to be tested. Critical first steps here would involve an assessment of the dependence of spontaneous activity in isolated neurons on intact mitochondria. It may also be possible to disrupt mitochondrial Ca^{2+} signaling in the glabrous skin or DRG in a behavioral assay of ongoing pain such as the conditioned place preference test.

As mentioned earlier, a sign of CIPN that is observed both in the clinic and preclinical studies is the loss of IENF. It is generally assumed that the loss of IENF accounts for the numbness observed in CIPN. This would suggest that the fibers lost are low threshold mechanoreceptors. Given the relatively selective manifestation of changes in Ca^{2+} regulation in putative nociceptive afferents, the increase in mitochondrial volume described in this thesis is unlikely to be associated with a decrease in the epidermal density of this fiber type. However, the nature of the fibers lost has yet to be unequivocally determined. It is therefore possible that at least some of the fibers lost are nociceptive. Furthermore, with evidence that patients suffering

from CIPN tend to have cold hands and feet (Boyette-Davis et al., 2011b), combined with evidence that one of the efferent functions of peptidergic nociceptive afferents is to maintain vasal tone, it is reasonable to speculate that there is at least some loss of nociceptive afferent terminals. It is therefore possible that the changes in mitochondria observed in putative nociceptive afferents is associated with a decrease in nociceptive IENF density. One way to assess such an association would be by to determine the impact of disrupting mitochondrial Ca^{2+} regulation in skin on a paclitaxel-induced decrease in IENF density. Potential outcomes of such an experiment include enhancement, reduction of, or no effect on the IENF density, all of which would have important implications. A reduction of IENF loss would imply that mitochondrial changes that we observed in soma are also taking place in the distal ends of the neurons. An enhancement of the IENF loss would imply that in contrast to the cell body, there is a decrease in mitochondrial function and/or mitotoxicity taking place at the distal terminals. A negative result should be followed up with control experiments and interpreted carefully, however it may indicate that the mitochondrial changes we have characterized and the IENF loss occur in different neurons. When coupled with experiments specifically targeting the mitochondrial Ca^{2+} regulation in the cell bodies of these neurons, the results of such experiments should provide information critical to our understanding of the implications of mitochondrial changes due to paclitaxel treatment.

While I have implicated a mitochondria-dependent mechanism for CIPN in this thesis work, it would be extremely difficult to target mitochondria, ER, or any other organelle specifically in one subpopulation without affecting any other cells. Therefore other avenues need to be taken to target the paclitaxel-induced changes to organelle functions in specific subpopulations. For example, NCX3 activity is in putative nociceptive afferents innervating the

glabrous skin does not differ in paclitaxel and vehicle conditions and there is evidence that other NCX isoforms are activated in neurons innervating other regions. Therefore, treatments aiming to reduce only NCX3 activity instead of using a general NCX inhibitor may provide relief that also has some degree of specificity for the putative nociceptors innervating the glabrous skin.

Based on our findings, inhibition of SERCA is another treatment option. However, SERCA is expressed at high levels in muscle tissue, therefore treatments targeting SERCA has to be local or neuron-specific. Currently there are multiple SERCA inhibitors, most of which have a higher affinity to SERCA1 over other isoforms although they inhibit all three isoforms (Michelangeli and East, 2011). SERCA1 is most common in muscle tissue but non-muscle tissues including neurons express either SERCA2b alone or in combination with SERCA3 (Michelangeli and East, 2011). Unfortunately, there are no isoform-specific inhibitors for SERCA2 splice variants or SERCA3 (Michelangeli and East, 2011) Therefore if selective inhibitors are characterized, the first step would be to determine which SERCA isoform(s) and/or splice variants are expressed in these specific subpopulation of sensory neurons to be able to block SERCA activity specifically in these neurons without affecting muscle functioning. Otherwise, neuron-specific virus-mediated gene therapy targeting SERCA or perineural injection of SERCA inhibitors may be effective to provide relief without muscle dysfunction.

There is also preclinical evidence about the effectiveness of Li⁺ treatment to prevent or attenuate CIPN (Mo et al., 2012, Pourmohammadi et al., 2012). It is suggested that Li⁺ treatment alters Ca²⁺ regulation via multiple pathways (Meltzer, 1986, Mo et al., 2012), therefore it is possible that in these studies Li⁺ provided relief by ameliorating Ca²⁺ dysregulation. For example, in the study from Mo et al., paclitaxel treatment was associated with decreases in intracellular Ca²⁺ signaling, and lithium treatment inhibited the development of paclitaxel-

induced hypersensitivity by via neuronal calcium sensor 1 (NCS-1), and the inositol 1,4,5-trisphosphate receptor (IP₃R) pathways (Mo et al., 2012).

In summary, I aimed to characterize a novel mechanism of CIPN in this study. While the data I presented in this document contributes to the literature of CIPN mechanisms, additional studies are needed to translate findings of this thesis work into effective treatment options.

BIBLIOGRAPHY

- (American Cancer Society, 2015) Cancer Facts and Figures. Atlanta, GA: American Cancer Society.
- Ahn HK, Jung M, Sym SJ, Shin DB, Kang SM, Kyung SY, Park JW, Jeong SH, Cho EK (2014) A phase II trial of Cremorphor EL-free paclitaxel (Genexol-PM) and gemcitabine in patients with advanced non-small cell lung cancer. *Cancer Chemother Pharmacol* 74:277-282.
- Albrecht PJ, Hines S, Eisenberg E, Pud D, Finlay DR, Connolly MK, Pare M, Davar G, Rice FL (2006) Pathologic alterations of cutaneous innervation and vasculature in affected limbs from patients with complex regional pain syndrome. *Pain* 120:244-266.
- Amoscato AA, Sparvero LJ, He RR, Watkins S, Bayir H, Kagan VE (2014) Imaging mass spectrometry of diversified cardiolipin molecular species in the brain. *Anal Chem* 86:6587-6595.
- Andre N, Braguer D, Brasseur G, Goncalves A, Lemesle-Meunier D, Guise S, Jordan MA, Briand C (2000) Paclitaxel induces release of cytochrome c from mitochondria isolated from human neuroblastoma cells'. *Cancer Res* 60:5349-5353.
- Baccaglini PI, Hogan PG (1983) Some rat sensory neurons in culture express characteristics of differentiated pain sensory cells. *Proc Natl Acad Sci U S A* 80:594-598.
- Bennett GJ, Doyle T, Salvemini D (2014) Mitotoxicity in distal symmetrical sensory peripheral neuropathies. *Nat Rev Neurol* 10:326-336.
- Berridge MJ, Bootman MD, Roderick HL (2003) Calcium signalling: dynamics, homeostasis and remodelling. *Nat Rev Mol Cell Biol* 4:517-529.
- Berridge MJ, Lipp P, Bootman MD (2000) The versatility and universality of calcium signalling. *Nat Rev Mol Cell Biol* 1:11-21.

- Beyak MJ, Ramji N, Krol KM, Kawaja MD, Vanner SJ (2004) Two TTX-resistant Na⁺ currents in mouse colonic dorsal root ganglia neurons and their role in colitis-induced hyperexcitability. *Am J Physiol Gastrointest Liver Physiol* 287:G845-855.
- Blaustein MP, Lederer WJ (1999) Sodium/calcium exchange: its physiological implications. *Physiol Rev* 79:763-854.
- Bonetti A, Leone R, Muggia F, Howell SB (2009) *Platinum and Other Heavy Metal Compounds in Cancer Chemotherapy: Molecular Mechanisms and Clinical Applications*: Humana Press.
- Boyette-Davis J, Dougherty PM (2011) Protection against oxaliplatin-induced mechanical hyperalgesia and intraepidermal nerve fiber loss by minocycline. *Exp Neurol* 229:353-357.
- Boyette-Davis J, Xin W, Zhang H, Dougherty PM (2011a) Intraepidermal nerve fiber loss corresponds to the development of taxol-induced hyperalgesia and can be prevented by treatment with minocycline. *Pain* 152:308-313.
- Boyette-Davis JA, Cata JP, Driver LC, Novy DM, Bruel BM, Mooring DL, Wendelschafer-Crabb G, Kennedy WR, Dougherty PM (2013) Persistent chemoneuropathy in patients receiving the plant alkaloids paclitaxel and vincristine. *Cancer Chemother Pharmacol* 71:619-626.
- Boyette-Davis JA, Cata JP, Zhang H, Driver LC, Wendelschafer-Crabb G, Kennedy WR, Dougherty PM (2011b) Follow-up psychophysical studies in bortezomib-related chemoneuropathy patients. *J Pain* 12:1017-1024.
- Caffrey JM, Eng DL, Black JA, Waxman SG, Kocsis JD (1992) Three types of sodium channels in adult rat dorsal root ganglion neurons. *Brain Res* 592:283-297.
- Carafoli E (1991) The calcium pumping ATPase of the plasma membrane. *Annu Rev Physiol* 53:531-547.
- Cata JP, Weng HR, Dougherty PM (2008) The effects of thalidomide and minocycline on taxol-induced hyperalgesia in rats. *Brain Res* 1229:100-110.
- Caterina MJ, Julius D (1999) Sense and specificity: a molecular identity for nociceptors. *Curr Opin Neurobiol* 9:525-530.
- Cevenini E, Caruso C, Candore G, Capri M, Nuzzo D, Duro G, Rizzo C, Colonna-Romano G, Lio D, Di Carlo D, Palmas MG, Scurti M, Pini E, Franceschi C, Vasto S (2010) Age-related inflammation: the contribution of different organs, tissues and systems. How to face it for therapeutic approaches. *Curr Pharm Des* 16:609-618.

- Chaudhry V, Chaudhry M, Crawford TO, Simmons-O'Brien E, Griffin JW (2003) Toxic neuropathy in patients with pre-existing neuropathy. *Neurology* 60:337-340.
- Chen H, Chan DC (2009) Mitochondrial dynamics--fusion, fission, movement, and mitophagy--in neurodegenerative diseases. *Hum Mol Genet* 18:R169-176.
- Chen SR, Cai YQ, Pan HL (2009) Plasticity and emerging role of BKCa channels in nociceptive control in neuropathic pain. *J Neurochem* 110:352-362.
- Contreras L, Drago I, Zampese E, Pozzan T (2010) Mitochondria: the calcium connection. *Biochim Biophys Acta* 1797:607-618.
- Costigan M, Befort K, Karchewski L, Griffin RS, D'Urso D, Allchorne A, Sitarski J, Mannion JW, Pratt RE, Woolf CJ (2002) Replicate high-density rat genome oligonucleotide microarrays reveal hundreds of regulated genes in the dorsal root ganglion after peripheral nerve injury. *BMC Neurosci* 3:16.
- Cottet-Rousselle C, Ronot X, Leverve X, Mayol JF (2011) Cytometric Assessment of Mitochondria Using Fluorescent Probes. *Cytometry Part A* 79A:405-425.
- Davidson S, Copits BA, Zhang J, Page G, Ghetti A, Gereau RWt (2014) Human sensory neurons: Membrane properties and sensitization by inflammatory mediators. *Pain* 155:1861-1870.
- Davidson SM, Duchon MR (2012) Imaging mitochondrial calcium signalling with fluorescent probes and single or two photon confocal microscopy. *Methods Mol Biol* 810:219-234.
- Demaurex N, Poburko D, Frieden M (2009) Regulation of plasma membrane calcium fluxes by mitochondria. *Biochim Biophys Acta* 1787:1383-1394.
- Dimroth P, Kaim G, Matthey U (2000) Crucial role of the membrane potential for ATP synthesis by F(1)F(o) ATP synthases. *J Exp Biol* 203:51-59.
- DiPolo R, Beauge L (2006) Sodium/calcium exchanger: influence of metabolic regulation on ion carrier interactions. *Physiol Rev* 86:155-203.
- Dougherty PM, Cata JP, Cordella JV, Burton A, Weng HR (2004) Taxol-induced sensory disturbance is characterized by preferential impairment of myelinated fiber function in cancer patients. *Pain* 109:132-142.
- Drose S, Brandt U (2008) The mechanism of mitochondrial superoxide production by the cytochrome bc1 complex. *J Biol Chem* 283:21649-21654.
- Duncan C, Mueller S, Simon E, Renger JJ, Uebele VN, Hogan QH, Wu HE (2013) Painful nerve injury decreases sarco-endoplasmic reticulum Ca(2)(+)-ATPase activity in axotomized sensory neurons. *Neuroscience* 231:247-257.

- Eisner V, Csordas G, Hajnoczky G (2013) Interactions between sarco-endoplasmic reticulum and mitochondria in cardiac and skeletal muscle - pivotal roles in Ca(2)(+) and reactive oxygen species signaling. *J Cell Sci* 126:2965-2978.
- Ellis A, Bennett DL (2013) Neuroinflammation and the generation of neuropathic pain. *Br J Anaesth* 111:26-37.
- Evtodienko YV, Teplova VV, Sidash SS, Ichas F, Mazat JP (1996) Microtubule-active drugs suppress the closure of the permeability transition pore in tumour mitochondria. *FEBS Lett* 393:86-88.
- Fang X, Djouhri L, McMullan S, Berry C, Waxman SG, Okuse K, Lawson SN (2006) Intense isolectin-B4 binding in rat dorsal root ganglion neurons distinguishes C-fiber nociceptors with broad action potentials and high Nav1.9 expression. *J Neurosci* 26:7281-7292.
- Fernyhough P, Calcutt NA (2010) Abnormal calcium homeostasis in peripheral neuropathies. *Cell Calcium* 47:130-139.
- Fidanboylyu M, Griffiths LA, Flatters SJ (2011) Global inhibition of reactive oxygen species (ROS) inhibits paclitaxel-induced painful peripheral neuropathy. *PLoS One* 6:e25212.
- Fields RD, Lee PR, Cohen JE (2005) Temporal integration of intracellular Ca²⁺ signaling networks in regulating gene expression by action potentials. *Cell Calcium* 37:433-442.
- Flatters SJ, Bennett GJ (2006) Studies of peripheral sensory nerves in paclitaxel-induced painful peripheral neuropathy: evidence for mitochondrial dysfunction. *Pain* 122:245-257.
- Fonteriz RI, de la Fuente S, Moreno A, Lobaton CD, Montero M, Alvarez J (2010) Monitoring mitochondrial [Ca(2+)] dynamics with rhod-2, ratiometric pericam and aequorin. *Cell Calcium* 48:61-69.
- Fuchs A, Lirk P, Stucky C, Abram SE, Hogan QH (2005) Painful nerve injury decreases resting cytosolic calcium concentrations in sensory neurons of rats. *Anesthesiology* 102:1217-1225.
- Fuchs A, Rigaud M, Hogan QH (2007) Painful nerve injury shortens the intracellular Ca²⁺ signal in axotomized sensory neurons of rats. *Anesthesiology* 107:106-116.
- Garcia-Sancho J (2014) The coupling of plasma membrane calcium entry to calcium uptake by endoplasmic reticulum and mitochondria. *J Physiol* 592:261-268.
- Gelderblom H, Verweij J, Nooter K, Sparreboom A (2001) Cremophor EL: the drawbacks and advantages of vehicle selection for drug formulation. *Eur J Cancer* 37:1590-1598.

- Gemes G, Oyster KD, Pan B, Wu HE, Bangaru ML, Tang Q, Hogan QH (2012) Painful nerve injury increases plasma membrane Ca²⁺-ATPase activity in axotomized sensory neurons. *Mol Pain* 8:46.
- Gerencser AA, Chinopoulos C, Birket MJ, Jastroch M, Vitelli C, Nicholls DG, Brand MD (2012) Quantitative measurement of mitochondrial membrane potential in cultured cells: calcium-induced de- and hyperpolarization of neuronal mitochondria. *J Physiol* 590:2845-2871.
- Ghirardi O, Lo Giudice P, Pisano C, Vertechy M, Bellucci A, Vesci L, Cundari S, Miloso M, Rigamonti LM, Nicolini G, Zanna C, Carminati P (2005a) Acetyl-L-Carnitine prevents and reverts experimental chronic neurotoxicity induced by oxaliplatin, without altering its antitumor properties. *Anticancer Res* 25:2681-2687.
- Ghirardi O, Vertechy M, Vesci L, Canta A, Nicolini G, Galbiati S, Ciogli C, Quattrini G, Pisano C, Cundari S, Rigamonti LM (2005b) Chemotherapy-induced allodynia: neuroprotective effect of acetyl-L-carnitine. *In Vivo* 19:631-637.
- Glancy B, Hartnell LM, Malide D, Yu ZX, Combs CA, Connelly PS, Subramaniam S, Balaban RS (2015) Mitochondrial reticulum for cellular energy distribution in muscle. *Nature* 523:617-620.
- Gold MS, Gebhart GF (2010) Peripheral Pain Mechanisms and Nociceptor Sensitization. In: *Bonica's Management of Pain* (Fishman, S. M. et al., eds), pp 24 – 34: Lippincott, Williams & Wilkins.
- Gold MS, Thut PD (2001) Lithium increases potency of lidocaine-induced block of voltage-gated Na⁺ currents in rat sensory neurons in vitro. *J Pharmacol Exp Ther* 299:705-711.
- Gold MS, Traub RJ (2004) Cutaneous and colonic rat DRG neurons differ with respect to both baseline and PGE₂-induced changes in passive and active electrophysiological properties. *J Neurophysiol* 91:2524-2531.
- Goncalves A, Braguer D, Carles G, Andre N, Prevot C, Briand C (2000) Caspase-8 activation independent of CD95/CD95-L interaction during paclitaxel-induced apoptosis in human colon cancer cells (HT29-D4). *Biochem Pharmacol* 60:1579-1584.
- Gornstein E, Schwarz TL (2014) The paradox of paclitaxel neurotoxicity: Mechanisms and unanswered questions. *Neuropharmacology* 76 Pt A:175-183.
- Greger R, Windhorst U (2013) *Comprehensive Human Physiology: From Cellular Mechanisms to Integration*: Springer Berlin Heidelberg.
- Griffiths LA, Flatters SJ (2015) Pharmacological Modulation of the Mitochondrial Electron Transport Chain in Paclitaxel-Induced Painful Peripheral Neuropathy. *J Pain* 16:981-994.

- Grunberg SM, Sonka S, Stevenson LL, Muggia FM (1989) Progressive paresthesias after cessation of therapy with very high-dose cisplatin. *Cancer Chemother Pharmacol* 25:62-64.
- Hajnoczky G, Csordas G, Das S, Garcia-Perez C, Saotome M, Sinha Roy S, Yi M (2006) Mitochondrial calcium signalling and cell death: approaches for assessing the role of mitochondrial Ca²⁺ uptake in apoptosis. *Cell Calcium* 40:553-560.
- Harper AA, Lawson SN (1985) Conduction velocity is related to morphological cell type in rat dorsal root ganglion neurones. *J Physiol* 359:31-46.
- Harriott AM, Dessem D, Gold MS (2006) Inflammation increases the excitability of masseter muscle afferents. *Neuroscience* 141:433-442.
- Harriott AM, Gold MS (2009) Electrophysiological properties of dural afferents in the absence and presence of inflammatory mediators. *J Neurophysiol* 101:3126-3134.
- Hershman DL, Lacchetti C, Dworkin RH, Lavoie Smith EM, Bleeker J, Cavaletti G, Chauhan C, Gavin P, Lavino A, Lustberg MB, Paice J, Schneider B, Smith ML, Smith T, Terstriep S, Wagner-Johnston N, Bak K, Loprinzi CL, American Society of Clinical O (2014) Prevention and management of chemotherapy-induced peripheral neuropathy in survivors of adult cancers: American Society of Clinical Oncology clinical practice guideline. *J Clin Oncol* 32:1941-1967.
- Hershman DL, Unger JM, Crew KD, Minasian LM, Awad D, Moinpour CM, Hansen L, Lew DL, Greenlee H, Fehrenbacher L, Wade JL, 3rd, Wong SF, Hortobagyi GN, Meyskens FL, Albain KS (2013) Randomized double-blind placebo-controlled trial of acetyl-L-carnitine for the prevention of taxane-induced neuropathy in women undergoing adjuvant breast cancer therapy. *J Clin Oncol* 31:2627-2633.
- Hill A, Bergin P, Hanning F, Thompson P, Findlay M, Damianovich D, McKeage MJ (2010) Detecting acute neurotoxicity during platinum chemotherapy by neurophysiological assessment of motor nerve hyperexcitability. *BMC Cancer* 10:451.
- Hogan QH (2007) Role of decreased sensory neuron membrane calcium currents in the genesis of neuropathic pain. *Croat Med J* 48:9-21.
- Hogan QH, Sprick C, Guo Y, Mueller S, Bienengraeber M, Pan B, Wu HE (2014) Divergent effects of painful nerve injury on mitochondrial Ca²⁺ buffering in axotomized and adjacent sensory neurons. *Brain Res* 1589:112-125.
- Holzer P (1991) Capsaicin as a tool for studying sensory neuron functions. *Adv Exp Med Biol* 298:3-16.
- Hursting SD (2014) Obesity, energy balance, and cancer: a mechanistic perspective. *Cancer Treat Res* 159:21-33.

- Il'yasova D, Colbert LH, Harris TB, Newman AB, Bauer DC, Satterfield S, Kritchevsky SB (2005) Circulating levels of inflammatory markers and cancer risk in the health aging and body composition cohort. *Cancer Epidemiol Biomarkers Prev* 14:2413-2418.
- Iwamoto T, Shigekawa M (1998) Differential inhibition of Na⁺/Ca²⁺ exchanger isoforms by divalent cations and isothioureia derivative. *Am J Physiol* 275:C423-430.
- Jaggi AS, Singh N (2012) Mechanisms in cancer-chemotherapeutic drugs-induced peripheral neuropathy. *Toxicology* 291:1-9.
- Jin HW, Flatters SJ, Xiao WH, Mulhern HL, Bennett GJ (2008) Prevention of paclitaxel-evoked painful peripheral neuropathy by acetyl-L-carnitine: effects on axonal mitochondria, sensory nerve fiber terminal arbors, and cutaneous Langerhans cells. *Exp Neurol* 210:229-237.
- Johnson MS, Ryals JM, Wright DE (2008) Early loss of peptidergic intraepidermal nerve fibers in an STZ-induced mouse model of insensate diabetic neuropathy. *Pain* 140:35-47.
- Kao JP (1994) Practical aspects of measuring [Ca²⁺] with fluorescent indicators. *Methods Cell Biol* 40:155-181.
- Kawano T, Zoga V, Gemes G, McCallum JB, Wu HE, Pravdic D, Liang MY, Kwok WM, Hogan Q, Sarantopoulos C (2009) Suppressed Ca²⁺/CaM/CaMKII-dependent K(ATP) channel activity in primary afferent neurons mediates hyperalgesia after axotomy. *Proc Natl Acad Sci U S A* 106:8725-8730.
- Khare A, Raundhal M, Chakraborty K, Das S, Corey C, Kamga CK, Quesnelle K, St Croix C, Watkins SC, Morse C, Oriss TB, Huff R, Hannum R, Ray P, Shiva S, Ray A (2016) Mitochondrial HO in Lung Antigen-Presenting Cells Blocks NF-kappaB Activation to Prevent Unwarranted Immune Activation. *Cell Rep*.
- Kidd BL, Urban LA (2001) Mechanisms of inflammatory pain. *Br J Anaesth* 87:3-11.
- Kidd JF, Pilkington MF, Schell MJ, Fogarty KE, Skepper JN, Taylor CW, Thorn P (2002) Paclitaxel affects cytosolic calcium signals by opening the mitochondrial permeability transition pore. *J Biol Chem* 277:6504-6510.
- Koerber HR, Druzinsky RE, Mendell LM (1988) Properties of somata of spinal dorsal root ganglion cells differ according to peripheral receptor innervated. *J Neurophysiol* 60:1584-1596.
- Koltzenburg M, McMahon SB, Tracey I, Turk DC (2013) Wall & Melzack's Textbook of Pain, Expert Consult - Online and Print, 6: Wall & Melzack's Textbook of Pain: Elsevier/Saunders.

- Kostyuk E, Svichar N, Shishkin V, Kostyuk P (1999) Role of mitochondrial dysfunction in calcium signalling alterations in dorsal root ganglion neurons of mice with experimentally-induced diabetes. *Neuroscience* 90:535-541.
- Kostyuk E, Voitenko N, Kruglikov I, Shmigol A, Shishkin V, Efimov A, Kostyuk P (2001) Diabetes-induced changes in calcium homeostasis and the effects of calcium channel blockers in rat and mice nociceptive neurons. *Diabetologia* 44:1302-1309.
- Kulikov AV, Shilov ES, Mufazalov IA, Gogvadze V, Nedospasov SA, Zhivotovsky B (2012) Cytochrome c: the Achilles' heel in apoptosis. *Cell Mol Life Sci* 69:1787-1797.
- Lawson SN (2002) Phenotype and function of somatic primary afferent nociceptive neurones with C-, Delta- or Aalpha/beta-fibres. *Exp Physiol* 87:239-244.
- Ledeboer A, Jekich BM, Sloane EM, Mahoney JH, Langer SJ, Milligan ED, Martin D, Maier SF, Johnson KW, Leinwand LA, Chavez RA, Watkins LR (2007) Intrathecal interleukin-10 gene therapy attenuates paclitaxel-induced mechanical allodynia and proinflammatory cytokine expression in dorsal root ganglia in rats. *Brain Behav Immun* 21:686-698.
- Ledeboer A, Sloane EM, Milligan ED, Frank MG, Mahony JH, Maier SF, Watkins LR (2005) Minocycline attenuates mechanical allodynia and proinflammatory cytokine expression in rat models of pain facilitation. *Pain* 115:71-83.
- Lekan HA, Chung K, Yoon YW, Chung JM, Coggeshall RE (1997) Loss of dorsal root ganglion cells concomitant with dorsal root axon sprouting following segmental nerve lesions. *Neuroscience* 81:527-534.
- Li N, Ragheb K, Lawler G, Sturgis J, Rajwa B, Melendez JA, Robinson JP (2003) Mitochondrial complex I inhibitor rotenone induces apoptosis through enhancing mitochondrial reactive oxygen species production. *J Biol Chem* 278:8516-8525.
- Li Y, Adamek P, Zhang H, Tatsui CE, Rhines LD, Mrozkova P, Li Q, Kosturakis AK, Cassidy RM, Harrison DS, Cata JP, Sapire K, Zhang H, Kennamer-Chapman RM, Jawad AB, Ghetti A, Yan J, Palecek J, Dougherty PM (2015a) The Cancer Chemotherapeutic Paclitaxel Increases Human and Rodent Sensory Neuron Responses to TRPV1 by Activation of TLR4. *J Neurosci* 35:13487-13500.
- Li Y, Zhang H, Kosturakis AK, Cassidy RM, Zhang H, Kennamer-Chapman RM, Jawad AB, Colomand CM, Harrison DS, Dougherty PM (2015b) MAPK signaling downstream to TLR4 contributes to paclitaxel-induced peripheral neuropathy. *Brain Behav Immun* 49:255-266.
- Li Y, Zhang H, Zhang H, Kosturakis AK, Jawad AB, Dougherty PM (2014) Toll-like receptor 4 signaling contributes to Paclitaxel-induced peripheral neuropathy. *Journal of Pain* 15:712-725.

- Liu CC, Lu N, Cui Y, Yang T, Zhao ZQ, Xin WJ, Liu XG (2010) Prevention of paclitaxel-induced allodynia by minocycline: Effect on loss of peripheral nerve fibers and infiltration of macrophages in rats. *Mol Pain* 6:76.
- Loprinzi CL, Maddocks-Christianson K, Wolf SL, Rao RD, Dyck PJ, Mantyh P, Dyck PJ (2007) The Paclitaxel acute pain syndrome: sensitization of nociceptors as the putative mechanism. *Cancer J* 13:399-403.
- Lu SG, Gold MS (2008) Inflammation-induced increase in evoked calcium transients in subpopulations of rat dorsal root ganglion neurons. *Neuroscience* 153:279-288.
- Lu SG, Zhang X, Gold MS (2006) Intracellular calcium regulation among subpopulations of rat dorsal root ganglion neurons. *J Physiol* 577:169-190.
- Lu SG, Zhang XL, Luo ZD, Gold MS (2010) Persistent inflammation alters the density and distribution of voltage-activated calcium channels in subpopulations of rat cutaneous DRG neurons. *Pain* 151:633-643.
- Maestri A, De Pasquale Ceratti A, Cundari S, Zanna C, Cortesi E, Crino L (2005) A pilot study on the effect of acetyl-L-carnitine in paclitaxel- and cisplatin-induced peripheral neuropathy. *Tumori* 91:135-138.
- Mai JK, Paxinos G (2011) *The Human Nervous System*: Elsevier Science.
- Malin S, Molliver D, Christianson JA, Schwartz ES, Cornuet P, Albers KM, Davis BM (2011) TRPV1 and TRPA1 function and modulation are target tissue dependent. *J Neurosci* 31:10516-10528.
- Malin SA, Davis BM, Molliver DC (2007) Production of dissociated sensory neuron cultures and considerations for their use in studying neuronal function and plasticity. *Nat Protoc* 2:152-160.
- Mangiavacalli S, Corso A, De Amici M, Varettoni M, Alfonsi E, Lozza A, Lazzarino M (2010) Emergent T-helper 2 profile with high interleukin-6 levels correlates with the appearance of bortezomib-induced neuropathic pain. *Br J Haematol* 149:916-918.
- Marchi S, Patergnani S, Pinton P (2014) The endoplasmic reticulum-mitochondria connection: one touch, multiple functions. *Biochim Biophys Acta* 1837:461-469.
- Martin HA, Basbaum AI, Kwiat GC, Goetzl EJ, Levine JD (1987) Leukotriene and prostaglandin sensitization of cutaneous high-threshold C- and A-delta mechanonociceptors in the hairy skin of rat hindlimbs. *Neuroscience* 22:651-659.
- McIlvried LA, Borghesi LA, Gold MS (2015) Sex-, Stress-, and Sympathetic Post-Ganglionic Neuron-Dependent Changes in the Expression of Pro- and Anti-Inflammatory Mediators in Rat Dural Immune Cells. *Headache* 55:943-957.

- McIlvried LA, Cruz JA, Borghesi LA, Gold MS (2016) Sex-, stress-, and sympathetic post-ganglionic-dependent changes in identity and proportions of immune cells in the dura. Cephalalgia.
- McIntyre P, McLatchie LM, Chambers A, Phillips E, Clarke M, Savidge J, Toms C, Peacock M, Shah K, Winter J, Weerasakera N, Webb M, Rang HP, Bevan S, James IF (2001) Pharmacological differences between the human and rat vanilloid receptor 1 (VR1). *Br J Pharmacol* 132:1084-1094.
- Meltzer HL (1986) Lithium mechanisms in bipolar illness and altered intracellular calcium functions. *Biol Psychiatry* 21:492-510.
- Michaelis M, Liu X, Janig W (2000) Axotomized and intact muscle afferents but no skin afferents develop ongoing discharges of dorsal root ganglion origin after peripheral nerve lesion. *J Neurosci* 20:2742-2748.
- Michelangeli F, East JM (2011) A diversity of SERCA Ca²⁺ pump inhibitors. *Biochem Soc Trans* 39:789-797.
- Mielke S, Sparreboom A, Mross K (2006) Peripheral neuropathy: a persisting challenge in paclitaxel-based regimes. *Eur J Cancer* 42:24-30.
- Mo M, Erdelyi I, Szigeti-Buck K, Benbow JH, Ehrlich BE (2012) Prevention of paclitaxel-induced peripheral neuropathy by lithium pretreatment. *FASEB J* 26:4696-4709.
- Moccia F, Zuccolo E, Soda T, Tanzi F, Guerra G, Mapelli L, Lodola F, D'Angelo E (2015) Stim and Orai proteins in neuronal Ca(2+) signaling and excitability. *Front Cell Neurosci* 9:153.
- Mogil JS (2012) Sex differences in pain and pain inhibition: multiple explanations of a controversial phenomenon. *Nat Rev Neurosci* 13:859-866.
- Mogil JS, Bailey AL (2010) Sex and gender differences in pain and analgesia. *Prog Brain Res* 186:141-157.
- Molliver DC, Wright DE, Leitner ML, Parsadanian AS, Doster K, Wen D, Yan Q, Snider WD (1997) IB4-binding DRG neurons switch from NGF to GDNF dependence in early postnatal life. *Neuron* 19:849-861.
- Nishida K, Kuchiiwa S, Oiso S, Futagawa T, Masuda S, Takeda Y, Yamada K (2008) Up-regulation of matrix metalloproteinase-3 in the dorsal root ganglion of rats with paclitaxel-induced neuropathy. *Cancer Sci* 99:1618-1625.
- Nogales E, Wolf SG, Khan IA, Luduena RF, Downing KH (1995) Structure of tubulin at 6.5 Å and location of the taxol-binding site. *Nature* 375:424-427.

- Orrenius S, Gogvadze V, Zhivotovsky B (2007) Mitochondrial oxidative stress: implications for cell death. *Annu Rev Pharmacol Toxicol* 47:143-183.
- Pachman DR, Barton DL, Watson JC, Loprinzi CL (2011) Chemotherapy-induced peripheral neuropathy: prevention and treatment. *Clin Pharmacol Ther* 90:377-387.
- Pachman DR, Loprinzi CL, Grothey A, Ta LE (2014) The search for treatments to reduce chemotherapy-induced peripheral neuropathy. *J Clin Invest* 124:72-74.
- Parnas I, Parnas H (2010) Control of neurotransmitter release: From Ca²⁺ to voltage dependent G-protein coupled receptors. *Pflugers Arch* 460:975-990.
- Patel SR, Vadhan-Raj S, Papadopolous N, Plager C, Burgess MA, Hays C, Benjamin RS (1997) High-dose ifosfamide in bone and soft tissue sarcomas: results of phase II and pilot studies--dose-response and schedule dependence. *J Clin Oncol* 15:2378-2384.
- Patestas MA, Gartner LP (2016) *A Textbook of Neuroanatomy*: Wiley.
- Peters CM, Jimenez-Andrade JM, Jonas BM, Sevcik MA, Koewler NJ, Ghilardi JR, Wong GY, Mantyh PW (2007) Intravenous paclitaxel administration in the rat induces a peripheral sensory neuropathy characterized by macrophage infiltration and injury to sensory neurons and their supporting cells. *Exp Neurol* 203:42-54.
- Polomano RC, Mannes AJ, Clark US, Bennett GJ (2001) A painful peripheral neuropathy in the rat produced by the chemotherapeutic drug, paclitaxel. *Pain* 94:293-304.
- Polster BM, Nicholls DG, Ge SX, Roelofs BA (2014) Use of potentiometric fluorophores in the measurement of mitochondrial reactive oxygen species. *Methods Enzymol* 547:225-250.
- Pourmohammadi N, Alimoradi H, Mehr SE, Hassanzadeh G, Hadian MR, Sharifzadeh M, Bakhtiarian A, Dehpour AR (2012) Lithium attenuates peripheral neuropathy induced by paclitaxel in rats. *Basic Clin Pharmacol Toxicol* 110:231-237.
- Prota AE, Bargsten K, Zurwerra D, Field JJ, Diaz JF, Altmann KH, Steinmetz MO (2013) Molecular mechanism of action of microtubule-stabilizing anticancer agents. *Science* 339:587-590.
- Quasthoff S, Hartung HP (2002) Chemotherapy-induced peripheral neuropathy. *J Neurol* 249:9-17.
- Raffa RB, Langford R, Pergolizzi JV, Porreca F, Tallarida RJ (2012) *Chemotherapy-Induced Neuropathic Pain*: CRC Press.
- Ratte S, Zhu Y, Lee KY, Prescott SA (2014) Criticality and degeneracy in injury-induced changes in primary afferent excitability and the implications for neuropathic pain. *Elife* 3:e02370.

- Rizzuto R, De Stefani D, Raffaello A, Mammucari C (2012) Mitochondria as sensors and regulators of calcium signalling. *Nat Rev Mol Cell Biol* 13:566-578.
- Rowland AA, Voeltz GK (2012) Endoplasmic reticulum-mitochondria contacts: function of the junction. *Nat Rev Mol Cell Biol* 13:607-625.
- Scheff NN, Gold MS (2011) Sex differences in the inflammatory mediator-induced sensitization of dural afferents. *J Neurophysiol* 106:1662-1668.
- Scheff NN, Gold MS (2014) Persistent Inflammation-Induced Increase in the Trafficking of Na⁺/Ca²⁺ Exchanger Isoform 3 (NCX3) to Peripheral Terminals. In: International Association for the Study of Pain Meeting Abstracts
- Scheff NN, Gold MS (2015) Trafficking of Na⁺/Ca²⁺ exchanger to the site of persistent inflammation in nociceptive afferents. *J Neurosci* 35:8423-8432.
- Scheff NN, Lu SG, Gold MS (2013) Contribution of endoplasmic reticulum Ca²⁺ regulatory mechanisms to the inflammation-induced increase in the evoked Ca²⁺ transient in rat cutaneous dorsal root ganglion neurons. *Cell Calcium* 54:46-56.
- Scheff NN, Yilmaz E, Gold MS (2014) The properties, distribution and function of Na⁽⁺⁾-Ca⁽²⁺⁾ exchanger isoforms in rat cutaneous sensory neurons. *J Physiol* 592:4969-4993.
- Schneider BP, Hershman DL, Loprinzi C (2015) Symptoms: Chemotherapy-Induced Peripheral Neuropathy. *Adv Exp Med Biol* 862:77-87.
- Scholz J, Woolf CJ (2007) The neuropathic pain triad: neurons, immune cells and glia. *Nat Neurosci* 10:1361-1368.
- Schwarz TL (2013) Mitochondrial trafficking in neurons. *Cold Spring Harb Perspect Biol* 5.
- Serrano A, Mo G, Grant R, Pare M, O'Donnell D, Yu XH, Tomaszewski MJ, Perkins MN, Seguela P, Cao CQ (2012) Differential expression and pharmacology of native P2X receptors in rat and primate sensory neurons. *J Neurosci* 32:11890-11896.
- Shmigol A, Verkhatsky A, Isenberg G (1995) Calcium-induced calcium release in rat sensory neurons. *J Physiol* 489 (Pt 3):627-636.
- Shun CT, Chang YC, Wu HP, Hsieh SC, Lin WM, Lin YH, Tai TY, Hsieh ST (2004) Skin denervation in type 2 diabetes: correlations with diabetic duration and functional impairments. *Brain* 127:1593-1605.
- Siau C, Bennett GJ (2006) Dysregulation of cellular calcium homeostasis in chemotherapy-evoked painful peripheral neuropathy. *Anesth Analg* 102:1485-1490.

- Silverman JD, Kruger L (1990) Selective neuronal glycoconjugate expression in sensory and autonomic ganglia: relation of lectin reactivity to peptide and enzyme markers. *J Neurocytol* 19:789-801.
- Song M, Wu K, Ogino S, Fuchs CS, Giovannucci EL, Chan AT (2013) A prospective study of plasma inflammatory markers and risk of colorectal cancer in men. *Br J Cancer* 108:1891-1898.
- Stucky CL, Lewin GR (1999) Isolectin B(4)-positive and -negative nociceptors are functionally distinct. *J Neurosci* 19:6497-6505.
- Sukhorukov VM, Dikov D, Reichert AS, Meyer-Hermann M (2012) Emergence of the mitochondrial reticulum from fission and fusion dynamics. *PLoS Comput Biol* 8:e1002745.
- Sweitzer SM, Pahl JL, DeLeo JA (2006) Propentofylline attenuates vincristine-induced peripheral neuropathy in the rat. *Neurosci Lett* 400:258-261.
- Takeuchi A, Kim B, Matsuoka S (2015) The destiny of Ca(2+) released by mitochondria. *J Physiol Sci* 65:11-24.
- Tang Q, Bangaru ML, Kostic S, Pan B, Wu HE, Koopmeiners AS, Yu H, Fischer GJ, McCallum JB, Kwok WM, Hudmon A, Hogan QH (2012) Ca(2+)-dependent regulation of Ca(2+) currents in rat primary afferent neurons: role of CaMKII and the effect of injury. *J Neurosci* 32:11737-11749.
- Tanner KD, Reichling DB, Levine JD (1998) Nociceptor hyper-responsiveness during vincristine-induced painful peripheral neuropathy in the rat. *J Neurosci* 18:6480-6491.
- Thibault O, Gant JC, Landfield PW (2007) Expansion of the calcium hypothesis of brain aging and Alzheimer's disease: minding the store. *Aging Cell* 6:307-317.
- Turner PV, Brabb T, Pekow C, Vasbinder MA (2011) Administration of substances to laboratory animals: routes of administration and factors to consider. *J Am Assoc Lab Anim Sci* 50:600-613.
- Vaughn AH, Gold MS (2010) Ionic mechanisms underlying inflammatory mediator-induced sensitization of dural afferents. *J Neurosci* 30:7878-7888.
- Verdru P, De Greef C, Mertens L, Carmeliet E, Callewaert G (1997) Na(+)-Ca²⁺ exchange in rat dorsal root ganglion neurons. *J Neurophysiol* 77:484-490.
- Verkhatsky A, Toescu EC (2003) Endoplasmic reticulum Ca(2+) homeostasis and neuronal death. *J Cell Mol Med* 7:351-361.

- Vincent AM, Edwards JL, McLean LL, Hong Y, Cerri F, Lopez I, Quattrini A, Feldman EL (2010) Mitochondrial biogenesis and fission in axons in cell culture and animal models of diabetic neuropathy. *Acta Neuropathol* 120:477-489.
- Wakabayashi T (2002) Megamitochondria formation - physiology and pathology. *J Cell Mol Med* 6:497-538.
- Walczak CE, Heald R (2008) Mechanisms of mitotic spindle assembly and function. *Int Rev Cytol* 265:111-158.
- Wang MS, Davis AA, Culver DG, Glass JD (2002) WldS mice are resistant to paclitaxel (taxol) neuropathy. *Ann Neurol* 52:442-447.
- Wang XM, Lehky TJ, Brell JM, Dorsey SG (2012) Discovering cytokines as targets for chemotherapy-induced painful peripheral neuropathy. *Cytokine* 59:3-9.
- Watkins LR, Maier SF (2002) Beyond neurons: evidence that immune and glial cells contribute to pathological pain states. *Physiol Rev* 82:981-1011.
- Werth JL, Thayer SA (1994) Mitochondria buffer physiological calcium loads in cultured rat dorsal root ganglion neurons. *J Neurosci* 14:348-356.
- West AP, Shadel GS, Ghosh S (2011) Mitochondria in innate immune responses. *Nat Rev Immunol* 11:389-402.
- Wilson SM, Schmutzler BS, Brittain JM, Dustrude ET, Ripsch MS, Pellman JJ, Yeum TS, Hurley JH, Hingtgen CM, White FA, Khanna R (2012) Inhibition of transmitter release and attenuation of anti-retroviral-associated and tibial nerve injury-related painful peripheral neuropathy by novel synthetic Ca²⁺ channel peptides. *J Biol Chem* 287:35065-35077.
- Windebank AJ, Grisold W (2008) Chemotherapy-induced neuropathy. *J Peripher Nerv Syst* 13:27-46.
- Wolf S, Barton D, Kottschade L, Grothey A, Loprinzi C (2008) Chemotherapy-induced peripheral neuropathy: prevention and treatment strategies. *Eur J Cancer* 44:1507-1515.
- Woodbury CJ, Zwick M, Wang S, Lawson JJ, Caterina MJ, Koltzenburg M, Albers KM, Koerber HR, Davis BM (2004) Nociceptors lacking TRPV1 and TRPV2 have normal heat responses. *J Neurosci* 24:6410-6415.
- Woolf CJ, Ma Q (2007) Nociceptors--noxious stimulus detectors. *Neuron* 55:353-364.
- Xiao W, Naso L, Bennett GJ (2008) Experimental studies of potential analgesics for the treatment of chemotherapy-evoked painful peripheral neuropathies. *Pain Med* 9:505-517.

- Xiao WH, Bennett GJ (2008) Chemotherapy-evoked neuropathic pain: Abnormal spontaneous discharge in A-fiber and C-fiber primary afferent neurons and its suppression by acetyl-L-carnitine. *Pain* 135:262-270.
- Xiao WH, Zheng H, Bennett GJ (2012) Characterization of oxaliplatin-induced chronic painful peripheral neuropathy in the rat and comparison with the neuropathy induced by paclitaxel. *Neuroscience* 203:194-206.
- Xiao WH, Zheng H, Zheng FY, Nuydens R, Meert TF, Bennett GJ (2011) Mitochondrial abnormality in sensory, but not motor, axons in paclitaxel-evoked painful peripheral neuropathy in the rat. *Neuroscience* 199:461-469.
- Yaksh TL (2006) Calcium channels as therapeutic targets in neuropathic pain. *J Pain* 7:S13-30.
- Yilmaz E, Gold MS (2015) Sensory neuron subpopulation-specific dysregulation of intracellular calcium in a rat model of chemotherapy-induced peripheral neuropathy. *Neuroscience* 300:210-218.
- Yilmaz E, Gold MS (2016) Paclitaxel-induced increase in NCX activity in subpopulations of nociceptive afferents: A protective mechanism against chemotherapy-induced peripheral neuropathy? *Cell Calcium*.
- Yoshimura N, Seki S, Erickson KA, Erickson VL, Hancellor MB, de Groat WC (2003) Histological and electrical properties of rat dorsal root ganglion neurons innervating the lower urinary tract. *J Neurosci* 23:4355-4361.
- Yu SP, Choi DW (1997) Na⁽⁺⁾-Ca²⁺ exchange currents in cortical neurons: concomitant forward and reverse operation and effect of glutamate. *Eur J Neurosci* 9:1273-1281.
- Zhang H, Boyette-Davis JA, Kosturakis AK, Li Y, Yoon SY, Walters ET, Dougherty PM (2013) Induction of monocyte chemoattractant protein-1 (MCP-1) and its receptor CCR2 in primary sensory neurons contributes to paclitaxel-induced peripheral neuropathy. *J Pain* 14:1031-1044.
- Zhang H, Li Y, de Carvalho-Barbosa M, Kavelaars A, Heijnen CJ, Albrecht PJ, Dougherty PM (2016) Dorsal root ganglion infiltration by macrophages contributes to paclitaxel chemotherapy induced peripheral neuropathy. *J Pain*.
- Zhang H, Yoon SY, Zhang H, Dougherty PM (2012a) Evidence that spinal astrocytes but not microglia contribute to the pathogenesis of Paclitaxel-induced painful neuropathy. *J Pain* 13:293-303.
- Zhang XL, Mok LP, Katz EJ, Gold MS (2010) BKCa currents are enriched in a subpopulation of adult rat cutaneous nociceptive dorsal root ganglion neurons. *Eur J Neurosci* 31:450-462.

- Zhang XL, Mok LP, Lee KY, Charbonnet M, Gold MS (2012b) Inflammation-induced changes in BK(Ca) currents in cutaneous dorsal root ganglion neurons from the adult rat. *Mol Pain* 8:37.
- Zheng H, Xiao WH, Bennett GJ (2011) Functional deficits in peripheral nerve mitochondria in rats with paclitaxel- and oxaliplatin-evoked painful peripheral neuropathy. *Exp Neurol* 232:154-161.
- Zheng H, Xiao WH, Bennett GJ (2012) Mitotoxicity and bortezomib-induced chronic painful peripheral neuropathy. *Exp Neurol* 238:225-234.